Wave Energy Analysis and Capture Width Ratio for Floating Structures

Souhail Boulanoire

Submitted to the
Institute of Graduate Studies and Research
in partial fulfillment of the requirements for the degree of

Master of Science
in
Civil Engineering

Eastern Mediterranean University
May 2019
Gazimağusa, North Cyprus

Approval of the Institute of Graduate Studies and Research

Prof. Dr. Ali Hakan Ulusoy
Acting Director

I certify that this thesis satisfies all the requirements as a thesis for the degree of Master of Science in Civil Engineering.

Assoc. Prof. Dr. Serhan Şensoy
Chair, Department of Civil Engineering

We certify that we have read this thesis and that in our opinion it is fully adequate in scope and quality as a thesis for the degree of Master of Science in Civil Engineering.

Prof. Dr. Umut Türker
Supervisor

Examining Committee

1. Prof. Dr. Umut Türker

2. Asst. Prof. Dr. Gözen Elkıran

3. Asst. Prof. Dr. Mustafa Ergil

ABSTRACT

This study aims to focus on identifying the wave climate that presides over the Atlantic Ocean on the West side of Ireland. A series of quantitative analysis was carried out using data taken from a wave buoy placed offshore North-West Ireland. The analysis performed to calculate the dominant wind and wave directions annually. The number of occurrences of different wave heights with respect to varying wave periods is also delineated. The well-known spectral analysis is also carried out in order to find the energy capacity of the studied region. The results show that the region is governed by a wave height of 4 meters that mostly travels from West to East that occurs at a very narrow frequency and a wave power of around 60 kW/m. Three Floating structures, two floating breakwaters (π-type and box-type) and a floating Wave Energy Converter (Wave Dragon), are also proposed in the aim to know their level of power absorption and their capture width ratio. This has been achieved with the help of four different studies, three different wave transmission coefficient formula was derived from each study for each structure. The results show that the Wave Dragon is the most efficient in terms of power absorption and capture width ratio while testing them as a point wave absorber.

Keywords: Wave Energy, Wave Power, Capture width ratio, Transmission coefficient, Wave energy absorber.

ÖZ

Bu çalışma, İrlanda'nın Batı sahillerinde, Atlantik Okyanusu'nda dalga ikliminin belirlenmesine yönelik çalışmaları irdelemektedir. Kuzey-Batı İrlanda açık denizine yerleştirilmiş dalga şamandırasından alınan veriler kullanılarak bir dizi nicel analiz yapılmıştır. Bu analizlerle birlikte ham veri olarak bulunan bölgedeki hâkim rüzgâr yönü ve dalga bilgileri yıl bazında detaylı bir şekilde hazırlanmıştır. Farklı dalga yüksekliklerinin değişken dalga periyodlarına bağlı olarak bir yılda gösterdikleri tekerrür miktarları belirlenmiştir. Dünyada kullanımı sıklıkla uygulanan spektral analiz metotlarının uygulanması ile bölgenin enerji kapasitesi belirlenmiştir. Sonuçlar, bölgenin çoğunlukla Batı'dan Doğu'ya giden 4 metre dalga yüksekliğine tabi olduğunu göstermektedir. Bu dalgalar genellikle çok dar bir frekansta meydana gelmekte ve 60 kW/m civarında bir dalga gücü yaratmaktadırlar. Üç yüzer yapı, iki yüzer dalgakıran (Pi-tipi ve kutu tipi) ve bir yüzen Dalga Enerjisi Dönüştürücü (Wave Dragon), bölgedeki verimliliği analiz etme amacıyla "güç emme seviyeleri" ve "genişlik oranlarını kapsama" açısından incelenmiş ve analiz edilmiştir. Analizler daha önce gerçekleştirilmiş dört farklı çalışmadan elde edilen iletim katsayıları formüle edilerek her üç yapı için de uygulanmış ve sonuçlar Wave Dragon'un "güç emilimi" ve "genişlik oranını kapsama" bakımından en etkili olduğunu göstermiştir. Tüm bu çalışmalarda yüzer yapılar nokta dalga emici olarak kabul edilerek etkileri değerlendirilmiştir.

Anahtar kelimeler: Dalga Enerjisi, Dalga Gücü, Yakalama genişliği oranı, İletim katsayısı, Dalga enerjisi emici.

DEDICATION

I dedicate this study to my dad, who gave me the strength to achieve my goals, who never gave up on me, who always provided me all the support and the necessary needed. To my brothers, sister and friends who showed present whenever needed and for their encouragement to finish this thesis. And lastly, I dedicate this book to my beloved wife who has always been by my side in the good and hard time and to my future child who is in his mom's womb.

ACKNOWLEDGMENT

I wish to express my deep gratitude to my dear supervisor Prof. Dr. Umut Türker for his advice and support. I want to thank him for guiding me into this area of civil engineering study (Coastal & Marine engineering) where I got to know quite a bit about ocean wave power and energy and also about wave energy converters or breakwater structures. I am grateful for the monitoring, help and the valuable knowledge that he provided me during all this study. He went with me step by step and have always been present to guide me and make the adjustment needed for the accomplishment of this study.

I would like to thank my Department of civil engineering for the right and proper environment that they provided to us and for their appreciable effort to ease for us the accomplishment of our study.

TABLE OF CONTENTS

ABSTRACT iii

ÖZ iv

DEDICATION v

ACKNOWLEDGMENT vi

LIST OF TABLES ix

LIST OF FIGURES xiii

LIST OF SYMBOLS AND ABBREVIATIONS xvii

1 INTRODUCTION 1

1.1 Background, definition of the problem 1

1.2 The study environment 3

1.3 Aims and objectives of the research 4

1.4 Research questions 5

1.5 The proposed methodology 5

1.6 Outline of the study 6

1.7 Limitation of the study 7

1.8 Literature review 7

2 FUNDAMENTALS OF WAVES, WAVE ENERGY AND WAVE POWER 10

2.1 Waves 10

2.1.1 Linear Wave Definitions 11

2.1.2 Basic relationships of the wave variables 12

2.2 The wave height distribution models 13

Energy in waves 14

2.2.1 Spectral characteristics of waves 15

2.2.2 Model forms of wave spectrum 22
2.3 Wave Energy Flux 16
2.3.1 Capture width ratio 17
3 IRELAND ATLANTIC OCEAN WAVE ANALYSIS 20
3.1 Area of study and data source 20
3.2 Number of occurrences of significant wave height and average wave period 22
3.3 Monthly average sea state 30
3.4 Wave direction 33
4 RESULTS AND DISCUSSIONS 40
4.1 Probability of occurrence 40
4.2 The wave power 47
4.3 Wave energy spectra 51
4.4 Capture width ratio per unit width and potential power absorbed 55
5 CONCLUSION 63
REFERENCES 65
APPENDICES 70
Appendix A: Derived K_t formula 71
Appendix B: $P_{absorbed}$ and CWR 77

LIST OF TABLES

Table 3.1: Resultant occurrences for wave periods and wave heights for the year 2011 26

Table 3.2: Resultant occurrences for wave periods and wave heights for the year 2011 27

Table 3.3: Resultant occurrences for wave periods and wave heights for the year 2012 27

Table 3.4: Resultant occurrences for wave periods and wave heights for the year 2013 28

Table 3.5: Resultant occurrences for wave periods and wave heights for the year 2014 28

Table 3.6: Resultant occurrences for wave periods and wave heights for the year 2015 29

Table 3.7: Resultant occurrences for wave periods and wave heights for the year 2016 29

Table 3.8: Resultant occurrences for wave periods and wave heights for the year 2017 30

Table 3.9: Monthly significant wave height for all the years. (The max & min values are colored)..... 31

Table 3.10: Monthly significant wave period for all the years. (The max & min values are colored)..... 32

Table 3.11: Percentage of wave heights depending to their directions for 2010 34

Table 3.12: Percentage of wave heights depending to their directions for 2011 34

Table 3.13: Percentage of wave heights depending to their directions for 2012 35

Table 3.14: Percentage of wave heights depending to their directions for 2013 36
Table 3.15: Percentage of wave heights depending to their directions for 2014 36
Table 3.16: Percentage of wave heights depending to their directions for 2015 37
Table 3.17: Percentage of wave heights depending to their directions for 2016 38
Table 3.18: Percentage of wave heights depending to their directions for 2017 38
Table 4.1: Root mean square wave height and wave period for all the considered years 41
Table 4.2: Transmission coefficient of a Wave Dragon 55
Table 4.3: Transmission coefficient of a Cylindrical Floating Breakwater 56
Table 4.4: Transmission coefficient of a Board-net Floating Breakwater 56
Table B.1: Monthly average wave power results by using K_t from Abubaker and Türker 2019 77
Table B.2: Monthly average wave power results by using K_t from Macagnon 1954 77
Table B.3: Monthly average wave power results by using K_t from Ruol et. al. 201378
Table B.4: Monthly average wave power results by using K_t from Kriebel and Bollmann 1996 78
Table B.5: Monthly average capture width ratio results by using K_t from Abubaker and Türker 2019 79
Table B.6: Monthly average capture width ratio results by using K_t from Macagnon 1954 79
Table B.7: Monthly average capture width ratio results by using K_t from Ruol et. al. 2013 80
Table B.8: Monthly average capture width ratio results by using K_t from Kriebel and Bollmann 1996 80
Table B.9: Monthly average wave power results by using K_t from Macagnon 1954 81

Table B.10: Monthly average wave power results by using K_t from Ruol et. al. 2013 81
Table B.11: Monthly average wave power results by using K_t from Kriebel and Bollmann 1996 82
Table B.12: Monthly average wave power results by using K_t from Abubaker and Türker 2019 82
Table B.13: Monthly average capture width ratio results by using K_t from Macagnon 1954 83
Table B.14: Monthly average capture width ratio results by using K_t from Ruol et. al. 2013 83
Table B.15: Monthly average capture width ratio results by using K_t from Kriebel and Bollmann 1996 84
Table B.16: Monthly average capture width ratio results by using K_t from Abubaker and Türker 2019 84
Table B.17: Monthly average wave power results by using K_t from Abubaker and Türker 2019 85
Table B.18: Monthly average wave power results by using K_t from Macagnon 1954 85
Table B.19: Monthly average wave power results by using K_t from Ruol et. al. 2013 86
Table B.20: Monthly average wave power results by using K_t from Kriebel and Bollmann 1996 86
Table B.21: Monthly average capture width ratio results by using K_t from Abubaker and Türker 2019 87
Table B.22: Monthly average capture width ratio results by using K_t from Macagnon

1954 87

Table B.23: Monthly average capture width ratio results by using K_t from Ruol et. al. 2013 88

Table B.24: Monthly average capture width ratio results by using K_t from Kriebel and Bollmann 1996 88

LIST OF FIGURES

Figure 1.1: The relative strength of wave energy in kW/m observed all around the world. (URL:1)..... 4

Figure 2.1: Classification of ocean waves with respect to their periods (Munk, 1951). 11

Figure 2.2: An illustration of sinusoidal wave with important variables like wave amplitude, wave length etc. (Laing, 1998)..... 12

Figure 3.1: Map of the location of the wave buoy Belmullet Berth B..... 21

Figure 3.2: Sample of the data gathered from the wave buoy Belmullet Berth B 21

Figure 3.3: Pierson- Moskowitz and JONSWAP spectrum depicted graphically. 23

Figure 3.4: The maximum and minimum significant wave period that may occur in a year..... 32

Figure 3.5: The maximum and minimum significant wave height that may occur in a year..... 33

Figure 3.6: Main wave direction distribution and related wave height for 2010..... 34

Figure 3.7: Main wave direction distribution and related wave height for 2011..... 35

Figure 3.8: Main wave direction distribution and related wave height for 2012..... 35

Figure 3.9: Main wave direction distribution and related wave height for 2013..... 36

Figure 3.10: Main wave direction distribution and related wave height for 2014..... 37

Figure 3.11: Main wave direction distribution and related wave height for 2015..... 37

Figure 3.12: Main wave direction distribution and related wave height for 2016..... 38

Figure 3.13: Main wave direction distribution and related wave height for 2017..... 39

Figure 4.1: Probability of occurrence of significant wave height for 2010 41

Figure 4.2: Probability of occurrence of average wave period for 2010 41

Figure 4.3: Probability of occurrence of significant wave height for 2011 42
Figure 4.4: Probability of occurrence of average wave period for 2011 42
Figure 4.5: Probability of occurrence of significant wave height for 2012 42
Figure 4.6: Probability of occurrence of average wave period for 2012 43
Figure 4.7: Probability of occurrence of significant wave height for 2013 43
Figure 4.8: Probability of occurrence of average wave period for 2013 43
Figure 4.9: Probability of occurrence of significant wave height for 2014 44
Figure 4.10: Probability of occurrence of average wave period for 2014 44
Figure 4.11: Probability of occurrence of significant wave height for 2015 44
Figure 4.12: Probability of occurrence of average wave period for 2015 45
Figure 4.13: Probability of occurrence of significant wave height for 2016 45
Figure 4.14: Probability of occurrence of average wave period for 2016 45
Figure 4.15: Probability of occurrence of significant wave height for 2017 46
Figure 4.16: Probability of occurrence of average wave period for 2017 46
Figure 4.17: Wave power based on wave period and wave height for 2010 48
Figure 4.18: Wave power based on wave period and wave height for 2011 48
Figure 4.19: Wave power based on wave period and wave height for 2012 48
Figure 4.20: Wave power based on wave period and wave height for 2013 49
Figure 4.21: Wave power based on wave period and wave height for 2014 49
Figure 4.22: Wave power based on wave period and wave height for 2015 49
Figure 4.23: Wave power based on wave period and wave height for 2016 50
Figure 4.24: Wave power based on wave period and wave height for 2017 50
Figure 4.25: Wave energy spectra for 2010 52
Figure 4.26: Wave energy spectra for 2011 52
Figure 4.27: Wave energy spectra for 2012 52

Figure 4.28: Wave energy spectra for 2013 53
Figure 4.29: Wave energy spectra for 2014 53
Figure 4.30: Wave energy spectra for 2015 53
Figure 4.31: Wave energy spectra for 2016 54
Figure 4.32: Wave energy spectra for 2017 54
Figure 4.33: Average power absorbed by Wave Dragon 58
Figure 4.34: Average capture width ratio for a Wave Dragon 59
Figure 4.35: Average power absorbed by a Cylindrical Floating Breakwater 59
Figure 4.36: Average capture width ratio for a Cylindrical Floating Breakwater 59
Figure 4.37: Average power absorbed by a Board-net Floating Breakwater 60
Figure 4.38: Average capture width ratio for a Board-net Floating Breakwater 60
Figure A.1: The change of K_t w.r.t B/L retrieved from Abubaker and Türker 2019 for Wave Dragon 71
Figure A.2: The change of K_t w.r.t B/L retrieved from Macagnon 1954 for Wave Dragon 71
Figure A.03: The change of K_t w.r.t B/L retrieved from Ruol et. al. 2013 for Wave Dragon 72
Figure A.4: The of K_t w.r.t B/L retrieved from Kriebel and Bollmann 1996 for Wave Dragon 72
Figure A.5: The change of K_t w.r.t H/L retrieved from Macagnon 1954 for Cylindrical Floating Breakwater 73
Figure A.6: The of K_t w.r.t H/L retrieved from Abubaker and Türker 2019 for Cylindrical Floating Breakwater 73
Figure A.7: The change of K_t w.r.t H/L retrieved from Ruol et. al. 2013 for Cylindrical Floating Breakwater 74

Figure A.8: The change of K_t w.r.t H/L retrieved from Kriebel and Bollmann 1996 for Cylindrical Floating Breakwater 74
Figure A.9: The change of K_t w.r.t H/L retrieved from Abubaker and Türker 2019 for Board-net Floating Breakwater 75
Figure A.10: The change of K_t w.r.t H/L retrieved from Ruol et. al. 2013 for Board-net Floating Breakwater 75
Figure A.11: The change of K_t w.r.t H/L retrieved from Kriebel and Bollmann 1996 for Board-net Floating Breakwater 76
Figure A.12: The change of K_t w.r.t H/L retrieved from Macagnon 1954 for Board-net Floating Breakwater 76

LIST OF SYMBOLS AND ABBREVIATIONS

A_γ	Normalizing Factor
a	Wave anplitude
AMETS	Atlantic Marine Energy Test Site
B	Width of the structure
BnFB	Board-net Floating Breakwater
C	Rate of propagation
C_g	Wave group speed
CFB	Cylindrical Floating Breakwater
CWR	Capture Width Ratio
CW	Capture Width
E_{total}	Total Energy
$E_{kinetic}$	Kinetic Energy
$E_{potential}$	Potential Energy
f	Wave frequency
f_p	Peak wave frequency
g	Gravitational acceleration
H	Wave Height
H_{rms}	Root mean square of wave height
H_s	significant wave height
H_{lee}	Wave height at the lee side
$H_{incident}$	Incident wave height
JONSWAP	Joint North Sea Wave Project
k	Wave number

K_t	Wave transmission coefficient
L	Wave lenght
n	Number of waves
P	Wave Power
pdf	Probability Density Function
$P_{absorbed}$	Absorbed Wave power
P	Wave Power or Energy flux
P_{lee}	Wave power at the lee side
$P_{incident}$	Incident Wave power
P_R	Rayleigh probability desinsity function
RMS	Root Mean Square
S(f)	Wave energy spectrum with respect to frequency
S(T)	Wave energy spectrum with respect to period
S_j	JONSWAP spectrum
S_{PM}	Pierson Moskowitz spectrum
SEAI	Sustainable Energy Authority of Ireland
T	Wave period
T_{av}	Average wave period
T_{rms}	Root mean square of wave period
T_{m01}	Mean wave period
T_{m02}	Mean zero up-crossing period
T_p	Peak Peariod
w	Angular frequency
WD	Wave Dragon
WEC	Wave Energy Converter

λ	Wave length
η	Wave profile
ρ	Density
γ	Peak shape parameter
σ	Spectral width parameter

Chapter 1

INTRODUCTION

1.1 Background, definition of the problem

Over a century, human beings have been consuming non-renewable fuels to generate energy. Although this has been done in sake of development and growth, the survival and sustainability of the nature has always been disregarded (Gökçekuş et al. 2011). Therefore, nowadays, using coal and oil for such energy requirements is backfiring in the form of climate change which can be treated as one of the greatest environmental encounters in the form of droughts (Payab and Türker, 2018) and floods. On the other hand, the common sources of energy such as oil and natural gas are not used under the philosophy of conservation of mass. This means that the rate at which we use them is not same as the rate they replenish themselves. As such, according to Shafiee and Topal (2009), the fossil fuel time depletion all around the world is estimated to be around 35, 107 and 37 years for oil, coal and gas resources, respectively. Even though main non-renewable energy sources are oil, coal and natural gas, there are other sources like nuclear energy. Nuclear energy is simply the outcomes of fission or fusion of atoms. Fission is the splitting of big atoms like plutonium and uranium whereas, fusion is the merging of smaller atoms like hydrogen. However, due to the high initial cost and negative environmental effects of nuclear wastes, this technology itself cannot be an alternative energy resource for the future. As a result, research studies and investment on alternative energy sources which does not deplete as it is used (renewable energy sources) should be encouraged.

Most common renewable energy sources are solar energy, wind energy, hydroelectric power, bioenergy, geothermal energy and the ocean energy. The sun is the main source of the solar energy and generates this energy through radiating. This energy is commonly used for heating and lighting purposes for commercial and industrial uses. The wind is used to generate energy by the help of turbines. Wind turbines are capable to convert the captured kinetic energy of the air into mechanical energy which is then converted into electricity through the generators. The wind energy, in the form of electricity is generally consumed at homes, schools and other public places.

Hydroelectric power is generated by using the head difference between the upstream and downstream elevations of water resources. Usually the upstream part is the stored water at high elevations like reservoir of a dam and downstream elevation is close to the base of the dam where turbines are ready to be rotated by water flowing through a penstock by the help of the gravity. Rotating turbines in turn drive generators to convert mechanical energy into electricity. The electricity captured by hydroelectric power can be transferred long distances in the form of high voltages to be consumed at any other place rather than the generated location. Bioenergy, on the other hand, is another type of renewable energy that is captured from lately active natural, biological organic resources known as biomass. Geothermal energy is the power generated by the internal heat of the earth itself. Geothermal energy is renewable since the heat is continuously produced inside the earth and is captured for the purpose of bathing, heating the buildings and generate electricity.

In fact, ocean energy describes different types of energy sources generated from various sea states. Tidal energy is the one of the well-known ocean energy generating source whereas, wind waves, storm waves, sea currents and tide waves are other

energy producing sea states used to produce electricity. Among the above sea state conditions the waves are an undulating movement of the sea. They are generated by the wind that transfers energy from the atmosphere into the sea. Transformed energy generates waves characterized by their height, period and the direction of their propagation. There are different devices to exploit this energy. Many systems are currently under study, some are already on the market but none have reached the stage of industrial maturity. Nevertheless, it is clear that decrease in the amount of fossil fuels motivate researchers to search for renewable energy sources like ocean energy and to increase the number of possible alternatives for generating renewable energy sources.

Therefore, in this study the author will concentrate on estimating how much renewable energy sources can be harvested from North-East Atlantic; ocean close to the offshore Ireland. This will be achieved by using the wave climate data measured from one of the wave gauges installed at North-East Atlantic.

1.2 The study environment

This study involved an investigation of wave data of the East Atlantic Ocean (Ireland). The data used to evaluate the wave characteristics and related wave power was collected from the Irish Weather Buoy Network. The buoy network delivers essential data for shipping bulletins, weather forecasts, swell and storm warnings and also data for research or general public information. The name of the wave buoy is Belmullet Wave Buoy Berth B, and it has been measured the wave data since the last months of 2009. The data used for this study covers wave information for the years 2010 to 2017. The data is retrieved from a buoy which is placed offshore at the north-west side of Ireland at a latitude of 54.23 and longitude of -10.14. The retrieved data consists of wave period and wave height together with the other parameters like wind

direction. The data is recorded in every 30 minutes. All the data is downloaded from the web page of the Marine Institute of Ireland. Marine Institute of Ireland is the state agency who is responsible all kinds of marine research, technology development and innovation in Ireland. Their web page is:

https://www.marine.ie/Home/home

The main idea of using the data obtained from Belmullet Wave Buoy Berth B is the information received from wave energy map of the world. According to the map (Fig. 1.1) west of Ireland at Atlantic Ocean is a region with high wave power potential.

Figure 1.1: The relative strength of wave energy in kW/m observed all around the world. (URL:1).

1.3 Aims and objectives of the research

The main idea behind this study is to find out the wave energy capacity of East of Atlantic Ocean and assess how much energy can be captured (absorbed power) if different types of floating structure is installed at Atlantic Ocean close to the data extracted region. In order to do so, data received from the wave buoy every 30 minutes between 2010 and 2017 is analysed. This will help in revealing the wave energy and the wave power that can be captured from east of Atlantic Ocean. The data covers the information regarding the wave height and the wave period. Initially the number of

occurrences of waves with respect to their height and period is evaluated. The probability of occurrence of waves and accordingly the annual wave power with respect to significant wave heights and average wave period are evaluated.

The wave power generated at Atlantic Ocean is then used to check the possible usage of floating structures at the region. The incident wave energy captured at the region is tested over the data predicted for box type, π-type, and wave dragon structures by previous research studies. The transmission coefficient magnitudes obtained in these studies are used to measure absorbed wave power.

1.4 Research questions

The research is whispered to answer several questions that motivated the author to complete the study. Some of these questions are as below, and the answers to these questions are almost answered within this thesis.

- What is the significant wave height per year at the western coast of Ireland?
- What is the energy potential between 2010 and 2017 at the study area?
- What is the wave energy spectrum for the chosen location?
- How much energy can be absorbed at the western coast of Ireland by using different wave energy capturing structures?
- Is there an any change in the wave height pattern within the study period?
- What kind of floating structures can achieve better energy absorption at the western coast of Ireland?

1.5 The proposed methodology

In order to estimate the wave energy and wave power available in the study area we are concerned about, the main methodology used for this study is quantitative. All data needed is available from Galway Bay and Belmullet wave energy test sites. The

quantitative results of our research questions will be achieved using mathematical and numerical methods with the help of Microsoft Excel software.

The method of work began by gathering the data about wave height, wave period and wind direction of the site we are interested in. The data is provided by Galway Bay and Belmullet wave energy test sites. The data is gathered from the buoy named "Bellmulet Berth B" which is placed offshore at the Atlantic Ocean in the North-West side of Ireland. The gathered data cover 7 years, from 2010 to 2017, of wave record. Since single day is a poor estimation of the wave energy/power, compared to a yearly average, it is decided to evaluate the wave records yearly over each year. This helped to produce more precise information on how much energy/power does exist in that area. As soon as the data is gathered, number of occurrence of wave heights and wave periods, the probability of occurrence of wave height and wave period, the monthly average significant wave height and wave period, the peak direction and wave height, and the wave power level with respect to wave height and wave period are evaluated and estimated for every year.

By the end, already available empirical relations derived for different types of floating structures are used to estimate absorbed wave power at the study area.

1.6 Outline of the study

This study comprises five different chapters. The first chapter is the introduction. First chapter includes; the background and definition of the problem, the study context as well as its aims and objectives and methodology used for this study. The second chapter deals with the fundamentals of waves, wave energy and wave power; and include all the necessary formulations required for this study. The 3rd chapter consist of information about North-East Atlantic wave analysis and all the outcomes of the study. Chapter 4 will be a discussion of the results obtained during this thesis study.

Finally, the Chapter 5 will be the conclusion of this theses where recommendation will be discussed for further studies.

1.7 Limitation of the study

Although the use of Pierson-Moskowitz and JONSWAP model is a fairly common approach to studying wave spectra model for two-dimensional wave analysis (wave height and direction), this study assesses the results based on one dimensional analysis. Furthermore, the study covers data analysis based on point data recorder. However, more reliable results can be obtained by reflecting the effect of regional data to the outcomes of the study. Finally, the capture width ratio calculated based on this study is valid only for the studied area.

1.8 Literature review

Generally, the advantages of wave energy is more than the advantages of other renewable energy sources while generating minimal impacts on the environment. The environmental impact of wave energy harvesting is only limited to the construction and installation of the wave absorbing structures (Hemer and Griffin, 2010). On the other hand, long term environmental concerns and uncertainties to be generated by wave energy converting structures remains unknown on the marine and coastal environments.

Continuous interaction of waves with coastlines and erosive properties by the force of waves has shown that ocean waves has considerable amount of energy potential. Converting such renewable energy potential into a usable electricity power is under the interest of researches for considerable amount of time period (Stahl, 1892; Leishman and Scobie, 1976; McCormick, 1981; Shaw, 1982).

The main focus on wave energy converting structures (WEC) goes parallel with the initial days of 1st World War. In those days the Japanese researcher Yoshio Masuda

initiated the first studies on devices that can be used to harvest the energy generated by the waves (Masuda, 1986). Until 1980 the interest on renewable energy concepts was not deeply studied and was under the interest of funding authorities. It was in 1980 when Kyoto protocol was signed and aims for the reduction of carbon emission became a vital environmental concern for all the countries all around the world. Since then, growing interest on renewable energy sources has taken over and parallel to this wave energy research and development studies funded by authorities (Falnes, 2007).

Currently there are many wave energy converting projects either based on field or laboratory studies. While some of them are harvesting efficient wave energy, others are still on testing levels. A few of these studies are used to supply electricity at regional base. However, the contribution of such projects on national energy production is far below the requirements and can be treated as at negligible levels (Hughes and Heap, 2010).

In the literature there exist two categories that wave energy research and development studies are based on. One of these categories is totally concentrated on the assessment and hindcasting of wave climate based on wave heights, periods and direction (Iglesias et al., 2009), whereas the second one takes into consideration the energy potential that can be captured from the waves and types and properties of WEC that optimizes these energy (Bernhoff et al., 2006; Henfridsson et al., 2007; Folley and Whittaker, 2009). There are some cases where both the categories are worked out in one research such as the study of Hughes and Heap in 2010 who has worked out the wave energy resource assessment of Australia (Babarit et al., 2012).

According to the wave power maps published usually through internet sources (URL1) the wave power energy around the Atlantic Ocean is worth to be analyzed. In the Atlantic Ocean, the wave power is about 40 kW/m (Mollison et al., 1976), and

according to Sinden, the wave power at the Atlantic Ocean is around 42 kW/m (Sinden, 2005). Nevertheless, one can say that the power at the Atlantic Ocean is more or less equal to 40 kW/m. Based on this information here in this study the author used the wave data captured by a wave buoy at the western part of Ireland and carried out a study based on both the categories defined above. The author first concentrated on the assessment of wave climate at the western part of Ireland, which is succeeded by calculations of incident wave energy. Later, by the help of the transmission coefficient values for different floating structures, the author find out the possible wave power absorption capacity of different floating structures at the western coast of Ireland.

Chapter 2

FUNDAMENTALS OF WAVES, WAVE ENERGY AND WAVE POWER

2.1 Waves

As a consequence of forces applied on the ocean surfaces, sea waves are generated. Mainly these forces are due to the shear stresses generated by winds while blowing over the ocean surface. Such waves are termed as ordinary gravity waves. At the same time, there are other types of waves occurring due to the naturally occurring external effects, such as, earthquakes, earth's rotation, interaction of moon and the sun etc. for the generation of different kind of waves. These waves are tsunami waves, tidal waves, storm surges, capillary waves etc. All these waves are differing from each other based on their periods. Wave period is defined as the time necessary for two successive wave-crest to pass a fixed point. The wave classification of different types of waves based on their periods are classified by Munk (1951) and is given in Figure 2.1.

The well-known and observed form of the waves is the wind-generated waves. These waves are taking place at the interface of ocean and the atmosphere. Gravity forces are the restoring and balancing forces of these waves; hence they are mentioned as wind generated ordinary gravity waves.

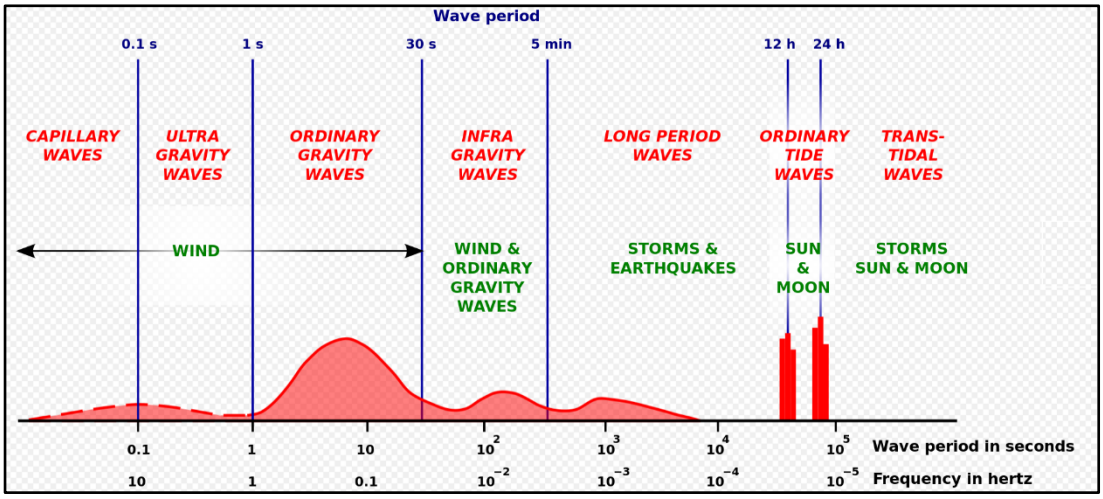

Figure 2.1: Classification of ocean waves with respect to their periods (Munk, 1951).

In general, the gravity waves are observed in rather complex pattern and are travelling randomly. It is necessary to understand the behavior of these waves so that one can easily analyze and model them. This can be achieved through simple assumptions such as; incompressibility of waves, important to build the continuity equation for the water particles; ignoring the friction forces and assuming that the fluid flow is irrotational. All these assumptions help defining several equations to describe the motion of the ocean as sea waves.

2.1.1 Linear Wave Definitions

The gravity waves are progressive, long crested and follow a sinusoidal pattern. Sinusoidal pattern in general repeats itself and follows a sine curve. Therefore, each individual wave experiences equal crests possessing same heights with the same frequency as shown in Figure 2.2.

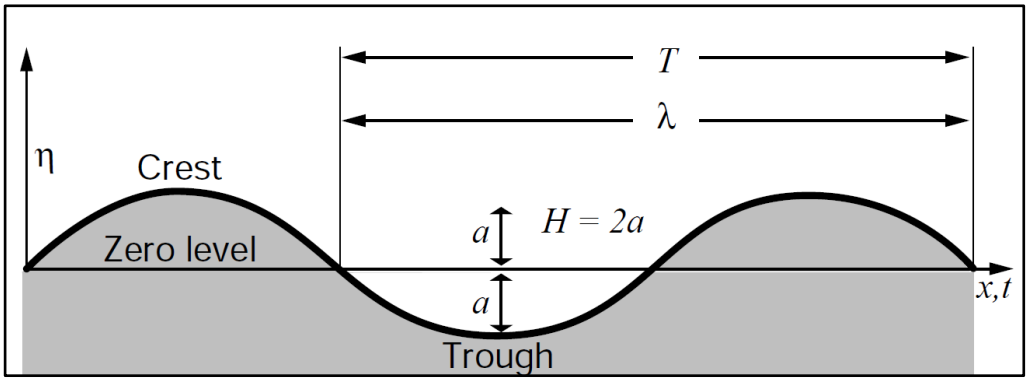

Figure 2.2: An illustration of sinusoidal wave with important variables like wave amplitude, wave length etc. (Laing, 1998).

As given in Figure 2.2 the wavelength is shown to be the horizontal distance between the two consecutive wave crests or trough. The wavelength is shown by a Greek symbol, λ. The wave length is usually defined in terms of meters. The number of crests or troughs passing a fixed point per unit time is called the wave frequency. The wave frequency, *f* is defined in terms of Hertz, and it is also defined as reciprocal of wave period, *T*. The vertical distance between the wave crest and the consecutive wave trough is known as wave height. The wave height, *H* is usually defined in terms of meters and is a primary wave energy indicator. On the other hand, the maximum deviation of wave form from mean sea level in the direction of either crest or trough is known as the wave amplitude, *a*. The speed of waves or in other terms the phase speed of waves is defined as the rate of propagation of the waves and is defined by symbol, *C*. The phase speed is the speed at which the wave profile travels. The wave travel can also be defined as the speed at which the wave crest or trough advances.

2.1.2 Basic relationships of the wave variables

As it was defined before, the wave profile can be defined in the shape of a sinusoidal wave and mathematically given as:

$$\eta(x,t) = a\,sin(kx - \omega t) \qquad (2.1)$$

In the above equation *k* represents the wave number and ω represents the angular

frequency of the waves. The wave number is the function of wave length and the angular frequency is function of wave period.

$$k = \frac{2\pi}{L} \quad and\ \omega = \frac{2\pi}{T} \tag{2.2}$$

Equation (2.1) shows that the wave profile is a function of both the time and the space. In reality, theoretically proved above relationship can never observed in real sea. Sometimes they can be observed in the form of swell which occurs in the condition where no wind occurs. In fact, in order to understand and describe the waves on the ocean surface simple relation given in Eq. (2.1) is frequently used. The models and analyses based on this simple definition have proven that it worth to be used and in practice gives reliable results.

2.2 The wave height distribution models

The spatial distribution of wave heights within the ocean is important. This helps to better understand the physical behavior of the ocean and resulting processes like construction of sea structures, sediment transport etc. In deep water wind generated wave height follows Rayleigh distribution based on their frequency of occurrences. There are many research studies that modified the definition of Rayleigh distribution to describe wave height effect on ocean works. Battjes (1972) and Collins (1970) are the two studies who initiate the Rayleigh distribution applications in coastal engineering. Longuet-Higgins (1975) was another scientist presenting analytical formulation of the probability distributions of the ocean waves.

Rayleigh distribution is a continuous probability distribution. The model is given good approximations especially when the wind velocity and its consequences are under consideration. The model works for non-negative random variables. Therefore, they are the most frequently used models to define wave climate in open sea conditions. The probability density function through Rayleigh helps to define the root-

mean-square wave height of the selected wave state. Actually, root mean square (RMS) wave height is defined as the square root average of squares of all the wave heights. It should also be noted that the model cannot be used for shallow sea state conditions.

The probability density function is denoted by $P_R(H)$ where subscript R mention that it is a Rayleigh probability distribution function (pdf) and H represent a specific wave height. The expression of Rayleigh probability density function is given as:

$$P_R(H) = \frac{2H}{{H_{rms}}^2} * exp^{\left(-\left(\frac{H}{H_{rms}}\right)^2\right)} \quad (2.3)$$

Where H_{rms} is defined, for data where similar records values are noticed, by the expression:

$$H_{rms} = \sqrt{\frac{\sum(H^2 n)}{\sum n}} \quad (2.4)$$

Where n denotes the number of waves occurring at a specific wave height.

By the help of Rayleigh pdf, one can produce representative graphs for the probability of occurrence for every wave height. Rayleigh pdf can also be used in order to represent, in a graph, the probability of occurrence of every wave period where the parameters H and H_{rms} will be replaced by T (wave period) and T_{rms} (root-mean-square period).

Energy in waves

The total wave energy can be described in terms of kinetic energy and potential energy. It is interesting that, while the wave propagates the total wave energy is equally divided between kinetic and potential energy. Any disturbance on the water surface due to the waves generates kinetic energy and this energy is always moving with the waves. On the other hand, while the wave propagates the water particles displace in

the vertical direction that affect the potential energy of the wave segment. The total energy due to the potential and kinetic energy can be given as

$$E_{total} = E_{kinetic} + E_{potential} \tag{2.5}$$

Which can be written in terms of related variables as

$$E_{total} = \frac{1}{16}\rho g H^2 + \frac{1}{16}\rho g H^2 = \frac{1}{8}\rho g H^2 \tag{2.6}$$

Where ρ is the density of the ocean water and g is the gravitational acceleration. The wave height is symbolized as H. E_{total} is the total of the potential and kinetic energies of all particles in the water column for one wavelength.

For the case of the real ocean conditions the wave energy is best described by means of the wave energy spectrum, *S(f)*. The wave energy spectrum is the spatial distribution of the sea wave energy as a function of the wave period, *T* or wave frequency, *f*. Spatially, the sea state is possessing a random wave characteristics generating constant changes within a given time span. Therefore, wave energy spectrum provides a clear illustration of the spatial energy distribution for a considerable time interval.

2.2.1 Spectral characteristics of waves

According to Goda, time wise changes of water surface profiles that consists of infinite number of wavelets with different periods, amplitudes, phase positions and directions can be integrated into an individual component by means of wave spectrum (Goda, 2010). In general, 1D- wave spectrum can be developed either by relating the wave energy in all directions, *S(f)* with the particular frequency, *f* or as an alternate by relating the wave energy in all directions, *S(T)* with the particular wave period, *T*.

Based on the linear wave theory, the definition of wave energy is as given in Eq. (2.5) or simply replacing wave height with wave amplitude as $\rho_w g a^2/2$. Defining the wave spectrum in terms of *E* were the initial representations of wave energy density

or spectrum of the wave energy. However, accepting that the density of sea water and the gravitational acceleration are always constant, it has become common practice to define the spectral wave energy in terms of wave amplitude as a^2. Therefore, plot of a^2 over the abscissa and the plot of either frequency or period on ordinate will show a continuous curve drawn typically as a bell shape as shown in Fig. (2.3). It should be noted that irregular sea conditions sometimes generate broad spectra which might give birth to several peaks. The wave spectrum ordinate that reflects the measure of the wave energy has a unit m^2/Hz.

It is important to note that most measurements do not provide information about the wave direction and therefore we can only calculate an energy distribution over wave frequencies, *E(f)*. In the vertical axis, a measure for the wave energy is plotted in units of m^2/Hz. This unit is usually for frequency spectra.

2.3 Wave Energy Flux

The wave energy flux per unit wave crest length or, equivalently, the rate the wave energy is transmitted across a plane of unit width, perpendicular to the direction of wave propagation direction, is the product of the total wave energy, including the kinetic and potential energies, and the wave group speed (Türker and Kabdaşlı, 2004). Using this definition, the energy flux attained in the wave propagation direction is defines as:

$$P = E_{tot} C_g \tag{2.8}$$

Where C_g is the wave group speed and given by the expression (for deep water):

$$C_g = g \frac{T_{av}}{4\pi} \tag{2.9}$$

Where g is gravitational acceleration and E_{tot} is the average total energy and, for ocean in deep sea, is given by:

$$E_{tot} = \rho g m_0 \tag{2.10}$$

Where

$$m_0 = \frac{{H_s}^2}{16} \tag{2.11}$$

Therefore, from Eq. (2.10) and Eq. (2.11), E_{tot} will be expressed as:

$$E_{tot} = \rho g \frac{{H_s}^2}{16} \tag{2.12}$$

Consequently, power *P* will be given as:

$$P = \frac{\rho g^2}{64\pi} {H_s}^2 T_{av} \tag{2.13}$$

With P in (kW/m), H_s in (m) and T_{av} in (sec). The wave power possessed by sea waves generally travels until they reach to a suitable location to dissipate their energy. Such conditions can be obtained in case of natural wave breaking conditions at coastal regions (Kabdaşlı and Türker, 2002) or at deep waters over submerged structures (Türker, 2014). The wave power simply is the wind energy which can be captured to be used in useful works such as production of electricity energy. However, in general the captured wave energy is not same as the energy absorbed by the system to convert wave energy to electricity energy. Due to the efficiency concerns in floating structures and wave energy converters not all the energy captured from waves is converted to useful form. Babarit (2015) worked on a ratio called Capture Width Ratio (CWR) in which helped to calculate the energy absorbed by floating structures or WEC's when the renewable energy sources are in concern.

2.3.1 Capture width ratio

The capture width (CW) phenomena was introduced early in 1975. It was initially defined by Falnes (1975). The ratio between the energy of the waves as a source (kW/m) and the wave power absorbed by the structures (kW) is simply defined as the

capture width (CW). The unit of capture width is in meters. The capture width can also be defined as the measurement of the efficiency of the system that optimizes the performance of floating structures. Capture width ratio (CWR) can be obtained by dividing the capture width into the characteristic length of the floating structures, such as the width of the system. Therefore, Babarit (2015) defined the Capture width ratio as the fraction of wave power flowing through the device that is absorbed by the device and define it as:

$$CWR = \frac{CW}{B} = \frac{P_{absorbed}}{B \times P_{incident}} \tag{2.14}$$

In other terms the Capture Width Ratio per unit width of floating device can simply be written as

$$CWR = \frac{P_{absorbed}}{P_{incident}} \tag{2.15}$$

Where $P_{incident}$ can be calculated through the wave power formula derived previously by the Eq. (2.13). On the other hand, coastal and ocean engineering studies has shown that the ratio between the wave energy before any floating structure and after floating structure can be defined by wave transmission coefficient. The effect of floating structure on the transmission coefficient have been studied by different researchers who have approved the above definition for transmission coefficients. These studies are performed by Martinelli et al. (2008), Diamantoulaki and Angelides (2011), Ruol et al. (2013) and recently by Alamailes and Türker (2019). Therefore, the wave transmission coefficient is defined as

$$K_t = \frac{H_{lee}}{H_{incident}} \tag{2.16}$$

Based on linear wave theory wave energy can be described in terms of square of wave height as:

$$K_t^2 = \frac{T_{av} 64 \pi \rho g^2 H_{lee}^2}{T_{av} 64 \pi \rho g^2 H_{incident}^2} \tag{2.17}$$

$$K_t^2 = \frac{P_{lee}}{P_{incident}} \tag{2.18}$$

$$K_t^2 = \frac{P_{incident} - P_{absorb}}{P_{incident}} \tag{2.19}$$

$$K_t^2 = 1 - \frac{P_{absorb}}{P_{incident}} \tag{2.20}$$

which can be written in terms of CWR as

$$CWR = 1 - K_t^2 \tag{2.21}$$

As a result, it is clear that the capture width ratio per unit width of any floating structure can be calculated if the transmission coefficient is known. Therefore, the amount of renewable energy that can be absorbed by floating structures at sea state conditions can be calculated.

Chapter 3

IRELAND ATLANTIC OCEAN WAVE ANALYSIS

3.1 Area of study and data source

In order to make testing of full-scale wave energy converters more accessible in an open environment, the Sustainable Energy Authority of Ireland (SEAI) developed the Atlantic Marine Energy Test Site (AMETS). AMETS is located in the Mullet Peninsula; the Belmullet area of county Mayo which is approximately 10 kilometers off Annagh head (Ceann Eanach). The area is known for its violent wind power coming from the Atlantic which could be the main reason of the location of AMETS since AMETS was created on the purpose of exploiting wave energy and it is known that in the case of wind waves; more powerful is the wind the more powerful are the waves.

The test site, where data were taken from, is located at the western coast of Ireland and it is focused on wave energy. It comprises two test area; one test area A is located 16 km far from the beach of Belderra Strand and has a 100 m water depth. The second test area B is located at 6 km away from the same beach; Belderra Strand, and has a 50 m water depth.

The test site focuses especially on wave powered technologies. The Atlantic Marine Energy Test Site offers real time data as well as historical data related to the wave climate at the Belmullet sites (Berth A and Berth B).

For this study, data were gathered from the second test area B; from the wave measurement buoy Bellmulet Berth B.

Figure 3.1: Map of the location of the wave buoy Belmullet Berth B

The wave buoy Belmullet Berth B is located at a longitude of -10.1429 degrees East and at a latitude of 54.233933 degrees North. The wave buoy take wave records every half hour and offers information about significant wave height, wave period, wave peak period, energy period, and wave direction.

A small part of the data extracted from Belmullet Berth B is shown in Fig. (3.2).

	longitude	latitude	time	station_id	PeakPeriod	PeakDirection	PeakSpread	EnergyPeriod	MeanWavePeriod_Tm01	MeanWavePeriod_Tm02	SignificantWaveHeight
2	degrees_eas	degrees_nort	UTC		s	degrees_true	degrees_true	s	s	s	m
3	-10.1429	54.233933	2009-12-15T16:36:00Z	Belmullet Wave Buoy Berth B	12.5	260.2	33.1	9.027324	7.25	6.25	2.07
4	-10.1429	54.233933	2009-12-15T17:06:00Z	Belmullet Wave Buoy Berth B	13.33	282.7	30.4	9.099861	7.21	6.154	1.98
5	-10.1429	54.233933	2009-12-15T17:36:00Z	Belmullet Wave Buoy Berth B	13.33	282.7	38.3	8.768274	7.01	6.154	2.1
6	-10.1429	54.233933	2009-12-15T18:06:00Z	Belmullet Wave Buoy Berth B	13.33	265.8	31.9	9.085818	7.15	6.154	2.02
7	-10.1429	54.233933	2009-12-15T18:36:00Z	Belmullet Wave Buoy Berth B	11.76	270	27.9	8.829636	7.14	6.25	2.19
8	-10.1429	54.233933	2009-12-15T19:06:00Z	Belmullet Wave Buoy Berth B	13.33	275.6	32.1	8.708892	7.13	6.349	2.22
9	-10.1429	54.233933	2009-12-15T19:36:00Z	Belmullet Wave Buoy Berth B	13.33	288.3	35.4	8.842119	7.22	6.452	2.15
10	-10.1429	54.233933	2009-12-15T20:06:00Z	Belmullet Wave Buoy Berth B	7.69	2.8	25.2	8.259191	6.92	6.25	2.13
11	-10.1429	54.233933	2009-12-15T20:36:00Z	Belmullet Wave Buoy Berth B	11.76	281.3	41.1	8.3589	6.91	6.25	2.13
12	-10.1429	54.233933	2009-12-15T21:06:00Z	Belmullet Wave Buoy Berth B	11.76	272.8	29	8.741701	7.23	6.452	2.18
13	-10.1429	54.233933	2009-12-15T21:36:00Z	Belmullet Wave Buoy Berth B	13.33	289.7	34	8.775845	7.22	6.452	2.14
14	-10.1429	54.233933	2009-12-15T22:06:00Z	Belmullet Wave Buoy Berth B	13.33	285.5	35.9	8.906202	7.24	6.452	2.11
15	-10.1429	54.233933	2009-12-15T22:36:00Z	Belmullet Wave Buoy Berth B	7.69	14.1	24.3	8.560669	7.18	6.452	2.17
16	-10.1429	54.233933	2009-12-15T23:06:00Z	Belmullet Wave Buoy Berth B	7.69	9.8	27.1	8.671747	7.27	6.557	2.1
17	-10.1429	54.233933	2009-12-15T23:36:00Z	Belmullet Wave Buoy Berth B	7.69	15.5	24.5	8.65815	7.19	6.452	1.98
18	-10.1429	54.233933	2009-12-16T00:06:00Z	Belmullet Wave Buoy Berth B	8.33	21.1	23.8	8.675851	7.23	6.557	1.97
19	-10.1429	54.233933	2009-12-16T00:36:00Z	Belmullet Wave Buoy Berth B	7.69	4.2	27.3	8.719723	7.23	6.452	1.95
20	-10.1429	54.233933	2009-12-16T01:06:00Z	Belmullet Wave Buoy Berth B	7.69	12.7	26.2	8.588437	7.23	6.557	1.89
21	-10.1429	54.233933	2009-12-16T01:36:00Z	Belmullet Wave Buoy Berth B	7.69	9.8	22.6	8.864164	7.42	6.667	2.03
22	-10.1429	54.233933	2009-12-16T02:06:00Z	Belmullet Wave Buoy Berth B	7.69	12.7	24.7	9.049387	7.34	6.557	1.93
23	-10.1429	54.233933	2009-12-16T02:36:00Z	Belmullet Wave Buoy Berth B	7.69	12.7	20.5	8.563532	7.05	6.25	1.91
24	-10.1429	54.233933	2009-12-16T03:06:00Z	Belmullet Wave Buoy Berth B	7.69	11.3	21	8.380185	7.02	6.349	1.93
25	-10.1429	54.233933	2009-12-16T03:36:00Z	Belmullet Wave Buoy Berth B	7.69	7	26.3	8.513842	6.82	6.061	1.81
26	-10.1429	54.233933	2009-12-16T04:06:00Z	Belmullet Wave Buoy Berth B	15.38	277	34.1	8.738696	6.98	6.154	1.89
27	-10.1429	54.233933	2009-12-16T04:36:00Z	Belmullet Wave Buoy Berth B	15.38	281.3	33.1	8.853807	6.96	6.061	1.86
28	-10.1429	54.233933	2009-12-16T05:06:00Z	Belmullet Wave Buoy Berth B	14.29	274.2	30.3	8.658287	6.83	5.97	1.73
29	-10.1429	54.233933	2009-12-16T05:36:00Z	Belmullet Wave Buoy Berth B	14.29	272.8	33.3	8.21816	6.52	5.797	1.93

Figure 3.2: Sample of the data gathered from the wave buoy Belmullet Berth B

3.1.1 Model forms of wave spectrum

Sea state can easily be influenced by factors that can reshape the wave characteristics of the region. These factors can be summarized as wave breaking, reflection and refraction conditions, the fetch length and the depth of the region, and the current magnitudes and directions. Based on these factors spectral models are developed with limitations depending on the sea state conditions, such as the deep-water conditions, fully developed sea conditions etc. Therefore, there are many models developed based on the spatial conditions and limitations that indicates the importance of significant wave height (H_s) and the peak period (T_p) validated for a given specific sea conditions. Together with the significant wave height and the peak period spectral models also influenced by wind or swell or a combination of both of them. Thus, each model due to their specific conditions and limitations can be worked out to generate their own fitting real spectra.

The Pierson-Moskowitz spectrum (Pierson and Moskowitz, 1964) and the observations made during the Joint North Sea Wave Project (JONSWAP) (Hasselmann et al., 1973) are the two famous spectrum models that value the real state sea conditions and reflect the energy potential at the open sea. Fig. (2.3) demonstrates the general difference between the wave spectrum curves of Pierson-Moskowitz and JONSWAP.

Pierson-Moskowitz model is the model that is mostly used for spectral analysis of the waves. This model is proposed for a fully developed sea where the fetch is unlimited. Further studies showed that this model correspond just partially to a fully developed sea condition. JONSWAP model is formulated as a modification of the Pierson-Moskowitz spectrum for a developing sea state in a fetch limited situation and is widely used in oceanography studies.

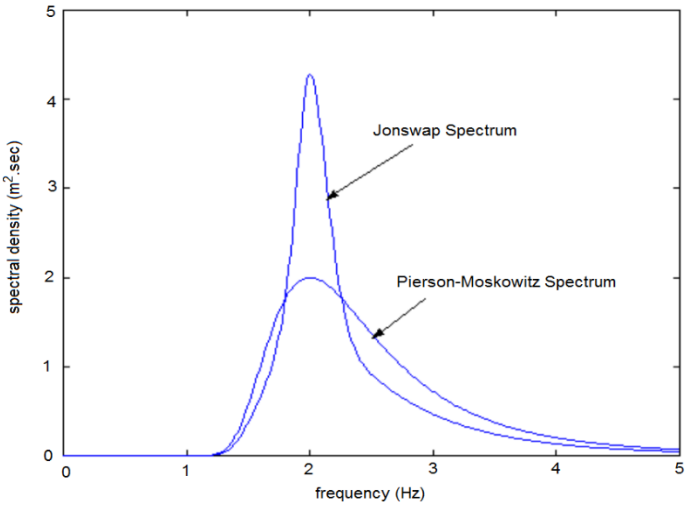

Figure 3.3: Pierson- Moskowitz and JONSWAP spectrum depicted graphically.

According to Recommended Practice DNV-RP-H103, April 2011; JONSWAP spectrum is modelized by the expression:

$$S_j(f) = A_y \, S_{PM}(f) \, \gamma^{\delta} \tag{2.7}$$

Where:

- f is the frequency
- $S_{PM}(f)$ is the Pierson Moskovitz spectrum and
  - $S_{PM}(f) = \frac{5}{16} H_s{}^2 (\frac{2\pi}{T_p})^4 f^{-5} exp^{(\frac{-5}{4} f (\frac{T_p}{2\pi})^{-4})}$
- A_γ is a normalizing factor and $A_\gamma = 1-0.287\ln(\gamma)$
- γ is a non-dimensional peak shape parameter
- $\delta = \exp\{(-0.5)[(f-f_p)/(\sigma f_p)]^2\}$ and f_p is the peak frequency
- σ = spectral width parameter
  - $\sigma = \sigma_a$ for $f \leq f_p$
  - $\sigma = \sigma_b$ for $f > f_p$

For an experimental data, using JONSWAP model, it is found that average values for the peak shape parameter is 3.3 ($\gamma = 3.3$). on the other hand, in order to calculate

spectral width parameter, the magnitude of σ_a and σ_b are given as 0.07 and 0.09, respectively. When γ is equal to 1, the JONSWAP model reduces to the spectrum model of Pierson-Moskowitz. When no values are given for the peak shape parameter (γ), the division of the peak frequency (Tp) over the square root of the significant wave height ($H_s^{0.5}$) should be studied; when:

- $(T_p / H_s^{0.5}) \leq 3.6 \rightarrow \gamma = 5$
- $(T_p / H_s^{0.5}) \geq 5 \rightarrow \gamma = 1$
- $3.6 < (T_p / H_s^{0.5}) < 5 \rightarrow \gamma = \exp(5.75\text{-}1.15(T_p / H_s^{0.5}))$

3.2 Number of occurrences of significant wave height and average wave period

The data gathered from Galway Bay and Belmullet wave energy test sites, specifically from the buoy "Bellmulet Berth B" which is placed offshore at the North Sea in the North-West side of Ireland, gives information about wave height and period over 9 years; from 2009 to 2018. The data related to the years 2009 and 2018 were excluded from this study and only years from 2010 to 2017 were taken into account as recordings related to those excluded years were not complete.

One can use these tables in order to have an idea over the wave climate that govern that particular location; the height and period at which the waves occur the most.

From the data the information about wave period were given as spectral wave period parameters; T_{m01} (mean wave period) and T_{m02} (mean zero crossing period). The wave periods (T_{m01} and T_{m02}) given in the data were estimated from the moments of the wave spectrum given by the wave buoy where T_{m01} represent the mean wave period using spectral moments of 0 and 1 and T_{m02} represent the mean wave period using spectral moments of 0 and 2. Although T_{m02}, which represent the mean zero up-crossing period, is the commonly used period in ocean studies, the author preferred to

get the average period (T_{av}) as an average value of T_{m01} and T_{m02}.

These two periods were used to relate an average wave period (T_{av}), where T_{av} will be given as:

$$T_{av} = \frac{T_{m01} + T_{m02}}{2} \tag{3.1}$$

During the analysis of the variable raw data, the average wave period for every single record is calculated based on Eq. (3.1). The number of wave occurrences as a function of the wave height and wave period with an increment of 0.5 meter for wave height and an increment of 1 second for wave period is also calculated. The increment for wave period was started from the lowest wave period recorded within that year; for example, in 2010 there was no wave record for a wave period value between 0 to 3 seconds. Thus, the counting of wave occurrence started from an interval of average wave period between 3 and 4 seconds. This was then followed by 4 and 5 seconds and so on with every time an increment of 1 second, until a wave period value where no wave is recorded. The significant wave height, given in data, represent the average of the highest third wave height and the wave period, which is given in terms of mean wave period and zero crossing period, are recorded by the buoy in a span time of 30 minutes.

Using the years 2010 to 2017 wave record information, the number of occurrences of waves as a function of wave height and period were calculated and presented through Table (3.1) to Table (3.8) for each year.

The given Tables (3.1) to (3.8) are representing the number of wave occurrence as a function of average wave period and wave height for every year under consideration. In these tables, each cell represented the number of wave occurring at a defined interval of wave height and wave period; for example the first column in Table (3.1) represented an average wave period interval of 3 to 4 seconds ($3 \leq P_{av} < 4$) and the

first line represented an interval of wave height of 0 to 0.5 seconds ($0 \leq H_s < 0.5$) and their intersection represented the cell where the number of wave occurring at those specific wave period and height was calculated.

Table 3.1: Resultant occurrences for wave periods and wave heights for the year 2011

Significant wave height, Hs (m) \ Average wave period, Tav (s)	3~4	4~5	5~6	6~7	7~8	8~9	9~10	10~11	11~12	12~13	13~14	SUM
0~0,5	0	0	0	0	0	0	0	0	0	0	0	0
0,5~1	24	170	298	170	83	28	0	0	0	0	0	773
1~1,5	0	380	724	896	567	241	23	0	0	0	0	2831
1,5~2	0	103	823	1086	845	453	50	7	0	0	0	3367
2~2,5	0	2	350	838	649	385	105	47	1	0	0	2377
2,5~3	0	0	98	650	767	471	148	32	1	0	0	2167
3~3,5	0	0	8	261	610	381	143	28	2	0	0	1433
3,5~4	0	0	0	73	395	233	98	10	5	0	0	814
4~4,5	0	0	0	14	196	182	53	11	0	0	0	456
4,5~5	0	0	0	0	75	136	57	9	0	0	0	277
5~5,5	0	0	0	0	8	93	43	5	0	0	0	149
5,5~6	0	0	0	0	1	28	51	7	0	0	0	87
6~6,5	0	0	0	0	0	13	56	6	2	0	0	77
6,5~7	0	0	0	0	0	0	26	19	4	2	0	51
7~7,5	0	0	0	0	0	0	6	17	0	5	0	28
7,5~8	0	0	0	0	0	0	2	12	2	0	0	16
8~8,5	0	0	0	0	0	0	2	5	2	2	0	11
8,5~9	0	0	0	0	0	0	2	4	5	4	1	16
9~9,5	0	0	0	0	0	0	0	4	2	3	0	9
9,5~10	0	0	0	0	0	0	0	7	0	0	0	7
10~11	0	0	0	0	0	0	0	0	2	0	0	2
11~12	0	0	0	0	0	0	0	1	3	0	0	4
12~14	0	0	0	0	0	0	0	0	1	4	0	5
SUM	24	655	2301	3988	4196	2644	865	231	32	20	1	

Table 3.2: Resultant occurrences for wave periods and wave heights for the year 2011

Significant wave height, Hs (m) \ Average wave period, Tav (s)	2~3	3~4	4~5	5~6	6~7	7~8	8~9	9~10	10~11	11~12	12~13	13~14	14~16	SUM
0~0,5	0	0	0	0	0	0	0	0	0	0	0	0	0	0
0,5~1	2	67	131	181	134	26	4	0	0	0	0	0	0	545
1~1,5	0	0	146	500	501	274	125	10	0	0	0	0	0	1556
1,5~2	0	0	46	524	533	385	339	205	35	3	0	0	0	2070
2~2,5	0	0	3	282	549	499	248	132	19	0	0	0	0	1732
2,5~3	0	0	0	63	632	614	309	134	17	1	0	0	0	1770
3~3,5	0	0	0	1	373	553	323	178	44	16	2	0	0	1490
3,5~4	0	0	0	0	89	566	312	179	82	13	2	0	0	1243
4~4,5	0	0	0	0	5	387	442	149	100	16	0	0	0	1099
4,5~5	0	0	0	0	0	148	432	175	54	18	0	2	1	830
5~5,5	0	0	0	0	0	48	354	146	59	43	4	1	4	659
5,5~6	0	0	0	0	0	6	209	127	39	44	12	3	4	444
6~6,5	0	0	0	0	0	0	66	96	28	15	12	4	3	224
6,5~7	0	0	0	0	0	0	19	82	32	11	9	2	5	160
7~7,5	0	0	0	0	0	0	4	72	25	7	1	0	1	110
7,5~8	0	0	0	0	0	0	1	55	47	8	0	0	0	111
8~8,5	0	0	0	0	0	0	0	23	24	12	0	0	0	59
8,5~9	0	0	0	0	0	0	0	7	31	5	0	0	0	43
9~9,5	0	0	0	0	0	0	0	2	11	3	0	0	0	16
9,5~10	0	0	0	0	0	0	0	0	16	4	0	0	0	20
10~11	0	0	0	0	0	0	0	0	4	16	0	0	0	20
11~12	0	0	0	0	0	0	0	0	0	5	1	0	0	6
12~14	0	0	0	0	0	0	0	0	0	3	3	0	0	6
SUM	2	67	326	1551	2816	3506	3187	1772	667	243	46	12	18	

Table 3.3: Resultant occurrences for wave periods and wave heights for the year 2012

Significant wave height, Hs (m) \ Average wave period, Tav (s)	3~4	4~5	5~6	6~7	7~8	8~9	9~10	10~11	11~12	12~13	13~20	SUM
0~0,5	0	9	7	0	0	0	0	0	0	0	0	16
0,5~1	23	244	270	187	50	2	0	0	0	0	0	776
1~1,5	3	237	670	539	270	83	0	0	0	0	0	1802
1,5~2	0	92	590	634	441	236	13	0	0	0	0	2006
2~2,5	0	1	375	913	616	317	85	4	0	0	0	2311
2,5~3	0	0	57	739	704	382	144	19	2	0	0	2047
3~3,5	0	0	0	388	717	395	109	27	1	0	0	1637
3,5~4	0	0	0	137	698	428	151	14	6	0	0	1434
4~4,5	0	0	0	4	322	358	138	2	0	0	0	824
4,5~5	0	0	0	1	88	300	133	21	0	0	0	543
5~5,5	0	0	0	0	8	235	104	15	0	0	0	362
5,5~6	0	0	0	0	4	137	101	12	1	0	0	255
6~6,5	0	0	0	0	0	63	77	15	0	0	0	155
6,5~7	0	0	0	0	0	17	92	15	0	0	0	124
7~7,5	0	0	0	0	0	1	34	24	5	0	0	64
7,5~8	0	0	0	0	0	0	23	19	16	0	0	58
8~8,5	0	0	0	0	0	0	25	13	6	3	0	47
8,5~9	0	0	0	0	0	0	8	14	15	2	0	39
9~9,5	0	0	0	0	0	0	0	6	14	4	0	24
9,5~10	0	0	0	0	0	0	0	0	6	7	0	13
10~11	0	0	0	0	0	0	0	0	0	4	0	4
11~12	0	0	0	0	0	0	0	0	0	1	0	1
12~14	0	0	0	0	0	0	0	0	0	0	0	0
SUM	26	583	1969	3542	3918	2954	1237	220	72	21	0	

Table 3.4: Resultant occurrences for wave periods and wave heights for the year 2013

Significant wave height, Hs (s) \ Average wave period, Tav (s)	3~4	4~5	5~6	6~7	7~8	8~9	9~10	10~11	11~12	12~13	13~14	SUM
0~0,5	23	29	52	33	0	0	0	0	0	0	0	137
0,5~1	72	251	441	355	117	6	0	0	0	0	0	1242
1~1,5	11	225	619	457	300	37	0	0	0	0	0	1649
1,5~2	0	59	519	563	303	130	14	0	0	0	0	1588
2~2,5	0	3	216	544	323	109	55	0	0	0	0	1250
2,5~3	0	0	63	519	613	300	57	0	1	0	0	1553
3~3,5	0	0	6	238	551	168	82	1	2	0	0	1048
3,5~4	0	0	0	49	511	223	84	25	2	0	0	894
4~4,5	0	0	0	0	191	247	52	19	0	1	0	510
4,5~5	0	0	0	0	97	238	108	11	8	3	0	465
5~5,5	0	0	0	0	15	217	151	8	12	4	0	407
5,5~6	0	0	0	0	4	112	188	27	3	14	0	348
6~6,5	0	0	0	0	0	55	96	53	0	4	2	210
6,5~7	0	0	0	0	0	24	101	58	5	0	0	188
7~7,5	0	0	0	0	0	0	73	60	2	0	0	135
7,5~8	0	0	0	0	0	0	36	51	7	0	0	94
8~8,5	0	0	0	0	0	0	9	37	16	0	0	62
8,5~9	0	0	0	0	0	0	2	25	17	0	0	44
9~9,5	0	0	0	0	0	0	0	11	7	1	0	19
9,5~10	0	0	0	0	0	0	0	6	12	2	0	20
10~11	0	0	0	0	0	0	0	1	19	4	0	24
11~12	0	0	0	0	0	0	0	0	0	10	0	10
12~14	0	0	0	0	0	0	0	0	0	0	0	0
SUM	106	567	1916	2758	3025	1866	1108	393	113	43	2	

Table 3.5: Resultant occurrences for wave periods and wave heights for the year 2014

Significant wave height, Hs (m) \ Average wave period, Tav (s)	3~4	4~5	5~6	6~7	7~8	8~9	9~10	10~11	11~12	12~13	13~14	SUM
0~0,5	1	4	10	1	0	0	0	0	0	0	0	16
0,5~1	68	479	677	557	118	25	3	1	0	0	0	1928
1~1,5	5	338	794	710	324	144	12	2	3	0	0	2332
1,5~2	0	40	797	493	613	134	60	8	3	4	0	2152
2~2,5	0	2	334	785	581	291	39	36	11	4	0	2083
2,5~3	0	0	50	651	581	323	95	35	3	5	0	1743
3~3,5	0	0	0	242	603	287	127	40	2	0	0	1301
3,5~4	0	0	0	32	608	413	110	56	4	0	0	1223
4~4,5	0	0	0	6	378	524	255	46	3	0	0	1212
4,5~5	0	0	0	0	135	384	189	54	3	0	0	765
5~5,5	0	0	0	0	19	221	177	36	2	0	0	455
5,5~6	0	0	0	0	6	98	141	46	10	2	0	303
6~6,5	0	0	0	0	1	37	115	49	12	7	0	221
6,5~7	0	0	0	0	0	5	93	51	6	3	0	158
7~7,5	0	0	0	0	0	0	38	39	3	0	0	80
7,5~8	0	0	0	0	0	0	16	34	3	1	0	54
8~8,5	0	0	0	0	0	0	5	23	9	4	1	42
8,5~9	0	0	0	0	0	0	1	18	2	2	0	23
9~9,5	0	0	0	0	0	0	0	15	0	0	0	15
9,5~10	0	0	0	0	0	0	0	5	7	0	0	12
10~11	0	0	0	0	0	0	0	1	10	1	0	12
11~12	0	0	0	0	0	0	0	0	6	13	0	19
12~13	0	0	0	0	0	0	0	0	0	11	4	15
13~14	0	0	0	0	0	0	0	0	0	1	3	4
SUM	74	863	2662	3477	3967	2886	1476	595	102	58	8	

Table 3.6: Resultant occurrences for wave periods and wave heights for the year 2015

Significant wave height, Hs (m) \ Average wave period, Tav (s)	3~4	4~5	5~6	6~7	7~8	8~9	9~10	10~11	11~12	12~13	13~14	SUM
0~0,5	0	2	0	0	0	0	0	0	0	0	0	2
0,5~1	20	211	176	169	114	9	0	0	0	0	0	699
1~1,5	10	271	697	573	315	73	5	0	0	0	0	1944
1,5~2	0	46	564	450	431	283	39	16	4	0	0	1833
2~2,5	0	4	221	691	531	306	111	32	8	3	0	1907
2,5~3	0	0	37	522	636	377	95	22	8	0	0	1697
3~3,5	0	0	0	273	476	303	95	22	7	3	0	1179
3,5~4	0	0	0	136	591	253	132	20	17	1	0	1150
4~4,5	0	0	0	14	514	346	146	39	7	3	0	1069
4,5~5	0	0	0	0	262	457	151	57	4	1	0	932
5~5,5	0	0	0	0	74	441	196	45	9	1	0	766
5,5~6	0	0	0	0	5	255	226	60	13	2	0	561
6~6,5	0	0	0	0	0	103	213	96	13	10	0	435
6,5~7	0	0	0	0	0	36	200	82	15	9	1	343
7~7,5	0	0	0	0	0	2	183	70	5	9	0	269
7,5~8	0	0	0	0	0	0	86	60	8	0	0	154
8~8,5	0	0	0	0	0	0	38	82	13	0	0	133
8,5~9	0	0	0	0	0	0	6	61	11	2	0	80
9~9,5	0	0	0	0	0	0	2	39	21	3	0	65
9,5~10	0	0	0	0	0	0	0	10	20	3	0	33
10~11	0	0	0	0	0	0	0	0	22	8	1	31
11~12	0	0	0	0	0	0	0	1	12	6	0	19
12~14	0	0	0	0	0	0	0	0	2	2	0	4
SUM	30	534	1695	2828	3949	3244	1924	814	219	66	2	

Table 3.7: Resultant occurrences for wave periods and wave heights for the year 2016

Significant wave height, Hs (m) \ Average wave period, Tav (s)	3~4	4~5	5~6	6~7	7~8	8~9	9~10	10~11	11~12	12~13	13~14	SUM
0~0,5	1	1	0	0	0	0	0	0	0	0	0	2
0,5~1	20	231	334	315	150	3	0	0	0	0	0	1053
1~1,5	19	349	873	627	450	140	7	1	0	0	0	2466
1,5~2	0	101	815	944	474	311	117	11	0	0	0	2773
2~2,5	0	2	460	860	592	342	85	10	0	0	0	2351
2,5~3	0	0	118	875	761	460	110	37	7	0	0	2368
3~3,5	0	0	3	366	785	483	135	54	18	0	0	1844
3,5~4	0	0	0	89	590	401	142	28	2	1	0	1253
4~4,5	0	0	0	5	290	330	131	67	10	0	0	833
4,5~5	0	0	0	0	123	288	192	55	22	0	0	680
5~5,5	0	0	0	0	16	183	147	65	14	3	0	428
5,5~6	0	0	0	0	2	109	142	65	14	4	0	336
6~6,5	0	0	0	0	0	55	143	60	11	9	1	279
6,5~7	0	0	0	0	0	18	153	55	19	5	3	253
7~7,5	0	0	0	0	0	1	70	86	7	1	1	166
7,5~8	0	0	0	0	0	0	31	75	17	0	1	124
8~8,5	0	0	0	0	0	0	12	66	17	3	0	98
8,5~9	0	0	0	0	0	0	3	33	13	4	0	53
9~9,5	0	0	0	0	0	0	3	17	12	5	0	37
9,5~10	0	0	0	0	0	0	0	2	7	3	0	12
10~11	0	0	0	0	0	0	0	3	9	2	0	14
11~12	0	0	0	0	0	0	0	0	5	3	0	8
12~13	0	0	0	0	0	0	0	0	1	11	1	13
13~14	0	0	0	0	0	0	0	0	0	2	1	3
SUM	40	684	2603	4081	4233	3124	1623	790	205	56	8	

Table 3.8: Resultant occurrences for wave periods and wave heights for the year 2017

Significant wave height, Hs (m) \ Average wave period, Tav (s)	3~4	4~5	5~6	6~7	7~8	8~9	9~10	10~11	11~12	12~13	13~14	SUM
0~0,5	0	0	0	0	0	0	0	0	0	0	0	0
0,5~1	21	222	280	182	108	2	0	0	0	0	0	815
1~1,5	2	396	793	670	234	58	0	0	0	0	0	2153
1,5~2	0	75	1018	1098	540	68	33	0	0	0	0	2832
2~2,5	0	1	555	1182	677	287	77	6	0	0	0	2785
2,5~3	0	0	75	1034	834	391	148	37	4	0	0	2523
3~3,5	0	0	1	460	843	358	129	52	14	0	0	1857
3,5~4	0	0	0	69	731	428	135	19	5	1	0	1388
4~4,5	0	0	0	3	409	447	171	21	7	0	0	1058
4,5~5	0	0	0	1	153	368	123	28	2	0	0	675
5~5,5	0	0	0	0	22	241	102	51	8	0	0	424
5,5~6	0	0	0	0	4	125	87	64	14	0	0	294
6~6,5	0	0	0	0	1	51	76	29	41	2	0	200
6,5~7	0	0	0	0	0	20	83	11	31	3	0	148
7~7,5	0	0	0	0	0	7	50	29	7	15	0	108
7,5~8	0	0	0	0	0	0	27	40	1	2	0	70
8~8,5	0	0	0	0	0	0	7	37	3	5	0	52
8,5~9	0	0	0	0	0	0	0	21	4	0	0	25
9~9,5	0	0	0	0	0	0	0	3	16	0	0	19
9,5~10	0	0	0	0	0	0	0	1	12	1	0	14
10~11	0	0	0	0	0	0	0	0	5	1	0	6
11~12	0	0	0	0	0	0	0	0	1	1	0	2
12~14	0	0	0	0	0	0	0	0	0	0	0	0
SUM	23	694	2722	4699	4556	2851	1248	449	175	31	0	

3.3 Monthly average sea state

In order for a WEC and/or wave power generator to be efficient and operate on optimal conditions, the wave climate should carefully be studied and define how the sea state vary in time. A monthly average of significant wave height and period, over a year, is a good estimate over a year in order to understand the sea state governing the location.

Traditionally, the significant wave height or period is typically defined as four times their standard deviation or as four times the square root of the zeroth-order moment; H_{m0} for wave height and T_{m0} for wave period of the wave spectrum. However, the significant wave height H_s as well as the significant wave period T_s can be calculated by obtaining the average of the highest third of wave height and wave period data. Yet, the magnitude resulted from these two methods show a difference of only few percent.

In this study, the last method which consist of the average of the highest third of data has been used. Using the data, for each year, an average of the highest third

records of wave height and wave period data of each month is obtained; Table (3.9 & 3.10).

As it was expected the maximum significant wave heights at the region occur in winter months whereas minimum wave heights occur in summer seasons. Parallel behavior is also observed for wave periods.

Table 3.9: Monthly significant wave height for all the years. (The max & min values are colored)

	Significant wave height values (m)							
Time	2010	2011	2012	2013	2014	2015	2016	2017
Jan	3.60	4.26	6.41	5.74	5.94	8.04	6.01	5.42
Feb	3.53	6.19	4.19	9.54	5.76	6.52	7.07	5.33
Mar	3.53	4.80	4.73	-	5.16	6.25	5.12	5.02
Apr	3.25	3.97	3.52	-	3.38	3.80	4.11	3.68
May	2.61	4.55	1.94	5.14	3.12	4.08	3.04	2.50
Jun	2.46	3.05	2.33	3.01	1.62	3.41	2.72	3.17
July	3.51	2.71	-	2.38	2.52	2.54	2.59	2.97
Aug	2.50	2.56	2.64	3.06	2.99	3.28	3.21	2.68
Sep	3.35	4.83	4.38	4.49	2.96	1.71	3.82	4.15
Oct	4.39	5.26	3.50	3.93	5.05	4.19	3.19	4.53
Nov	5.31	5.31	4.56	5.32	3.81	5.95	4.50	4.85
Dec	3.38	7.19	5.14	6.87	6.96	5.96	6.64	5.71

Table 3.10: Monthly significant wave period for all the years. (The max & min values are colored)

	Significant wave period values (sec)							
Time	2010	2011	2012	2013	2014	2015	2016	2017
Jan	8.90	9.64	9.47	10.12	10.07	10.55	10.09	9.42
Feb	9.64	11.28	8.81	11.01	9.65	9.91	10.21	9.90
Mar	8.52	9.49	9.56	-	9.66	9.80	9.48	9.47
Apr	8.22	9.46	7.84	-	8.38	9.12	9.02	8.62
May	7.64	8.21	7.28	9.35	7.62	8.19	7.76	7.67
Jun	7.84	7.92	7.24	7.73	6.68	7.63	7.45	7.52
July	7.66	7.42	-	7.39	6.97	6.90	6.79	7.33
Aug	6.77	7.06	7.19	7.47	7.16	7.93	7.37	6.98
Sep	8.78	8.44	8.51	8.78	8.84	8.03	8.15	8.28
Oct	8.69	8.87	8.41	8.19	8.90	9.29	9.19	8.42
Nov	9.27	9.37	9.06	9.18	9.20	9.26	8.83	9.06
Dec	8.75	9.98	9.14	9.99	10.12	9.67	10.30	9.53

The maximum and minimum significant period and wave height that may occur in a year are represented in graphs as shown in Figure (3.3 & 3.4).

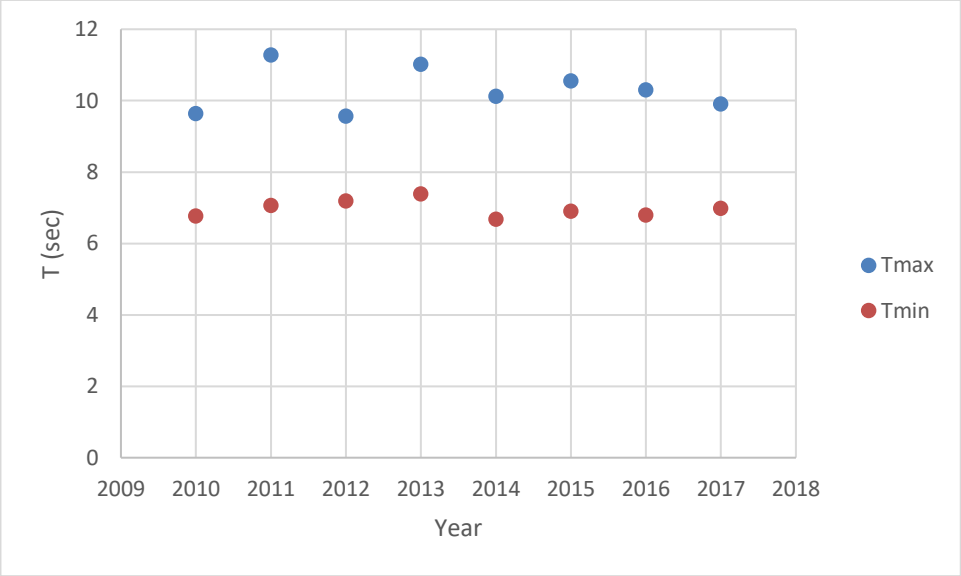

Figure 3.4: The maximum and minimum significant wave period that may occur in a year

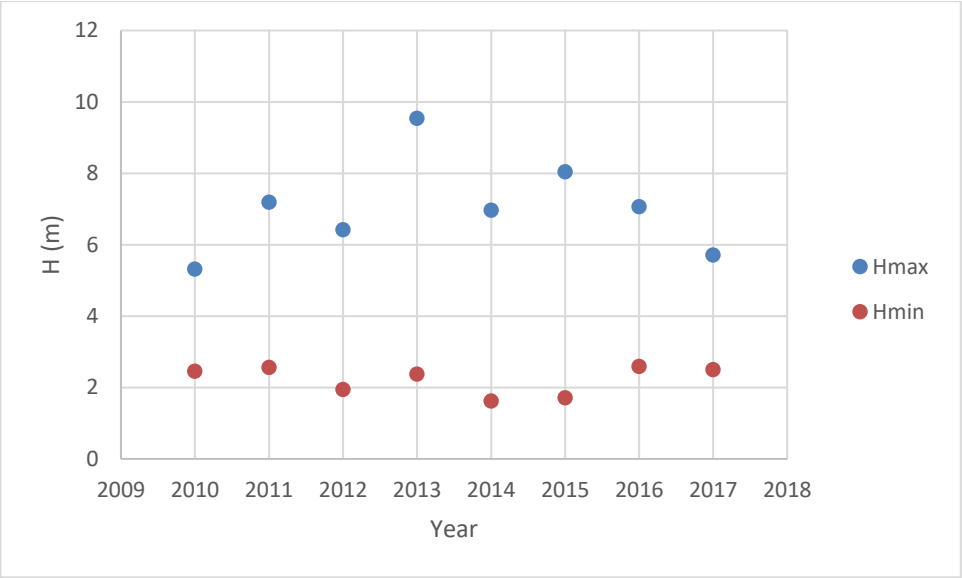

Figure 3.5: The maximum and minimum significant wave height that may occur in a year

3.4 Wave direction

The directional characteristics of wave climate are an important factor when dealing with both coastal and offshore structures like breakwater and WEC. When the structure is placed front to the direction of propagation of waves, this latter receives the full impact of the wave and therefore, the structure will work more efficiently. As an engineer, it is not useful to know the direction of propagation of waves which does not carry an important energy. Only most energetic waves are important when studying a location for the purpose of extracting energy and power in the case of a WEC structure or dissipate the waves that may have a considerable impact on the Ireland coast in the case of floating breakwater structure. The records about peak wave direction are the information which is most used by engineers when one want to put a structure into the sea. That is because peak wave direction represents the direction of the most energetic waves.

The data provide directions of waves as a decimal degrees values. These directions have been changed to cardinal degrees in order to be more understandable in a wave

rose diagram. The wave rose diagrams of the study area is given through Figures 3.5 to 3.12. at the same order the percentage of occurrence of wave heights depending on their direction for each year is given in Tables 3.11 to 3.18

Table 3.11: Percentage of wave heights depending to their directions for 2010

H (m)	N	NE	E	SE	S	SW	W	NW
0-1	1%	0%	0%	0%	0%	0%	2%	2%
1-2	11%	0%	0%	0%	0%	1%	17%	12%
2-3	9%	0%	0%	0%	0%	1%	12%	8%
3-4	4%	0%	0%	0%	0%	0%	7%	4%
4-5	1%	0%	0%	0%	0%	0%	3%	1%
5-6	1%	0%	0%	0%	0%	0%	1%	0%
6-7	0%	0%	0%	0%	0%	0%	0%	0%
>7	0%	0%	0%	0%	0%	0%	0%	0%

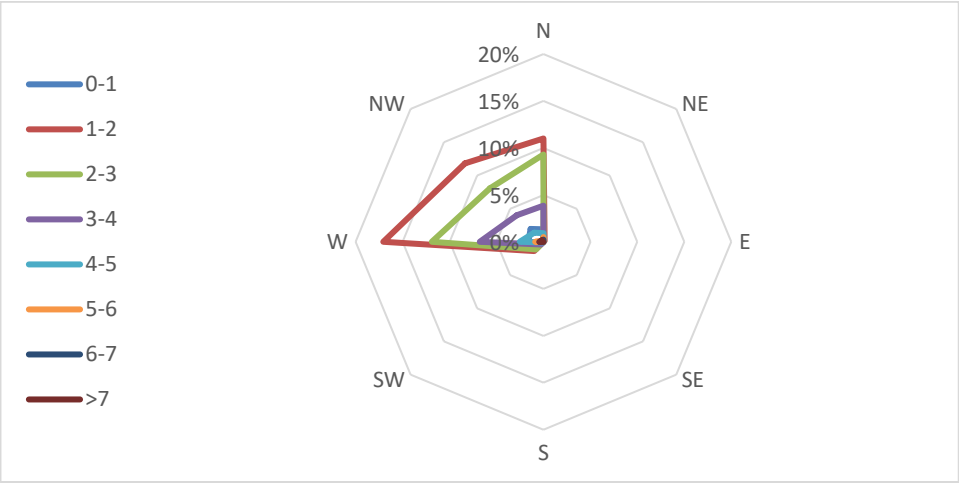

Figure 3.6: Main wave direction distribution and related wave height for 2010

Table 3.12: Percentage of wave heights depending to their directions for 2011

H (m)	N	NE	E	SE	S	SW	W	NW
0-1	0%	0%	0%	0%	0%	0%	2%	2%
1-2	2%	0%	0%	0%	0%	1%	12%	10%
2-3	3%	0%	0%	0%	0%	1%	11%	9%
3-4	2%	0%	0%	0%	0%	0%	8%	9%
4-5	1%	0%	0%	0%	0%	0%	6%	7%
5-6	0%	0%	0%	0%	0%	0%	4%	4%
6-7	0%	0%	0%	0%	0%	0%	1%	2%
>7	0%	0%	0%	0%	0%	0%	1%	2%

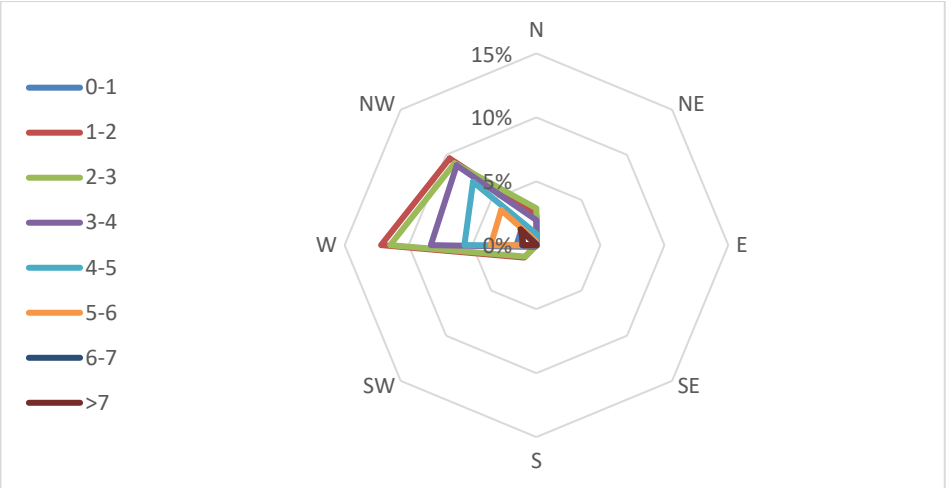

Figure 3.7: Main wave direction distribution and related wave height for 2011

Table 3.13: Percentage of wave heights depending to their directions for 2012

H (m)	N	NE	E	SE	S	SW	W	NW
0-1	1%	0%	0%	0%	0%	0%	2%	2%
1-2	7%	0%	0%	0%	0%	1%	11%	7%
2-3	5%	0%	0%	0%	0%	1%	13%	11%
3-4	2%	0%	0%	0%	0%	0%	10%	9%
4-5	1%	0%	0%	0%	0%	0%	3%	5%
5-6	1%	0%	0%	0%	0%	0%	1%	2%
>6	0%	0%	0%	0%	0%	0%	1%	2%

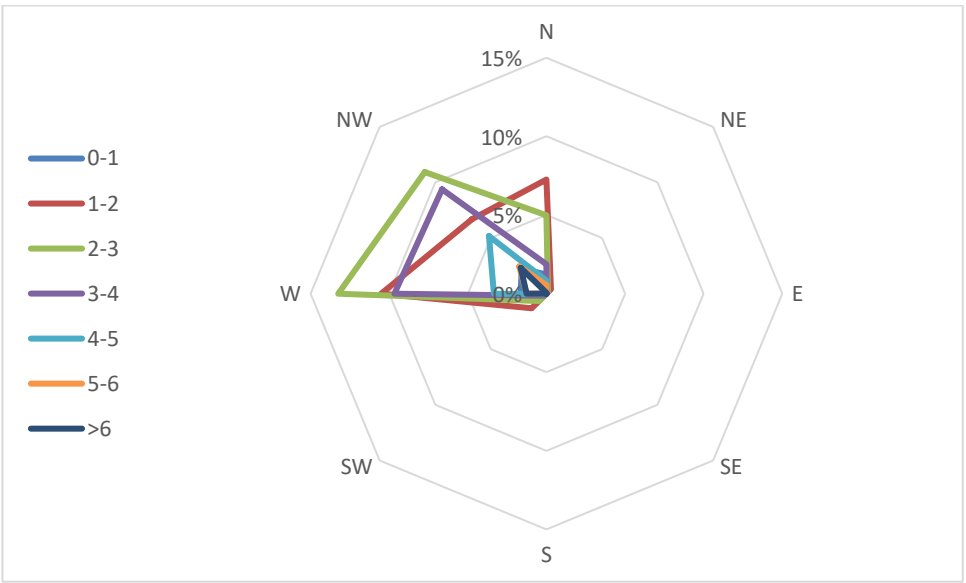

Figure 3.8: Main wave direction distribution and related wave height for 2012

Table 3.14: Percentage of wave heights depending to their directions for 2013

H(m)	N	NE	E	SE	S	SW	W	NW
0-1	0%	0%	0%	0%	0%	2%	7%	2%
1-2	3%	0%	0%	0%	0%	3%	13%	8%
2-3	3%	0%	0%	0%	0%	1%	9%	11%
3-4	1%	0%	0%	0%	0%	0%	6%	8%
4-5	1%	0%	0%	0%	0%	0%	3%	4%
5-6	1%	0%	0%	0%	0%	0%	2%	3%
>6	1%	0%	0%	0%	0%	0%	2%	4%

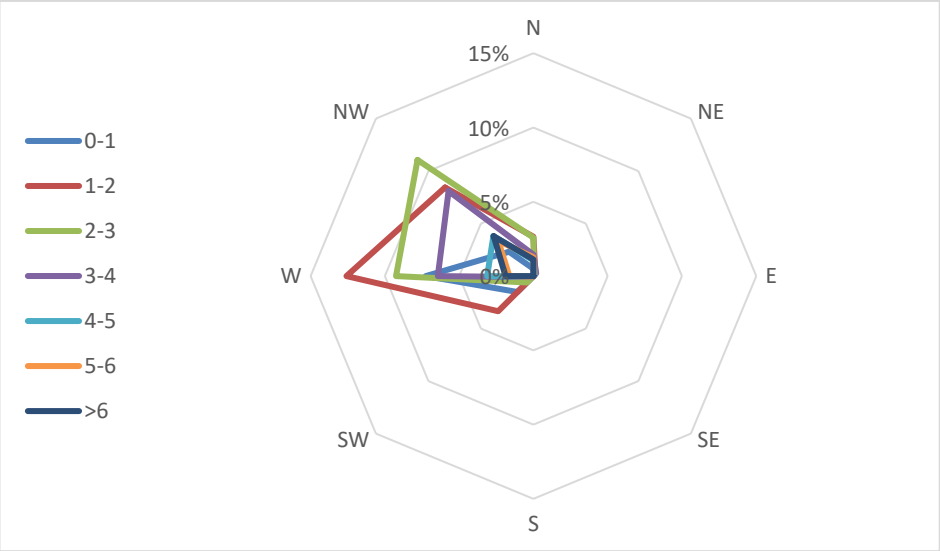

Figure 3.9: Main wave direction distribution and related wave height for 2013

Table 3.15: Percentage of wave heights depending to their directions for 2014

H(m)	N	NE	E	SE	S	SW	W	NW
0-1	3%	0%	0%	0%	0%	1%	5%	3%
1-2	5%	0%	0%	0%	0%	4%	12%	7%
2-3	3%	0%	0%	0%	0%	4%	10%	7%
3-4	2%	0%	0%	0%	0%	1%	6%	7%
4-5	2%	0%	0%	0%	0%	1%	3%	6%
5-6	1%	0%	0%	0%	0%	0%	1%	3%
6-7	0%	0%	0%	0%	0%	0%	0%	2%
>7	0%	0%	0%	0%	0%	0%	0%	2%

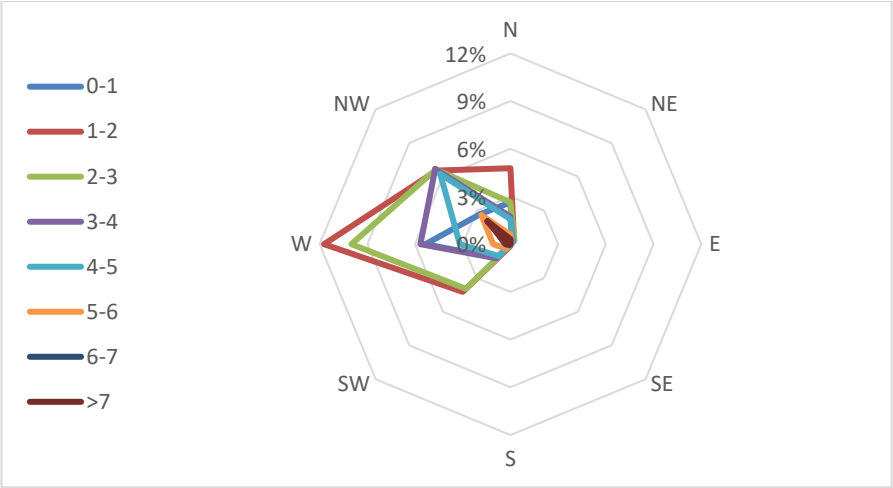

Figure 3.10: Main wave direction distribution and related wave height for 2014

Table 3.16: Percentage of wave heights depending to their directions for 2015

H(m)	N	NE	E	SE	S	SW	W	NW
0-1	1%	0%	0%	0%	0%	0%	1%	3%
1-2	3%	0%	0%	0%	0%	2%	10%	9%
2-3	2%	0%	0%	0%	0%	1%	11%	10%
3-4	1%	0%	0%	0%	0%	0%	7%	7%
4-5	0%	0%	0%	0%	0%	0%	7%	6%
5-6	0%	0%	0%	0%	0%	0%	5%	3%
6-7	0%	0%	0%	0%	0%	0%	2%	3%
>7	0%	0%	0%	0%	0%	0%	2%	3%

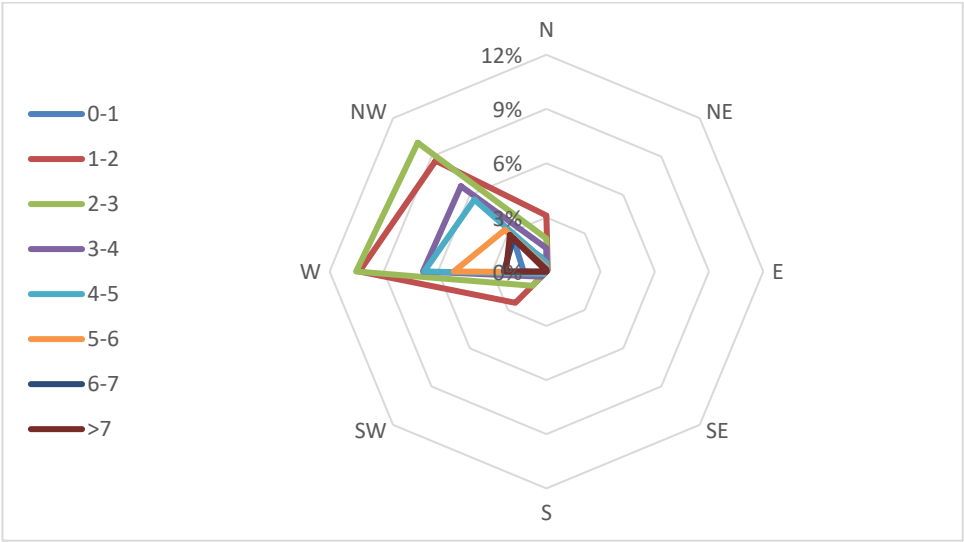

Figure 3.11: Main wave direction distribution and related wave height for 2015

Table 3.17: Percentage of wave heights depending to their directions for 2016

H(m)	N	NE	E	SE	S	SW	W	NW
0-1	1%	0%	0%	0%	0%	1%	3%	2%
1-2	7%	0%	0%	0%	0%	2%	15%	6%
2-3	4%	0%	0%	0%	0%	1%	14%	8%
3-4	1%	0%	0%	0%	0%	0%	10%	6%
4-5	0%	0%	0%	0%	0%	0%	5%	4%
5-6	0%	0%	0%	0%	0%	0%	2%	2%
6-7	0%	0%	0%	0%	0%	0%	1%	2%
>7	0%	0%	0%	0%	0%	0%	1%	2%

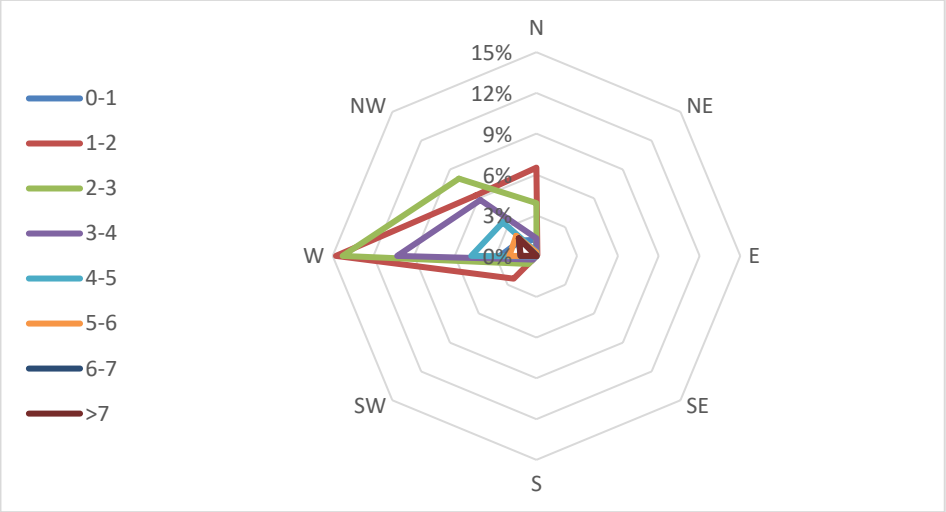

Figure 3.12: Main wave direction distribution and related wave height for 2016

Table 3.18: Percentage of wave heights depending to their directions for 2017

H(m)	N	NE	E	SE	S	SW	W	NW
0-1	1%	0%	0%	0%	0%	0%	2%	1%
1-2	5%	0%	0%	0%	0%	1%	13%	9%
2-3	4%	0%	0%	0%	0%	1%	16%	10%
3-4	1%	0%	0%	0%	0%	1%	10%	7%
4-5	1%	0%	0%	0%	0%	0%	4%	4%
5-6	0%	0%	0%	0%	0%	0%	2%	2%
6-7	0%	0%	0%	0%	0%	0%	1%	1%
>7	0%	0%	0%	0%	0%	0%	0%	1%

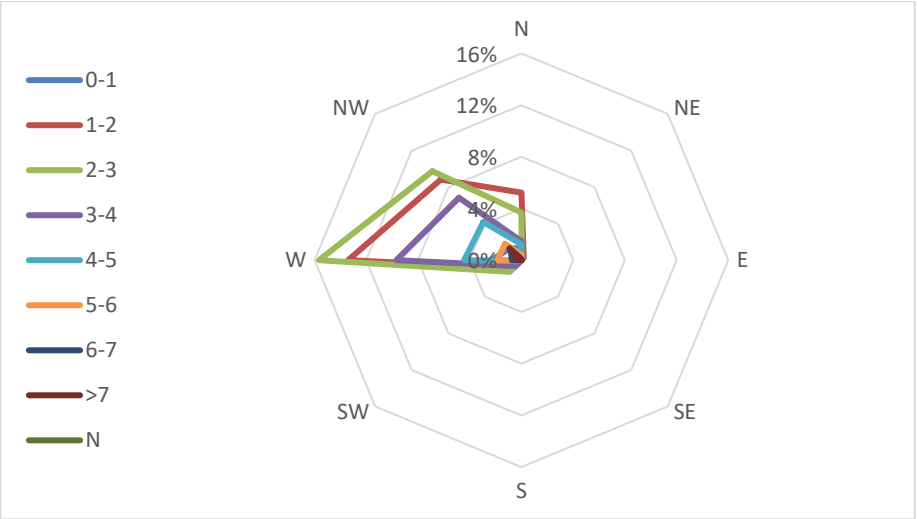

Figure 3.13: Main wave direction distribution and related wave height for 2017

The results indicate that the dominant wave directions around the study region is from West and North-West directions. There are waves approaching from North but not as much and effective as the waves approaching from West and North West.

Chapter 4

RESULTS AND DISCUSSIONS

4.1 Probability of occurrence

The data organized in Tables 3.1 to 3.8 can be used to calculate the probability of occurrence of wave height and wave period. Probability of occurrence analyses are performed for the years starting with 2010 up to 2017.

The Rayleigh probability density function, as was discussed in Chapter 2, Eq. (2.3), is used to perform the analysis. Based on the Tables 3.1 to 3.8 it is shown that there exist a constant interval between each significant wave height and wave period. Therefore, the average of each interval is used in order to have a specific value to be used in Eq. (2.3). As explained in Chapter 2, using the same equation, H and H_{rms} are replaced with period values T and T_{rms}. This has helped to calculate the probability of occurrence with respect to the wave period. The summation of all occurrences in each significant wave height interval independently of average wave period and summation of all occurrences in each average wave period interval independently of significant wave height were gathered for the use of Eq. (2.4). The summation of occurrences can be seen, highlighted with blue, on tables 3.1 to 3.8; horizontally for average wave period and vertically for significant wave height.

Using Eq. (2.4), root mean square of significant wave height (H_{rms}) and the average wave period root mean square (T_{rms}) is derived for each year as given in Table (4.1)

Figures 4.1 to 4.16 summarizes the results of the probability of occurrence of significant wave height and period for each year.

Table 4.1: Root mean square wave height and wave period for all the considered years

Year	H_{rms} (m)	T_{rms} (s)
2010	2.64	7.27
2011	3.54	7.87
2012	3.19	7.43
2013	3.39	7.43
2014	3.19	7.46
2015	3.85	7.76
2016	3.32	7.57
2017	3.16	7.37

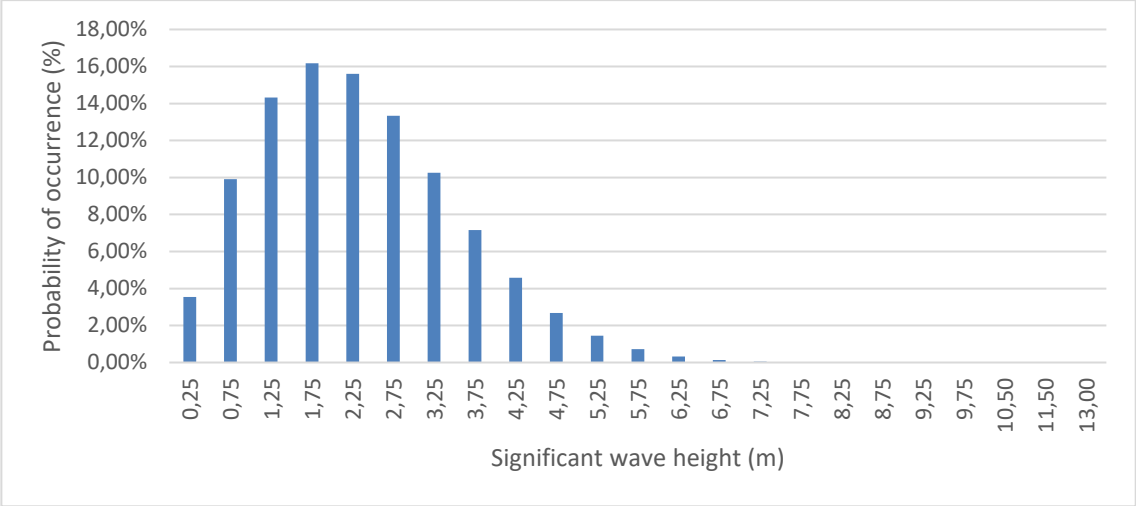

Figure 4.1: Probability of occurrence of significant wave height for 2010

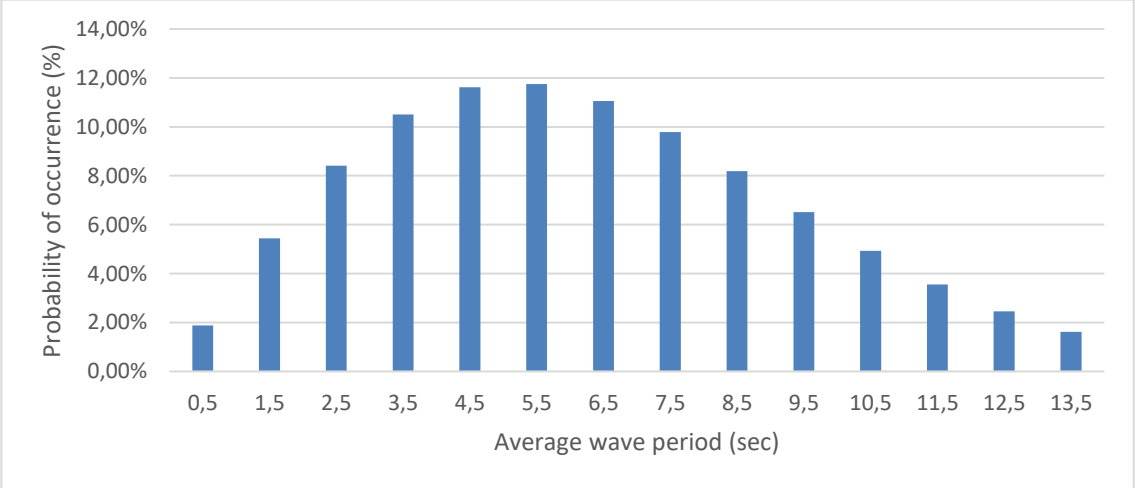

Figure 4.2: Probability of occurrence of average wave period for 2010

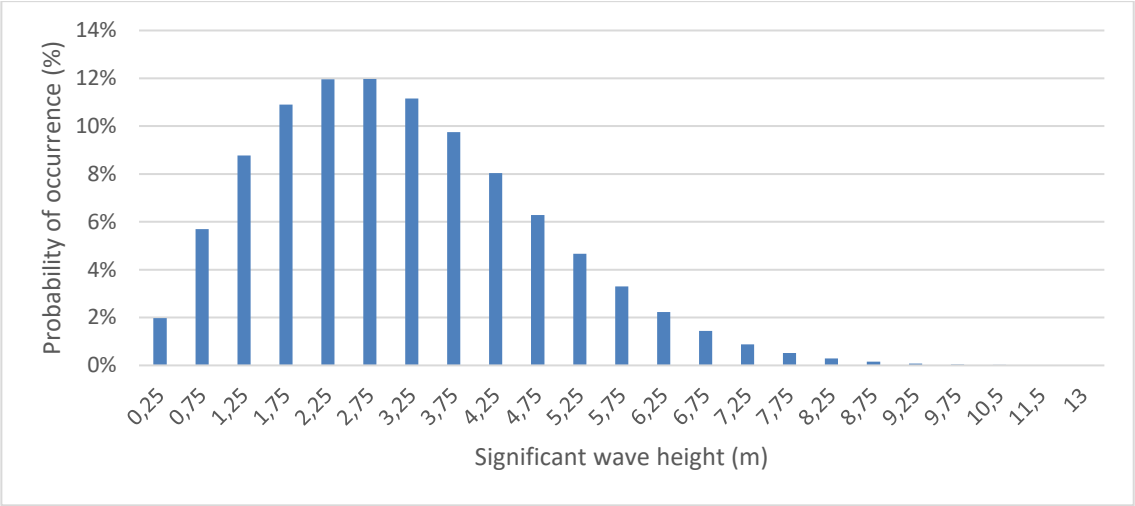

Figure 4.3: Probability of occurrence of significant wave height for 2011

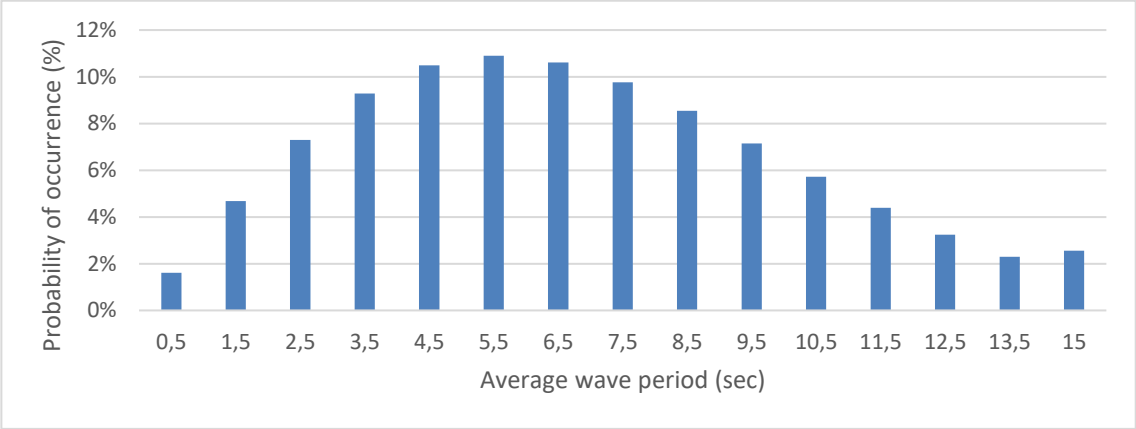

Figure 4.4: Probability of occurrence of average wave period for 2011

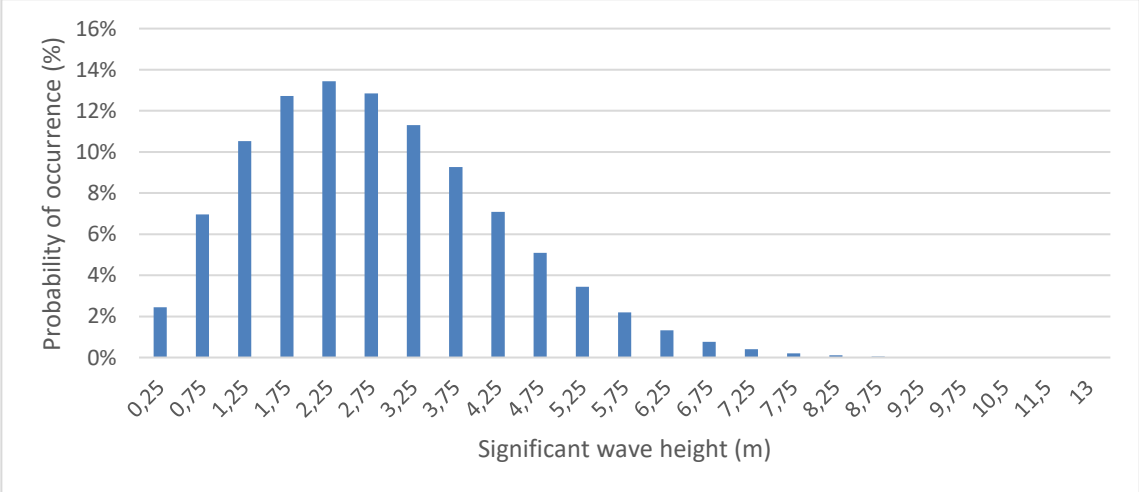

Figure 4.5: Probability of occurrence of significant wave height for 2012

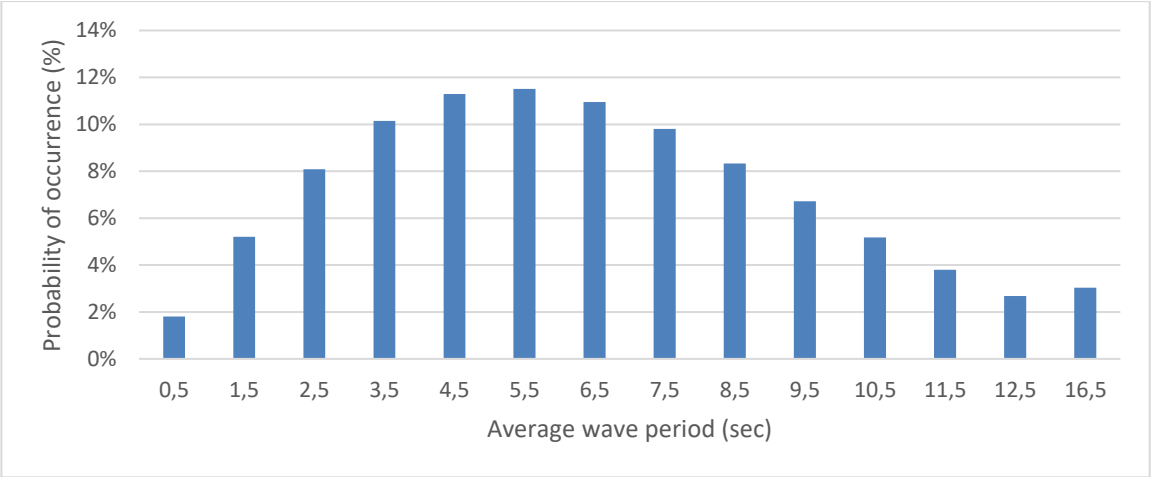

Figure 4.6: Probability of occurrence of average wave period for 2012

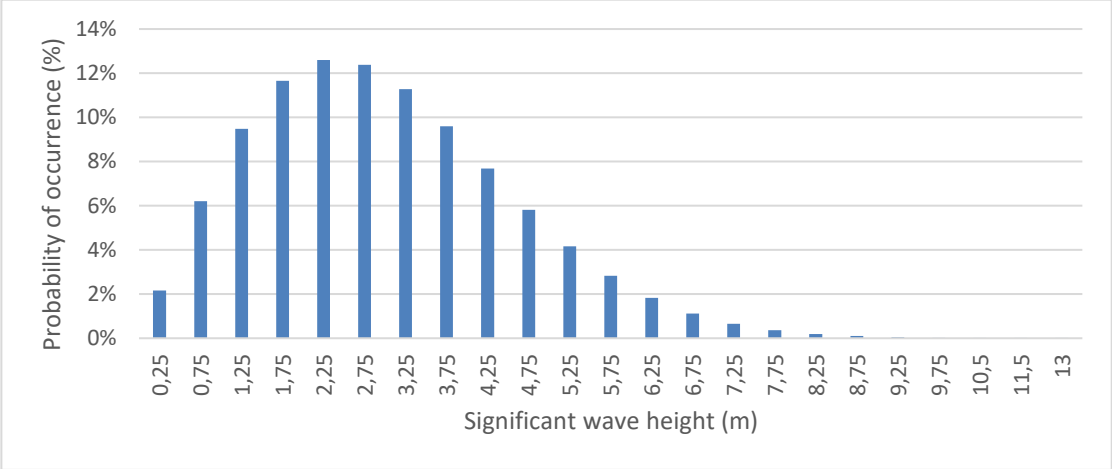

Figure 4.7: Probability of occurrence of significant wave height for 2013

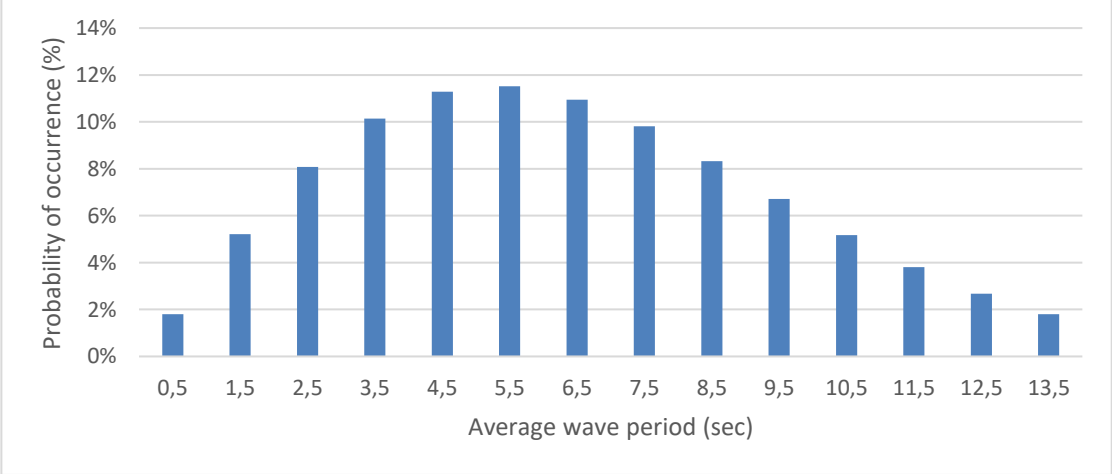

Figure 4.8: Probability of occurrence of average wave period for 2013

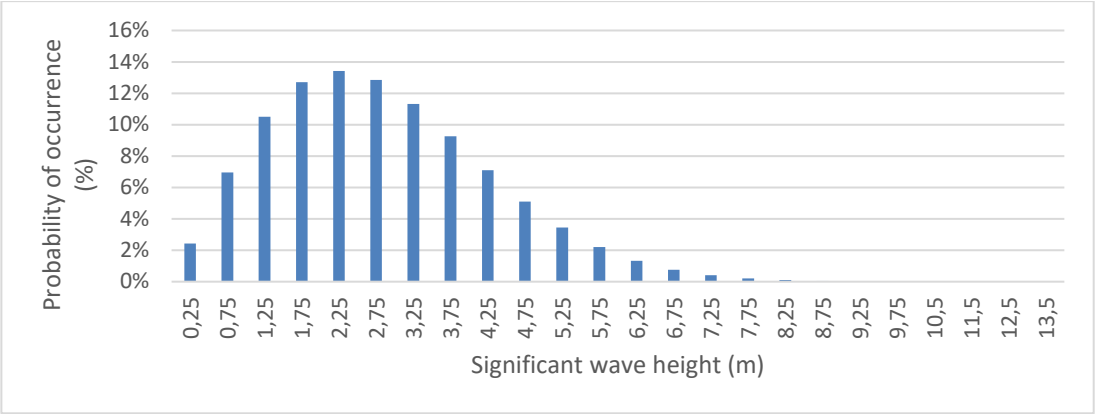

Figure 4.9: Probability of occurrence of significant wave height for 2014

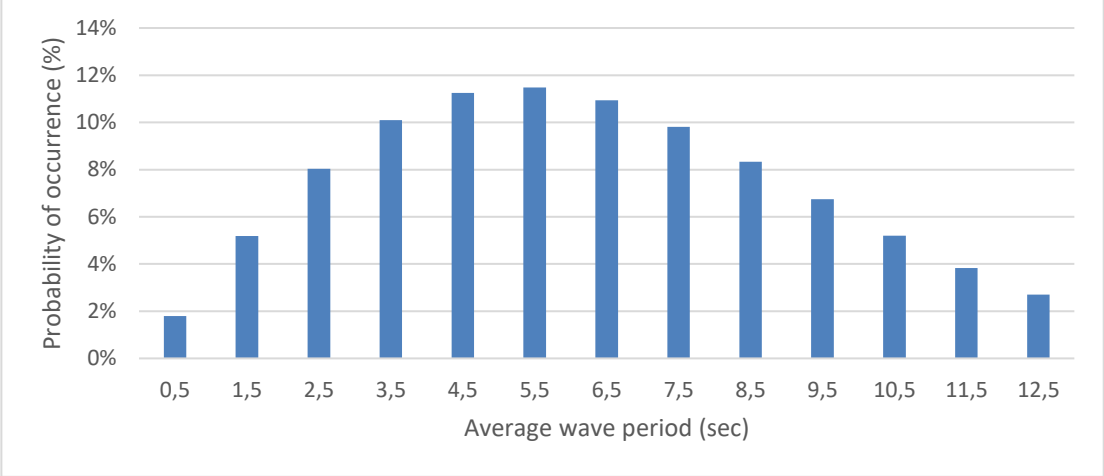

Figure 4.10: Probability of occurrence of average wave period for 2014

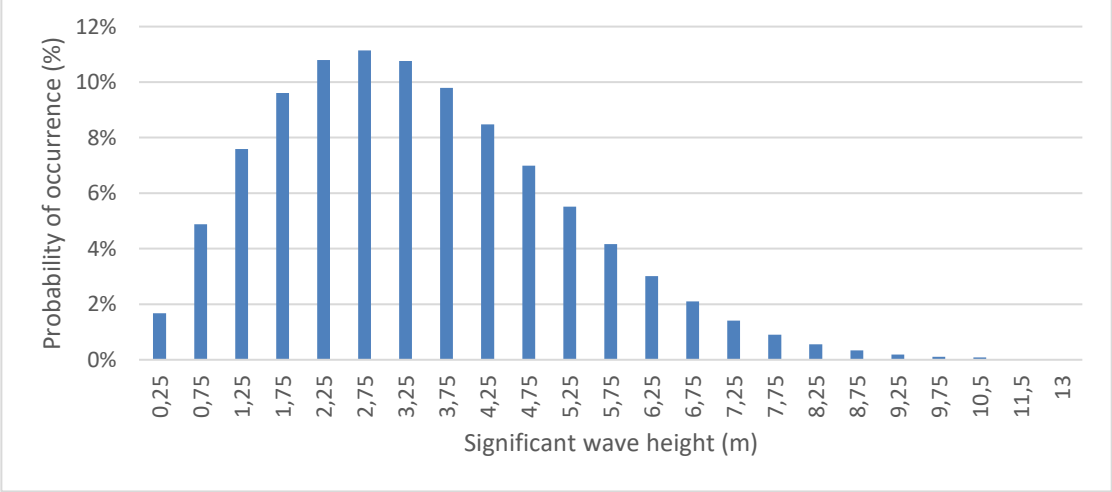

Figure 4.11: Probability of occurrence of significant wave height for 2015

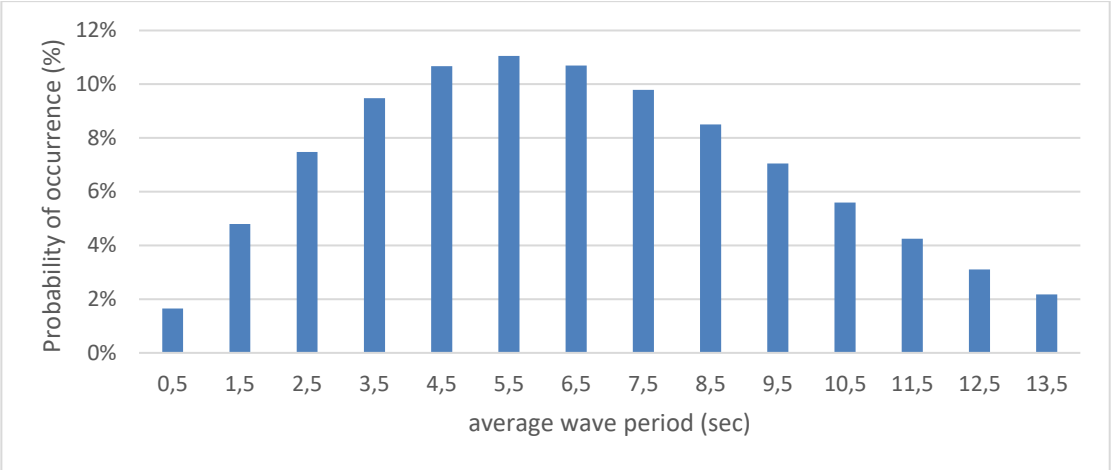

Figure 4.12: Probability of occurrence of average wave period for 2015

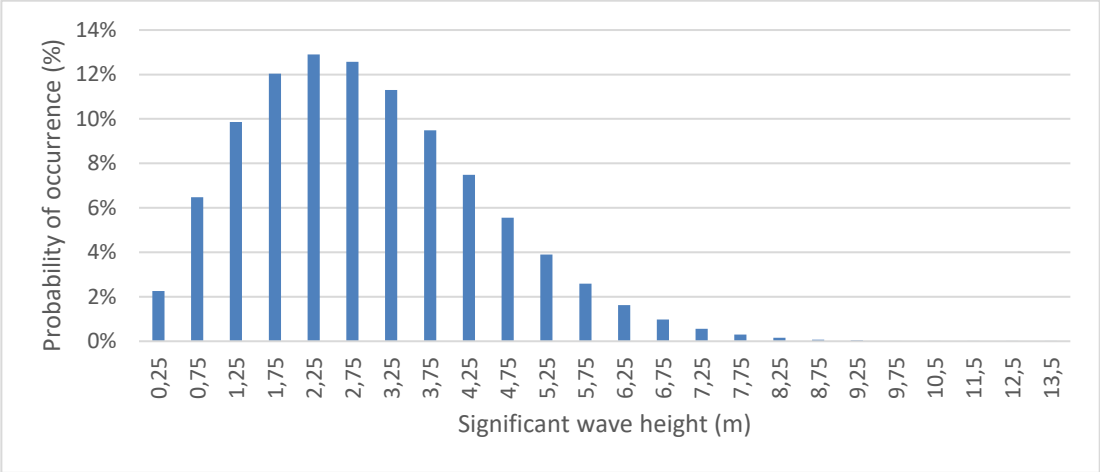

Figure 4.13: Probability of occurrence of significant wave height for 2016

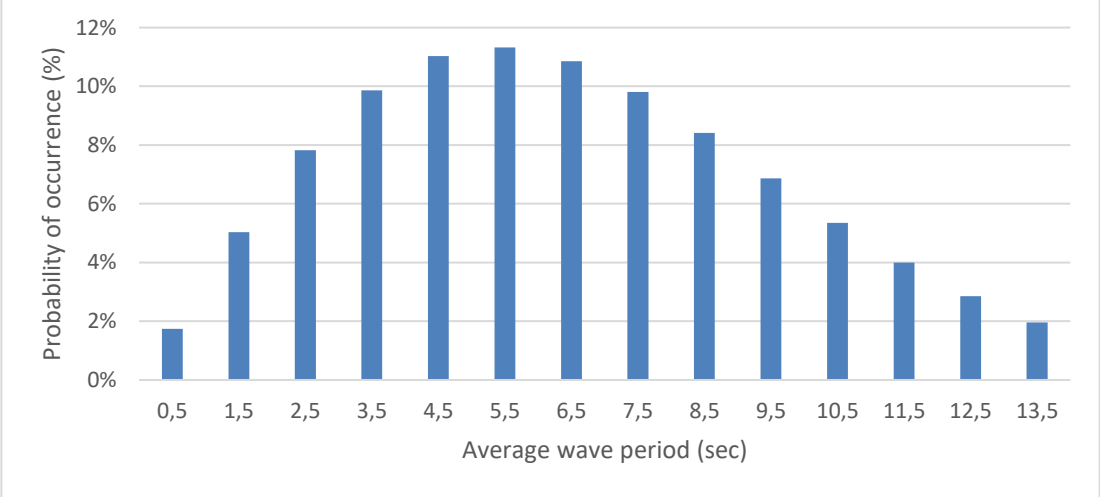

Figure 4.14: Probability of occurrence of average wave period for 2016

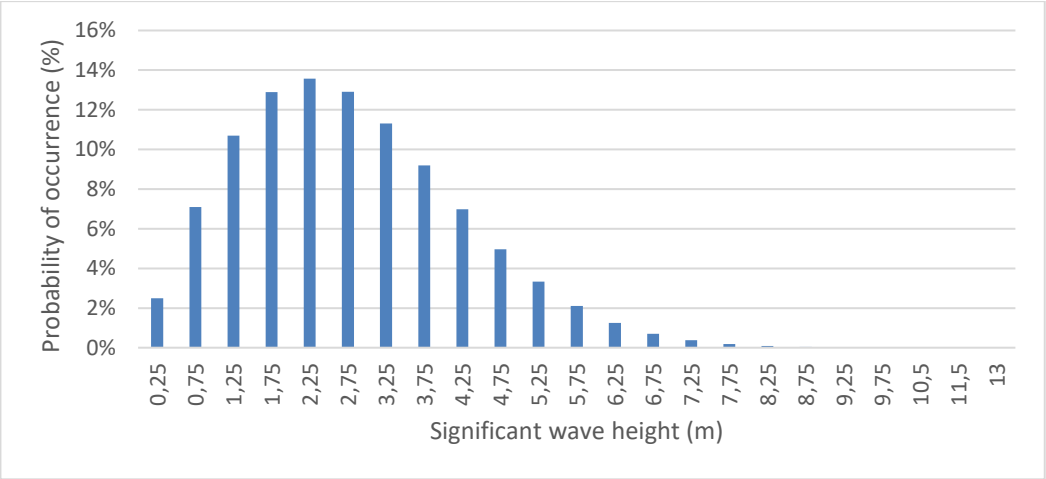

Figure 4.15: Probability of occurrence of significant wave height for 2017

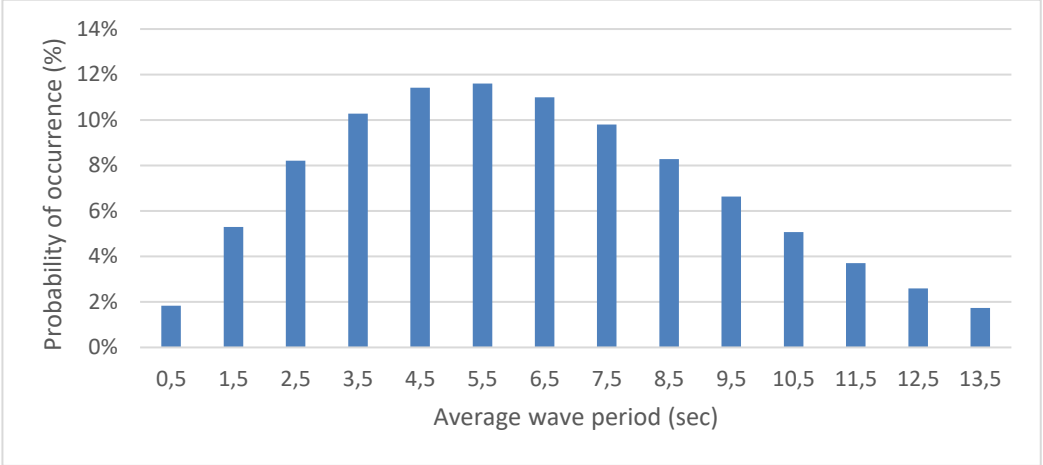

Figure 4.16: Probability of occurrence of average wave period for 2017

Figures show that the wave height distribution is positively skewed. This shows that the mean wave height is greater than the median and mode is the smallest. On the other hand, average wave period for all the years depicts normal distribution which means mean mode and median wave periods are approximately same. Mean is the average of all the data used in the study. Median, on the other hand, represents the middle value of all the numbers. The mode gives the maximum point of the distribution and is the number that appear more frequently.

The height and period of waves are given in percentage of their probability of occurrence. It is given, from the graphs obtained, that more than 60% of waves present

a height between 1.25m and 3.25m, and more than 50% of waves present a period between 3.5s and 7.5s. It is clear that probability distribution gives a more precise idea about the most frequent wave period and height that governs the location.

4.2 The wave power

In this section, the power that waves generate in a year span depending on their average wave period and significant wave height is to be calculated. The power capacity that is generated by waves during one year is calculated by the help of Eq. (2.13). This equation was derived for an individual wave height. Therefore, Eq. (2.13) is multiplied by the number of occurrences of each wave height/period, at Tables (3.1) to (3.8). Hence, the calculation was made using the formula of wave power; Eq. (2.13) multiplied the number of occurrences.

The density (ρ) of sea water which is roughly higher than normal water due to its salinity was chosen to be 1025 kg/m^3 which is the density of sea surface. This value has been chosen since the wave occurrence is at the ocean surface.

The wave power equation is depending on two constant which are the density ρ and the gravitational acceleration g; where their SI units are respectively kg/m^3 and m/s^2. When multiplying the density with the square of acceleration gravity gives units in $Watt/m^3.s$. Therefore, the equation of wave power has been multiplied by 10^{-3} to have the result in kilowatt. The final expression has a unit of kW/m.year since the power is calculated for the whole year.

The annual wave power available in Atlantic Ocean offshore of Ireland is represented in surface chart for each year as follows; at Figures (4.17) to (4.24)

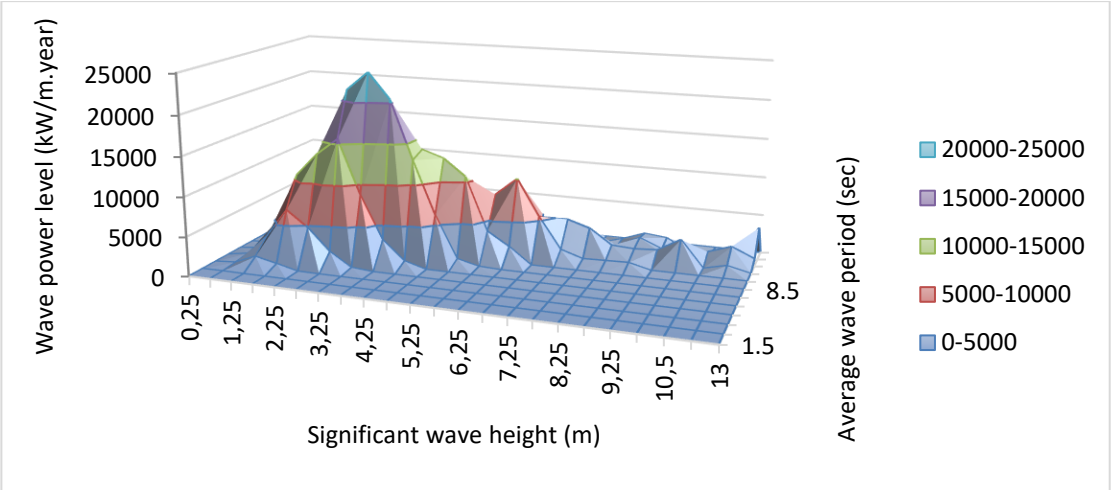

Figure 4.17: Wave power based on wave period and wave height for 2010

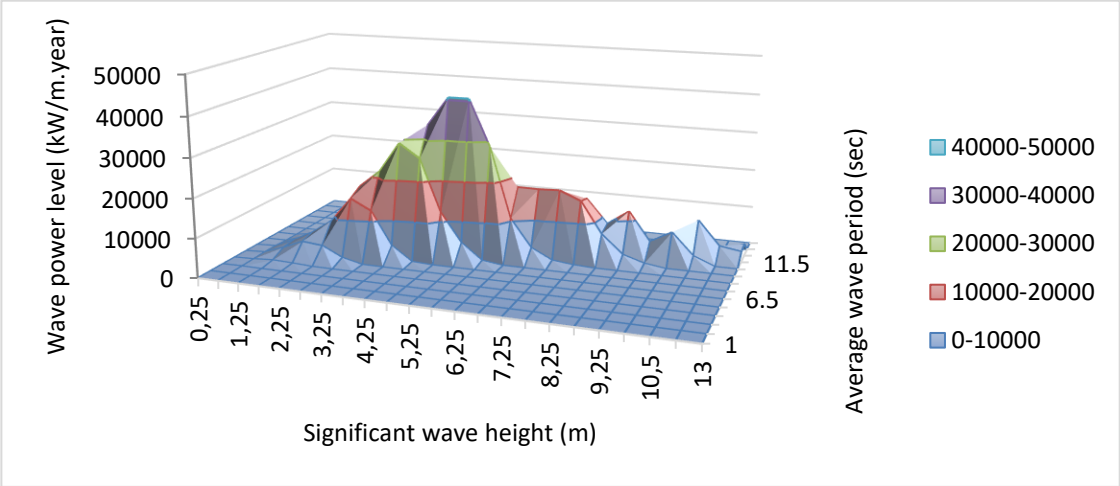

Figure 4.18: Wave power based on wave period and wave height for 2011

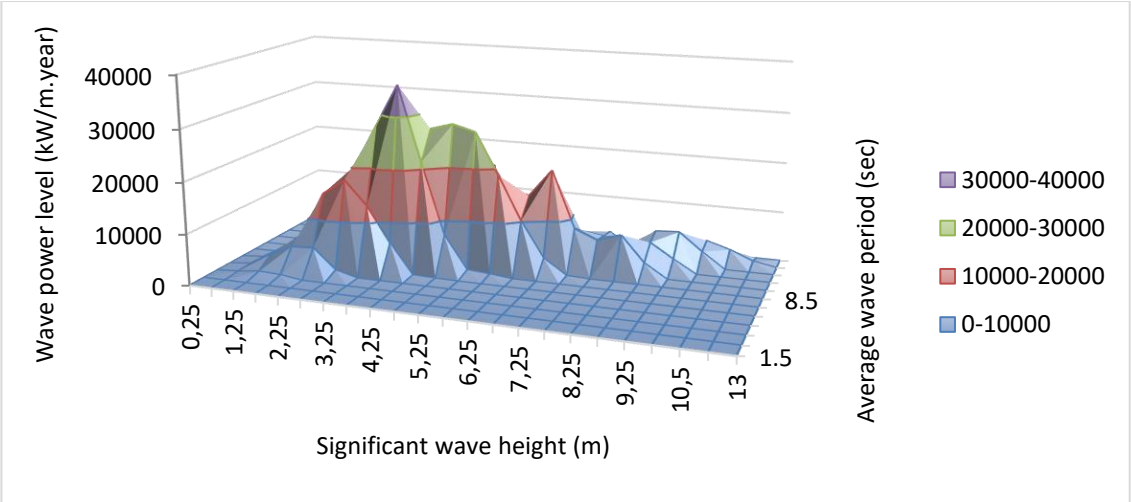

Figure 4.19: Wave power based on wave period and wave height for 2012

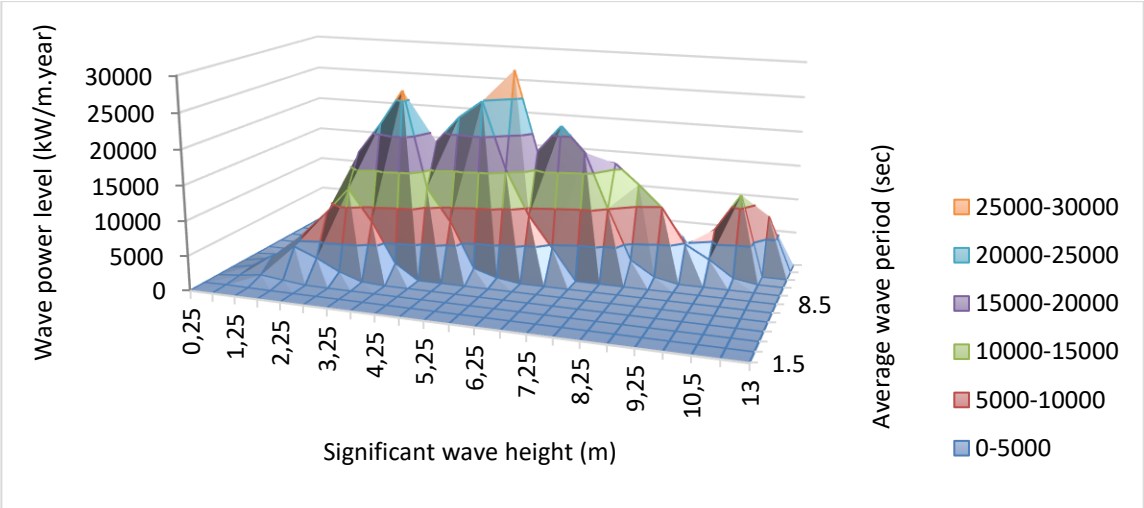

Figure 4.20: Wave power based on wave period and wave height for 2013

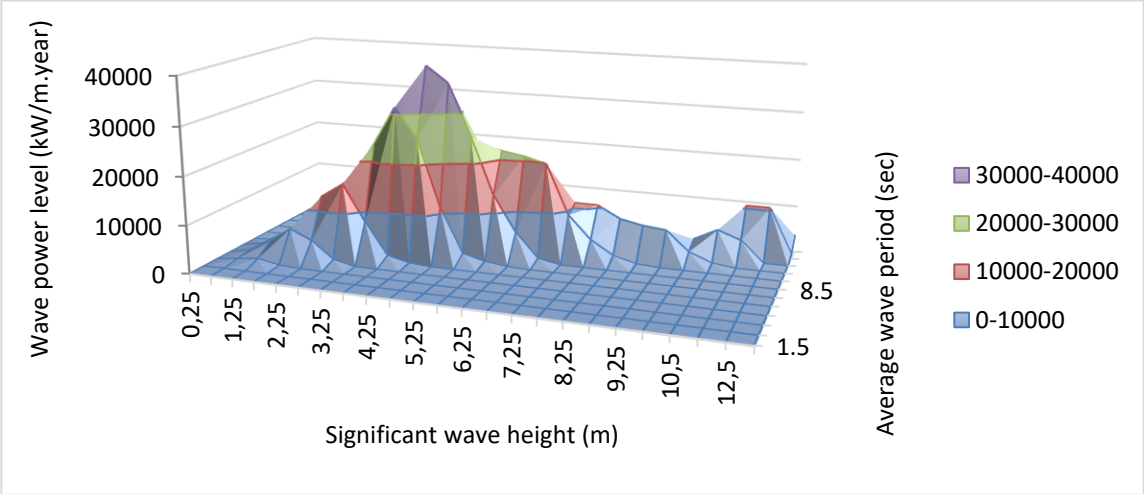

Figure 4.21: Wave power based on wave period and wave height for 2014

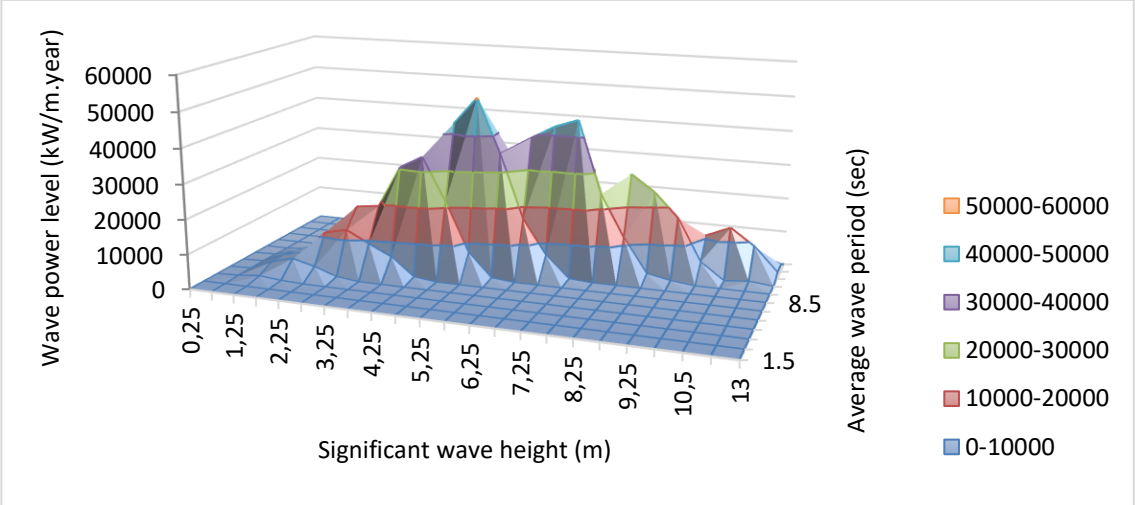

Figure 4.22: Wave power based on wave period and wave height for 2015

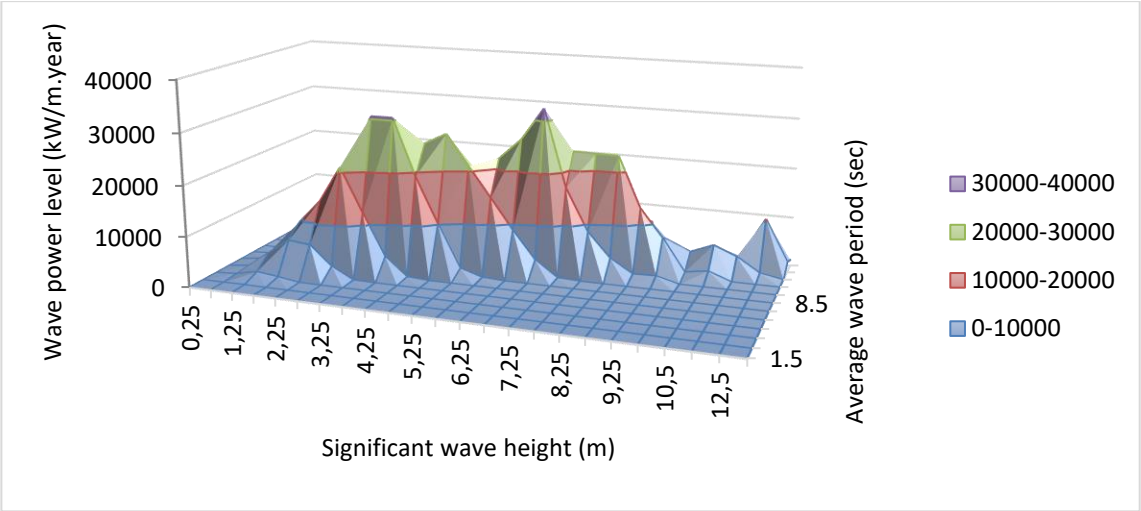

Figure 4.23: Wave power based on wave period and wave height for 2016

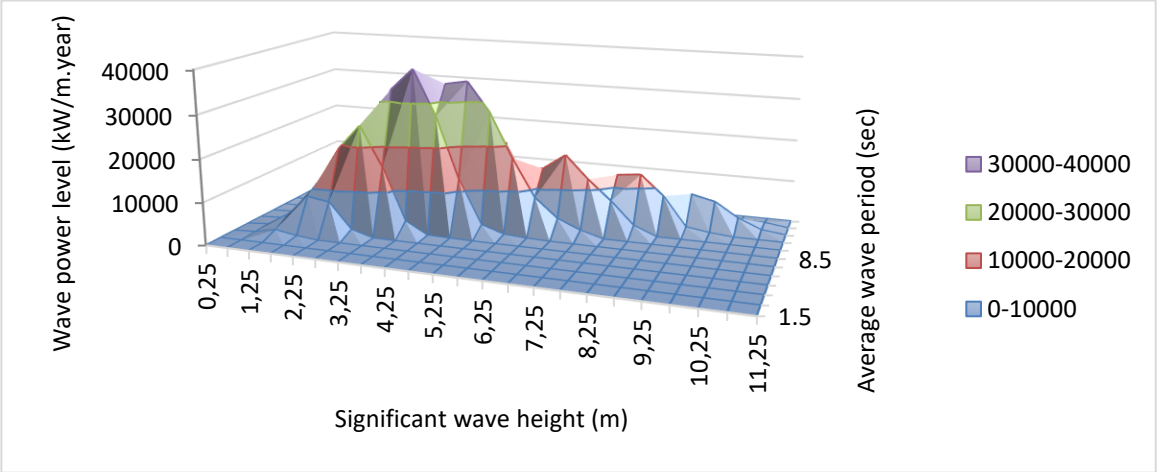

Figure 4.24: Wave power based on wave period and wave height for 2017

The surface chart representation of the wave power level (Figure 4.17 to 4.24) gives an idea about the power available in the waves over a whole year, which includes all sea state. The average wave energy available is estimated to be 19 kW/m for 2010, 37 kW/m for 2011, 29 kW/m for 2012, 30 kW/m for 2013, 27 kW/m for 2014, 42 kW/m for 2015, 30 kW/m for 2016 and 28 kW/m for 2017. A maximum average wave power may be estimated from Section (3.3), as the power is obtained from average of significant values of wave height and period. The power is then estimated to be 53 kW/m for 2010, 104 kW/m for 2011, 73 kW/m for 2012, 137 kW/m for 2013, 88 kW/m

for 2014, 115 kW/m for 2015, 97 kW/m for 2016 and 81 kW/m for 2017. We notice that some years present a very high-power level, that is due to some important stormy conditions that occur in the area.

4.3 Wave energy spectra

The spectrum which has been performed in this study is a representation of energy density in function of frequency.

Before representing the wave energy spectra, one should know which of the JONSWAP or Pierson-Moskovitz rule will be used. It is the peak shape parameter γ that will determine the rule to be used. Since no γ is given, the step to follow is to get the value of the ratio between the peak period and the root square of wave height. this ratio gives a hint about the value of the peak shape parameter; refer to Eq. (2.7).

Once all peak period records were gathered from data, their monthly highest value were identified. With the help of the monthly average significant wave height, Table (3.9), the relationship (T_p /$H_s^{1/2}$) can be obtained. The relationship was found, for all months of all years, to be greater or equal to five. From the rule of JONSWAP and the peak shape parameter, Section (2.3.2), it is concluded that the value of the peak shape parameter is equal to one ($\gamma = 1$). Thus, the JONSWAP spectrum reduces to the Pierson-Moskowitz spectrum.

The resulting wave energy spectra can be seen in figures (4.25) to (4.32).

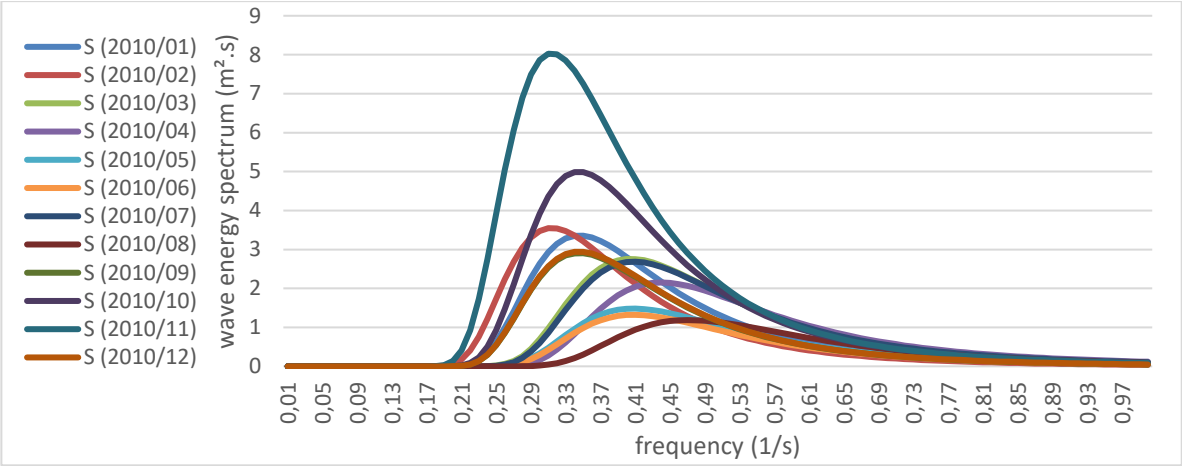

Figure 4.25: Wave energy spectra for 2010

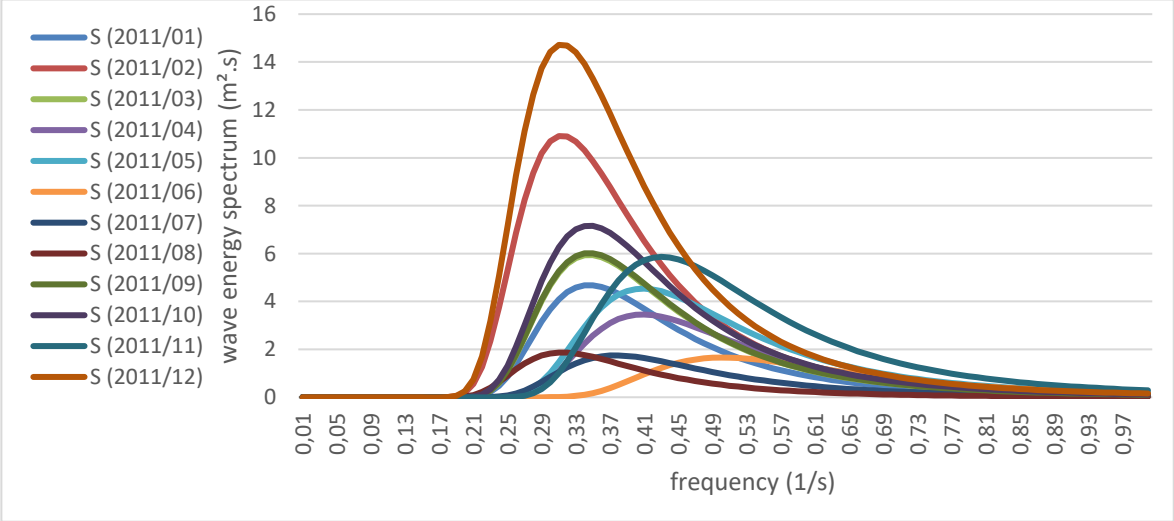

Figure 4.26: Wave energy spectra for 2011

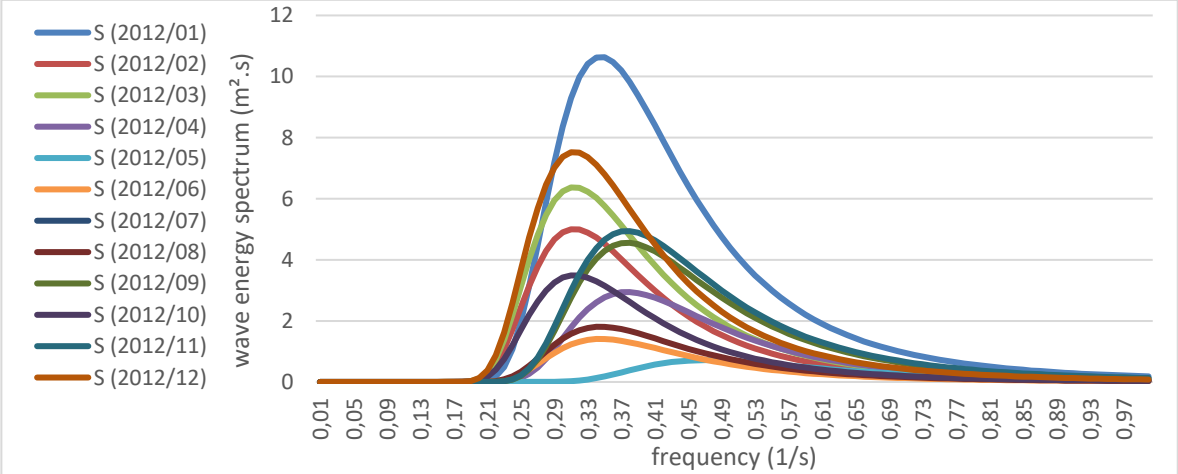

Figure 4.27: Wave energy spectra for 2012

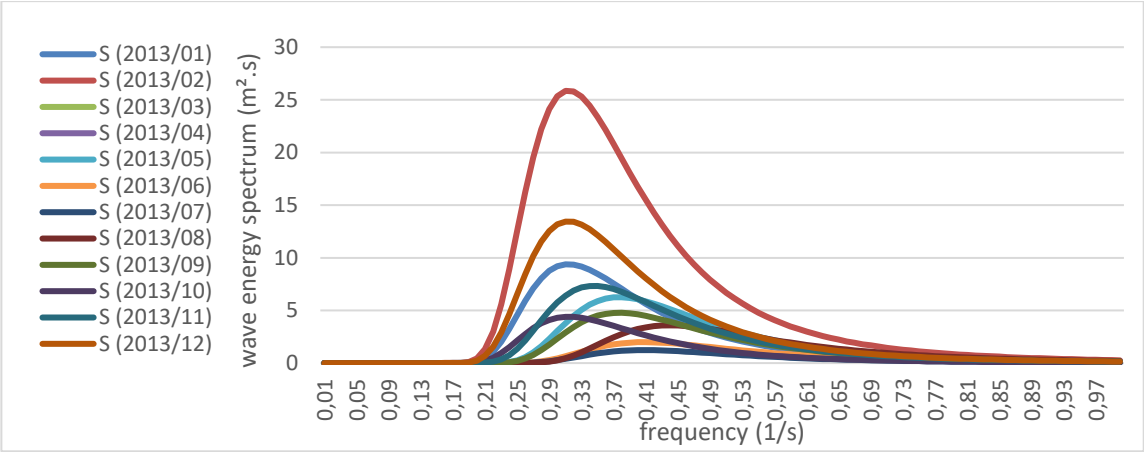

Figure 4.28: Wave energy spectra for 2013

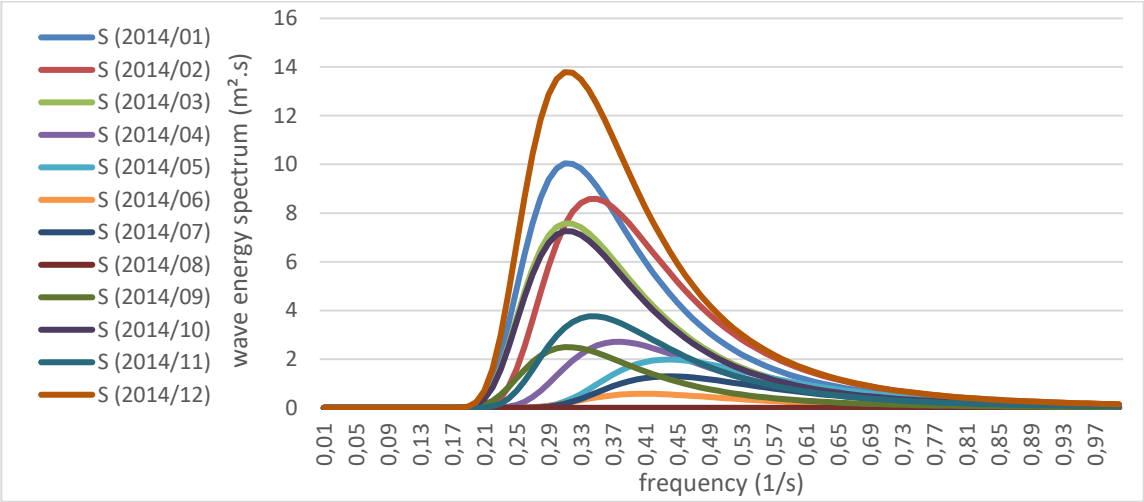

Figure 4.29: Wave energy spectra for 2014

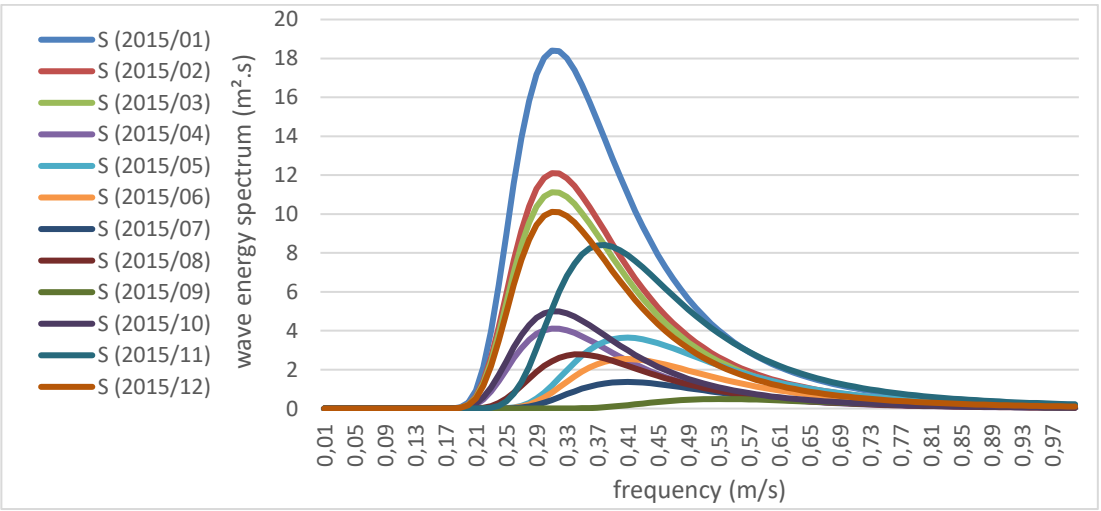

Figure 4.30: Wave energy spectra for 2015

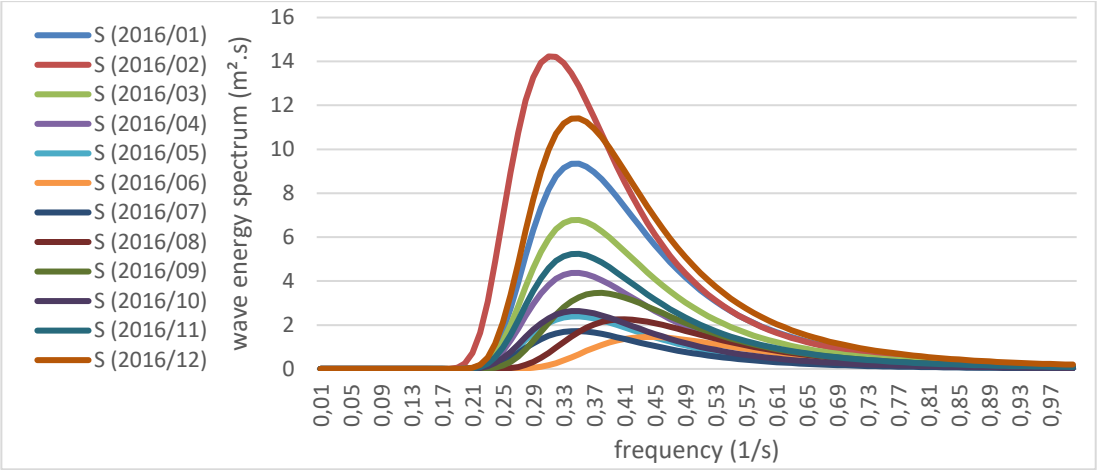

Figure 4.31: Wave energy spectra for 2016

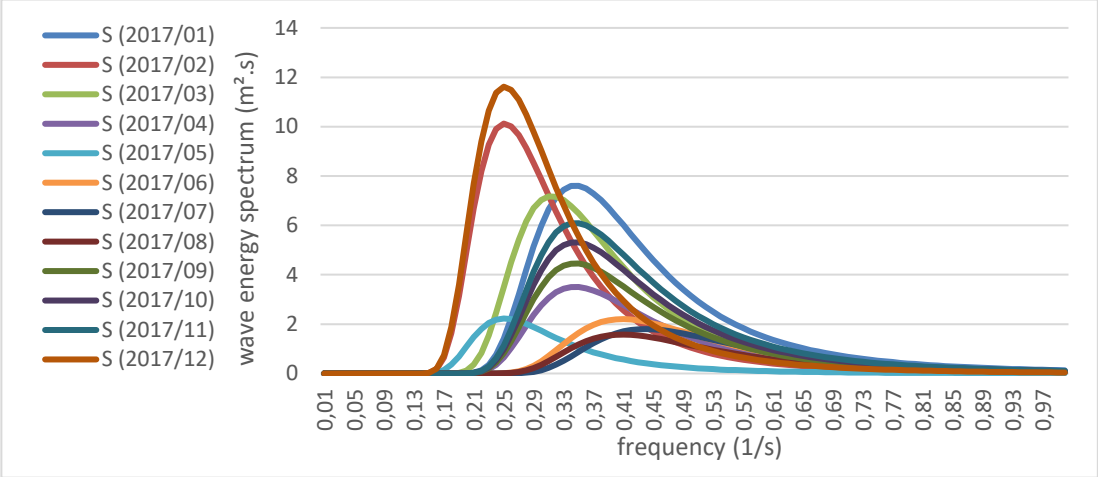

Figure 4.32: Wave energy spectra for 2017

The wave spectrum analysis comes to validate and to give a precise estimate of the seasons where the most energetic waves occur, and it can be seen that the most energetic waves happens specially during the winter season with a spectral wave energy, over all year, of about 15m²/Hz. More to that, the shape of the spectrum curve indicates that a peak of energy occur in a narrow frequency interval, meaning that the wave at the North-East Atlantic transport energy very frequently; in the order of 0.25~0.55 Hz.

4.4 Capture width ratio per unit width and potential power absorbed

This section, at the first, was performed in order to evaluate the performance of a type of wave energy converter; wave dragon (WD), and two floating breakwaters; a cylindrical floating breakwater (CFB) and a board-net floating breakwater (BnFB) which were created by Chun et al. (2015) and Dong et al. (2008), respectively. To be able to evaluate the performance of such structure, the wave transmission coefficient K_t should be studied, as this latter will help, by using Eq. (2.20), find the power absorbed by the structure and from that, using Eq. (2.15), the Capture Width Ratio per unit width will be obtained.

The wave transmission coefficient formula was derived using information given about the ratio *H/L*, in the case of breakwaters, or the ratio *B/L*, in the case of a wave dragon, and their K_t values obtained from different studies; Abubaker and Türker (2019) (A & T (2019)), Macagno (1954) (M (1954)), Ruol et al. (2013) (R (2013)), and Kriebel and Bollman (1996) (K & B (1996)). The data given in Tables (4.4), (4.5) & (4.6) are gathered from the above mentioned research studies.

Table 4.2: Transmission coefficient of a Wave Dragon

Wave Dragon				
	K_t			
B/L	A & T (2019)	M (1954)	R (2013)	K & B (1996)
1.488	0.64	0.72	0.80	0.50
1.186	0.69	0.81	0.77	0.57
0.985	0.72	0.87	0.84	0.61
0.905	0.72	0.90	0.88	0.63
0.748	0.74	0.94	0.94	0.65

Table 4.3: Transmission coefficient of a Cylindrical Floating Breakwater

Chun et al. (2005)				
	K_t			
H/L	A & T (2019)	M (1954)	R (2013)	K & B (1996)
	H=3m			
0.119	0.65	0.44	0.38	0.54
0.096	0.69	0.55	0.48	0.62
0.080	0.73	0.65	0.60	0.68
0.067	0.77	0.74	0.70	0.74
0.058	0.80	0.80	0.78	0.78
0.050	0.83	0.85	0.84	0.81
	H=4m			
0.128	0.70	0.55	0.48	0.62
0.106	0.73	0.65	0.60	0.68
0.089	0.77	0.74	0.70	0.74
0.077	0.80	0.80	0.78	0.78
0.067	0.83	0.85	0.84	0.81

Table 4.4: Transmission coefficient of a Board-net Floating Breakwater

Dong et al. (2018)				
	K_t			
H/L	A & T (2019)	M (1954)	R (2013)	K & B (1996)
	H=2.5m			
0.045	0.67	0.50	0.42	0.61
0.035	0.75	0.66	0.61	0.71
0.028	0.79	0.78	0.76	0.77
0.024	0.82	0.86	0.85	0.80
0.021	0.84	0.91	0.90	0.82
	H=4.5m			
0.082	0.68	0.50	0.42	0.61
0.062	0.75	0.66	0.61	0.71
0.051	0.80	0.78	0.76	0.77
0.043	0.82	0.86	0.85	0.80
0.037	0.84	0.91	0.90	0.82
	H=6m			
0.109	0.688	0.499	0.422	0.607
0.083	0.754	0.663	0.608	0.709
0.068	0.798	0.781	0.759	0.768
0.057	0.825	0.858	0.851	0.802
0.049	0.842	0.906	0.904	0.824

Tables (4.4), (4.5) & (4.6) have been used to make a scatter diagram where an average fitline is derived. The equation of each fit line derived represents the wave transmission coefficient (K_t) of each study dependently to the structure derived for. The equation will be in the form of $y = ax + b$, where *x* will represent *H/L*, in the case of the breakwater structures, or *B/L*, in the case of the Wave Dragon, and *y* represent K_t. the drawing related to each relationship is given in Appendix A.

The transmission coefficient equations derived are as follows:

- In the case of cylindrical floating breakwater:
    - Macagno: $K_t = -4.6451\frac{H}{L} + 1.088$
    - Ruol: $K_t = -5.525\frac{H}{L} + 1.1225$
    - Kriebel and Bollman: $K_t = -3.0451\frac{H}{L} + 0.9686$
    - Abubaker: $K_t = -2.0407\frac{H}{L} + 0.9276$
- In the case of Boared-net floating breakwater:
    - Abubaker: $K_t = -1.4466\frac{H}{L} + 0.8549$
    - Macagno: $K_t = -3.9507\frac{H}{L} + 0.9503$
    - Ruol: $K_t = -4.719\frac{H}{L} + 0.9582$
    - Kriebel and Bollman: $K_t = -2.0953\frac{H}{L} + 0.8529$

Where the wave length *L* is given as:

$$L = 1.56\,T^2 \tag{3.1}$$

In the case of a wave dragon, the transmission coefficient was given depending on the ratio B/L. where B is the total width of the WD and equal to 150 meters. The derived equations are as follows:

- Abubaker: $K_t = -0.1351\frac{B}{L} + 0.8446$

- Macagno: $K_t = -0.3097\frac{B}{L} + 1.1768$
- Ruol: $K_t = -0.1832\frac{B}{L} + 1.0413$
- Kriebel and Bollman: $K_t = -0.2081\frac{B}{L} + 0.8153$

The transmission coefficient values obtained from above relations can be used in the formula given as Eq. (2.20) and the absorbed wave power by different floating structures can be calculated as:

$$P_{absorb} = (1 - K_t^2)P_{incident} \tag{3.2}$$

A monthly absorbed wave power, for every single structure, is given in Tables in Appendix B. Once $P_{absorbed}$ is known the capture width ratio per unit length can be calculated using Eq. (2.15) or Eq. (2.21). The monthly average Capture width is presented in Tables given in Appendix B.

Yearly average of capture width ratio and power absorbed by different Floating Structures with respect to different studies are summarized in the figures (4.33) to (4.38).

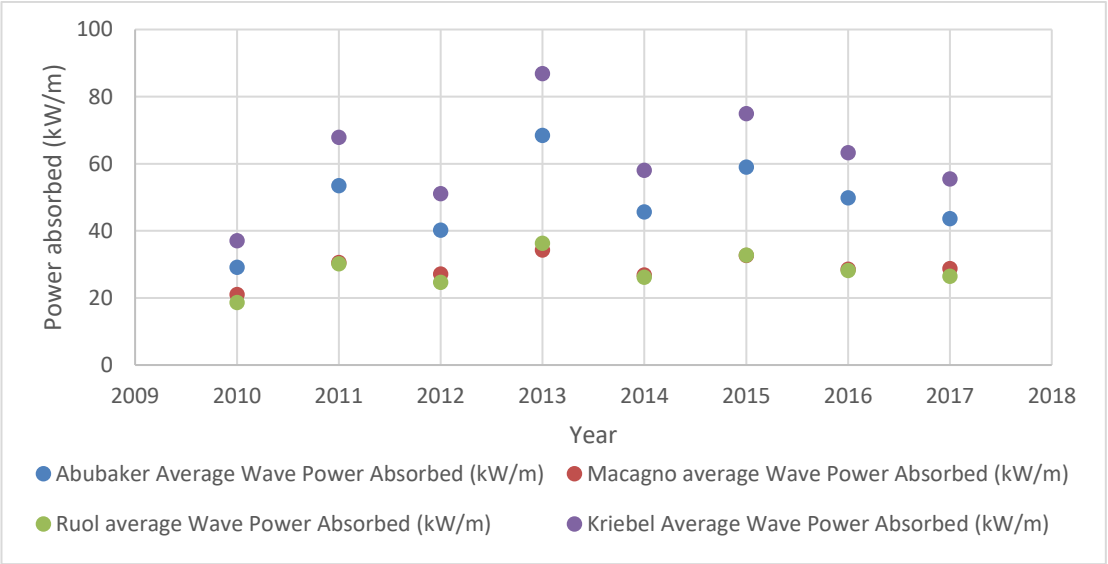

Figure 4.33: Average power absorbed by Wave Dragon

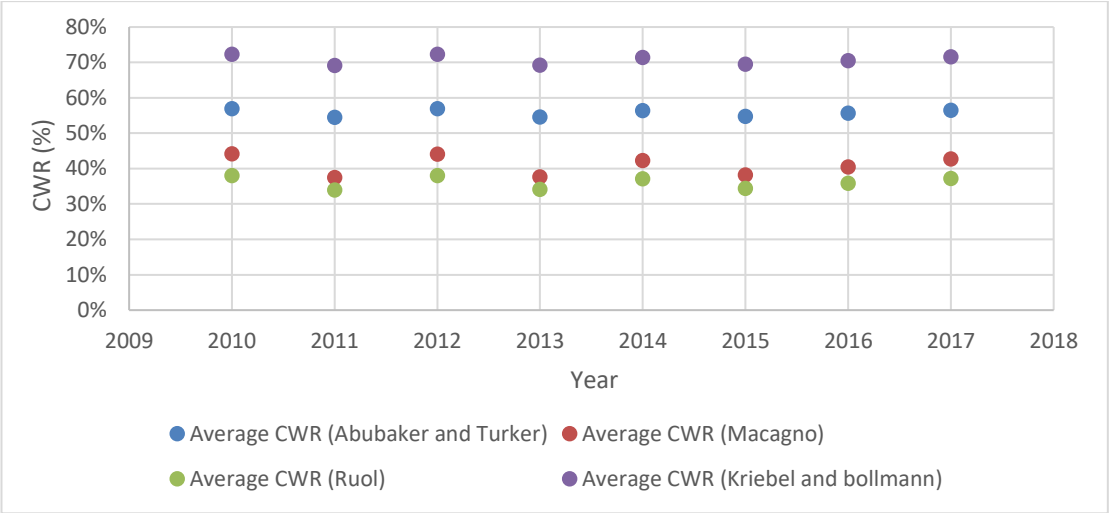

Figure 4.34: Average capture width ratio for a Wave Dragon

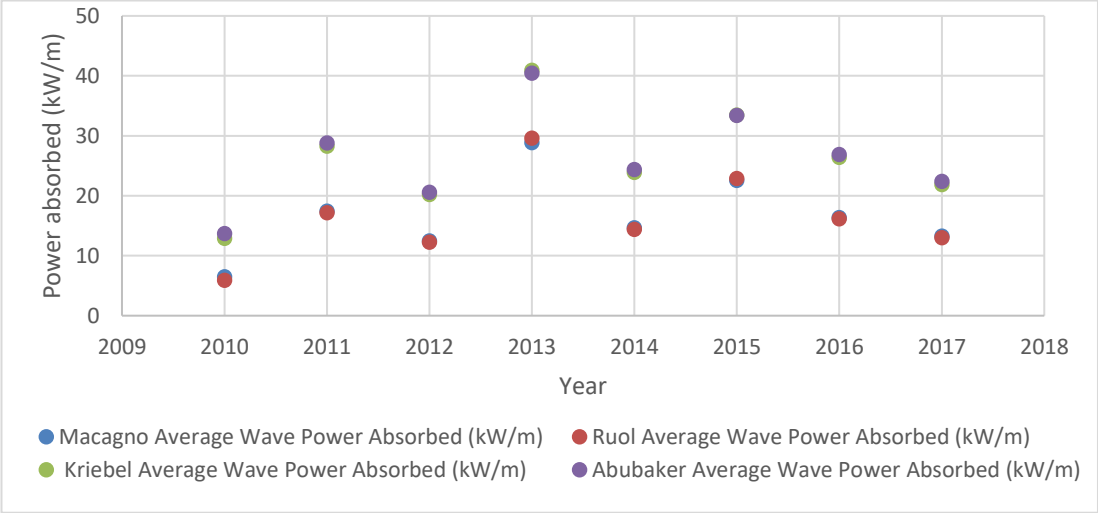

Figure 4.35: Average power absorbed by a Cylindrical Floating Breakwater

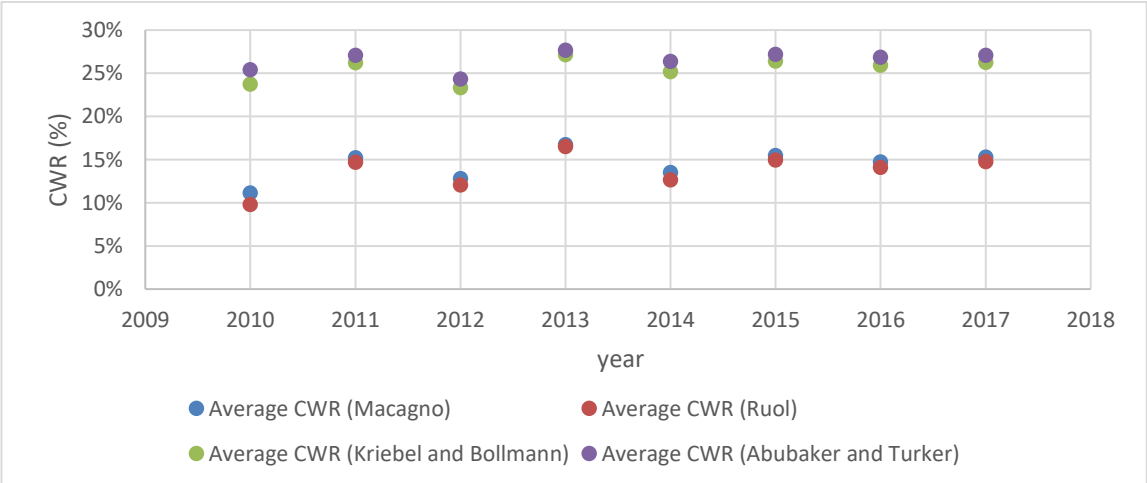

Figure 4.36: Average capture width ratio for a Cylindrical Floating Breakwater

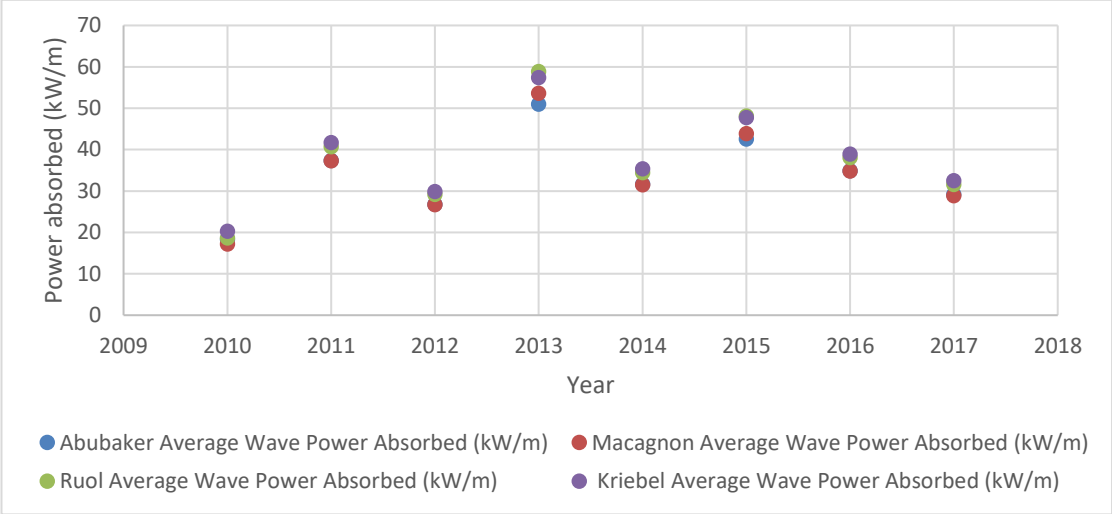

Figure 4.37: Average power absorbed by a Board-net Floating Breakwater

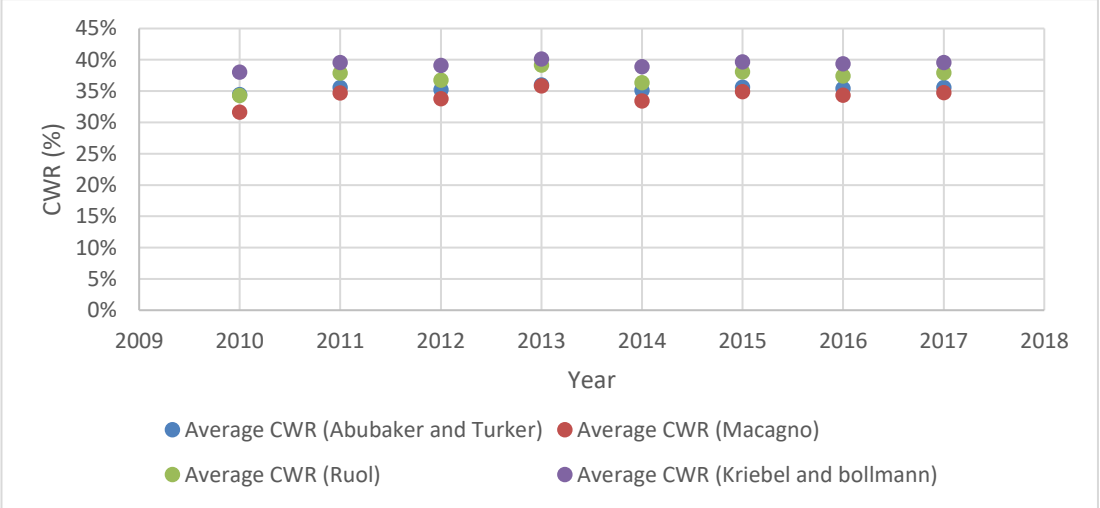

Figure 4.38: Average capture width ratio for a Board-net Floating Breakwater

The capture width of a value of 0% correspond to no absorption and a value of 100% correspond to a state of full absorption. For WD, it has been shown, from Figures in Annex B, that the capture width is higher at the months related to summer. This can be explained by the fact that most of waves, in terms of height, created at that period of the year are relatively small and hence, the wave may be, almost, completely absorbed by the structure. Using significant values of wave height and wave period,

already calculated in Section 4.3, the average wave power absorbed, over all the years, is estimated to be 49 kW/m, 29 kW/m, 28 kW/m and 62 kW/m for Abubaker and Türker (2019), Macagno (1954), Ruol et. al. (2013), and Kriebel and Bollman (1996), repectively. Parallelly, the average capture width over all the years is estimated to be 0.55 m/m, 0.41 m/m, 0.36 m/m and 0.71 m/m for the same studies respectivelly. The results obtained from the use of Kriebel and bollmann (1996) formula are considerably higher than the results obtained using the formula of the other authors. One can say that the method used by Kriebel and bollmann (1996) overestimate the results. For CFB, Ruol et. al. (2013) and Macagno (1954) methods gives lower results comparing to those of Abubaker and Kriebel. From the figures, given in Annex B, it is noticed that there is a peak in capture width ratio and power absorbed when the ratio H/L is important, in other words, the CFB structure depend on the ratio between wave height and wave period; when a wave is considerably high and its period is low, that is when the structure is more efficient. Nevertheless, the structure seems not to be very efficient, since the average capture width over all year is only about 0.14 m/m, 0.13 m/m, 0.25 m/m, 0.26m/m and a power absorption of about 16 kW/m, 16 kW/m, 26 kW/m, 26 kW/m for Macagno (1954), Ruol et. al. (2013), Kriebel and Bollmann (1996), and Abubaker and Türker (2019), respectively. In the case of BnFB structure, the capture width behaves like for the CFB structure; meaning that it increases when the ratio H/L increases as well. However, here all derived authors formulas gives approximately same result but one can still notice that Abubaker and Türker (2019) formula does not vary proportionally with the variation, over a year, of the Ratio H/L but varies very slightly comparing the pattern that follow other CWR results obtained using other authors formula. The maximum power absorbed by this Board-net floating breakwater is estimated for all years to be 34 kW/m, 34 kW/m, 37 kW/m and 38 kW/m,

and a capture width ratio of, about, 0.35 m/m, 0.34 m/m, 0.37 m/m and 0.39 m/m for Abubaker and Türker (2019), Macagno (1954), Ruol et. al. (2013), and Kriebel and bollmann (1996).

Chapter 5

CONCLUSION

This research was conducted for the purpose of identifying the wave climate that governs the Atlantic Ocean at the West side of Ireland as well as the efficiency of some floating structures in terms of their capture width ratio and their absorbed power. Based on quantitative analysis of ocean wave data that has been gathered from the Marine Institute of Ireland, it was found that the average significant wave height, observed from 8 years of records, is around 4 meters. However, it is noticed that the wave height pattern may change from year to year or over a year itself. This behavior may be explained by some hazardous stormy conditions that occur in the region. The waves were mostly found to come from the West. The region is able to produce an average wave power of 30 kW/m. This value is obtained from the observation of all wave parameters such as wave period and wave height obtained from the data in the period of 2010 to 2017. The significant values of the wave parameters were selected from data and a new significant average wave power was found to fluctuate around 90 kW/m. An average of these two values will be a good estimate of the real average wave power that may be produced by the waves on the region; and the wave power is then estimated to be around 60 kW/m which is in accordance with the information given in Fig. (1.1). The wave energy spectrum gives an idea about the frequency at which the most energetic waves appear and, based on this study, this frequency is around 0.35 Hz. The frequency indicates that the Ocean is a good source of power since a considerable energy is produced in a very narrow time interval.

Once the wave climate of the region has been studied and understood, three floating structures (Wave Dragon, Cylindrical Floating Breakwater and Board-net Floating Structure) were studied as well in the interest to know which of them is more efficient in terms of their capture width and power absorption. Four different formula retrieved from the literature were used for this purpose. The results obtained were different from author to author, that may be explained by the fact that each author take in account more or less parameters than the others in order to evaluate the capture width ratio of a floating structure in the Ocean. However, it is clear from the study that the Wave Dragon present the highest power absorption and capture width ratio.

REFERENCES

Alamailes, A., & Türker, U. (2019). Using Analytical Approach to Estimate Wave Transmission Coefficient in Floating Structures. *Journal of Waterway, Port, Coastal, and Ocean Engineering*, 145(3), 04019010.

Babarit, A., Hals, J., Muliawan, M. J., Kurniawan, A., Moan, T., & Krokstad, J. (2012). Numerical benchmarking study of a selection of wave energy converters. *Renewable energy*, (41), 44-63.

Babarit, A. (2015). A database of capture width ratio of wave energy converters. *Renewable Energy*, 80, 610-628.

Battjes, J. A. (1972). Long-term wave height distributions at seven stations around the British Isles. *Deutsche Hydrografische Zeitschrift*, 25(4), 179-189.

Bernhoff, H., Sjostedt, E., & Leijon, M. (2006). Wave energy resources in sheltered sea areas: a case study of the Baltic Sea. *Renewable Energy* 31, 2164–2170.

Budar, K., & Falnes, J. (1975). A resonant point absorber of ocean-wave power. *Nature*, 256(5517), 478.

Collins, J. I. (1970). Probabilities of breaking wave characteristics. *Coastal Engineering Proceedings*, 1(12), 25.

Diamantoulaki, I., & Angelides, D. C. (2011). Modeling of cable-moored floating

breakwaters connected with hinges. *Eng. Struct.*, 33(5), 1536–1552.

Falnes, J. (2007). A review of wave-energy extraction. *Marine structures*, 20(4), 185-201.

Folley, M., & Whittaker, T. J. T., (2009). Analysis of the nearshore wave energy resource. *Renewable Energy*. 34, 1709–1715.

Goda, Y. (2010). Random seas and design of maritime structures (Vol. 33). *World Scientific Publishing Company.*

Gökçekuş, H., Türker, U., & LaMoreaux J. W. (2011). Survival and Sustainability, *Environmental Earth Sciences*, 15 DOI 10.1007/978-3-540-95991-5_2, Springer-Verlag Berlin Heidelberg

Hemer, M.A., & Griffin, D.A. (2010). The wave energy resource along Australia's southern margin. *Journal of Renewable and Sustainable Energy*, 2, 041308, 1-10.

Henfridsson, U., Neimane, V., Strand, K., Kapper, R., Bernhoff, H., Danielsson, O., … Bergman, K. (2007). Wave energy potential in the Baltic Sea and the Danish part of the North Sea, with reflections on the Skagerrak. *Renewable Energy* (32), 2069–2084.

Hasselmann, K., Barnett, T. P., Bouws, E., Carlson, H., Cartwright, D. E., Enke, K., ... & Meerburg, A. (1973). Measurements of wind-wave growth and swell

decay during the Joint North Sea Wave Project (JONSWAP). *Ergänzungsheft 8-12)*.

Hughes, M.G., & Heap, A. D. (2010). National-scale wave energy resource assessment for Australia. *Renewable Energy*, 35(8), 1783-1791.

Iglesias, G., Lopez, M., Carballo, R., Castro, A., Fraguela, J.A., & Frigaard, P. (2009). Wave energy potential in Galicia (NW Spain). *Renewable Energy* (34), 2323–2333.

Kabdasli, M. S., & Türker, U. (2002). The wave breaking phenomena as a tool for environmental friendly shore protection. *Water science and technology*, 46(8), 153-160.

Laing, A. K. (1998). An Introduction to Ocean Waves. *World Meteorological Organization. Guide to Wave Analysis and Forecasting.* (2nd ed.). Switzerland: WMO, (702).

Leishman, J. M., & Scobie, G. (1976). *The development of wave power-a techno-economic study*. East Kilbride, Scotland: National Engineering Laboratory.

Longuet-Higgins, M. S. (1975). On the joint distribution of the periods and amplitudes of sea waves. *Journal of Geophysical Research*, 80(18), 2688-2694.

Martinelli, L., Ruol, P., & Zanuttigh, B. (2008). Wave basin experiments on floating breakwaters with different layouts. *Appl. Ocean Res.*, 30(3), 199–207.

Masuda, Y. (1986). An experience of wave power generator through tests and improvement. In *Hydrodynamics of ocean wave-energy utilization* (pp. 445-452). Springer, Berlin, Heidelberg.

McCormick, M.E. (1981). *Ocean wave energy conversion*. New York: Wiley.

Mollison, D., Salter, S. H., & Taylor, J. R. M., *Edinburgh Wave Power Project Report* No. 32 (1976)

Munk, W. H. (1951). *Origin and generation of waves* (No. SIO-REF-51-57). Scripps Institution of Oceanography. La Jolla, Calif.

Payab, A. H., & Türker, U. (2018). Analyzing temporal–spatial characteristics of drought events in the northern part of Cyprus. Environment, development and sustainability, 20(4), 1553-1574.

Pierson, W. J., & Moskowitz, L. (1964). *A proposed spectral form for fully developed wind-seas based on the similarity theory of S. A. Kitaigorodskii. J. Geophys.* Res., 69(24), 5181–5190.

Ruol, P., Martinelli, L., & Pezzutto, P. (2013). Formula to predict transmission for π-type floating breakwaters. *J. Waterway Port Coastal Ocean Eng.*, 10.1061/(ASCE)WW.1943-5460.0000153, 1–8.

Shafiee, S., & Topal, E. (2009). When will fossil fuel reserves be diminished? *Energy policy*, 37(1), 181-189.

Shaw, R. (1982). *Wave energy-a design challenge*. Chichester, England: Ellis Horwood Ltd.

Sinden, G. (2005). *Wind power and the UK wind resource*. Environmental Change Institute, University of Oxford.

Stahl, A. (1892). The utilization of the power of ocean waves. *Transactions of the American Society of Mechanical Engineering*, 13, 438–506.

Türker, U. (2014). Excess energy approach for wave energy dissipation at submerged structures. *Ocean Engineering*, 88, 194-203.

Türker, U., & Kabdasli, M. S. (2004). Average sediment dislocation analysis for barred profiles. *Ocean engineering*, 31(14-15), 1741-1756.

URL1, http://www.renewablegreenenergypower.com/what-is-wave-energy/

APPENDICES

Appendix A: Derived K_t formula

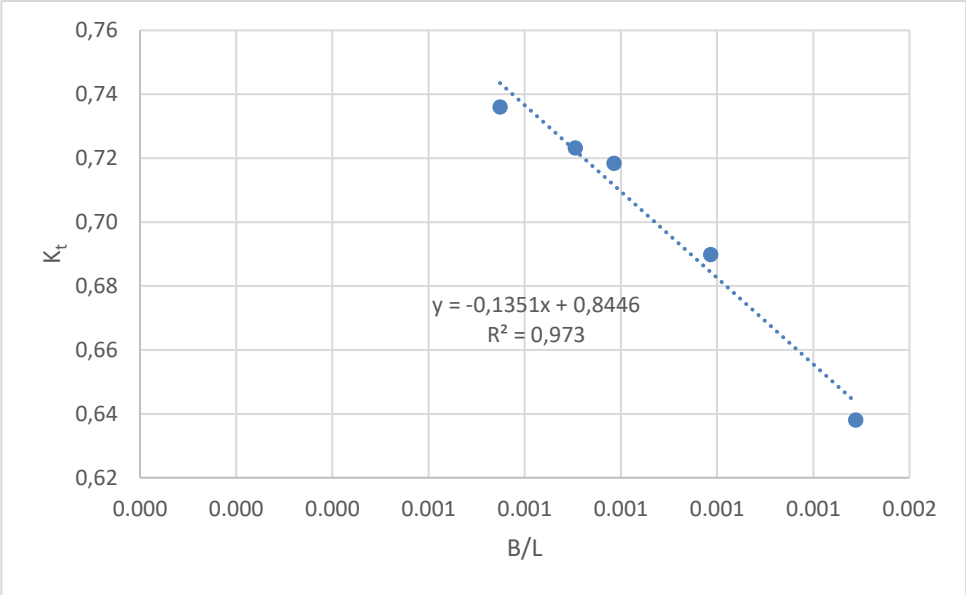

Figure A.1: The change of K_t w.r.t B/L retrieved from Abubaker and Türker 2019 for Wave Dragon

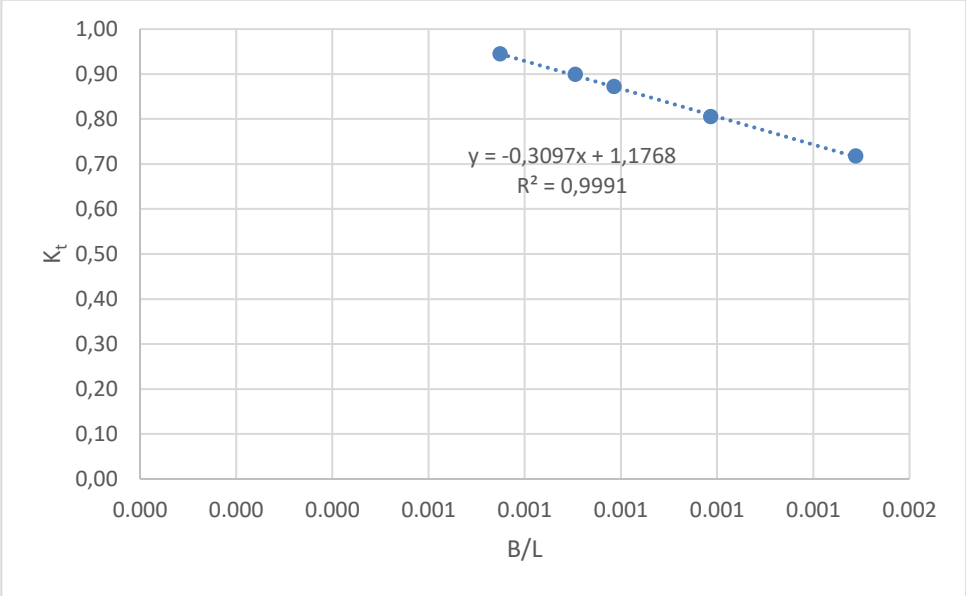

Figure A.2: The change of K_t w.r.t B/L retrieved from Macagnon 1954 for Wave Dragon

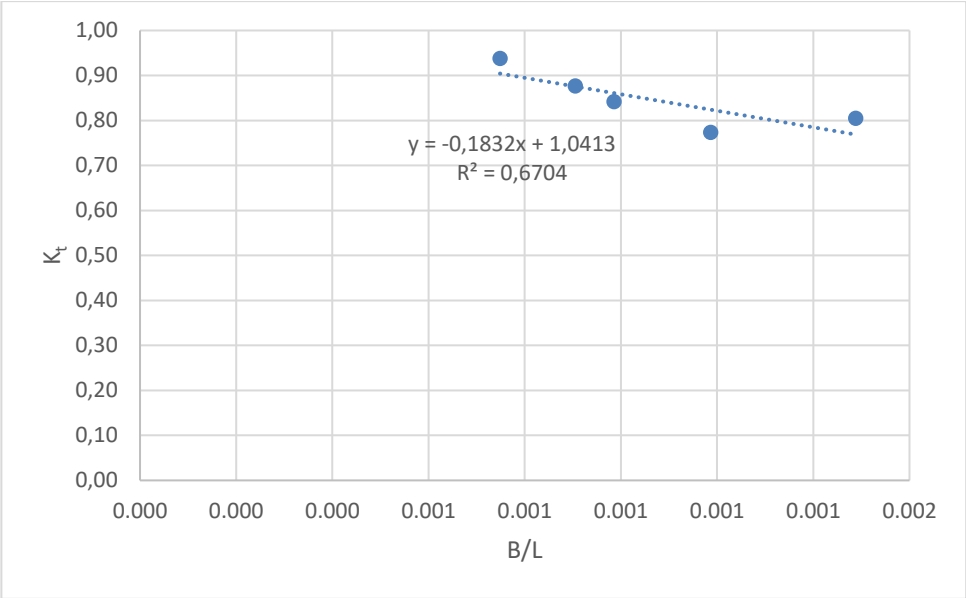

Figure A.03: The change of K_t w.r.t B/L retrieved from Ruol et. al. 2013 for Wave Dragon

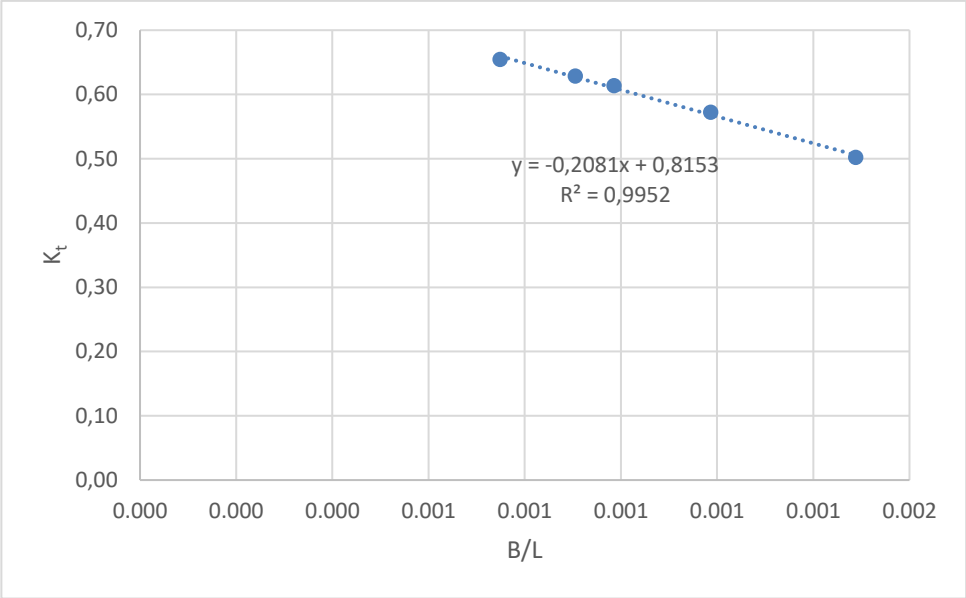

Figure A.4: The of K_t w.r.t B/L retrieved from Kriebel and Bollmann 1996 for Wave Dragon

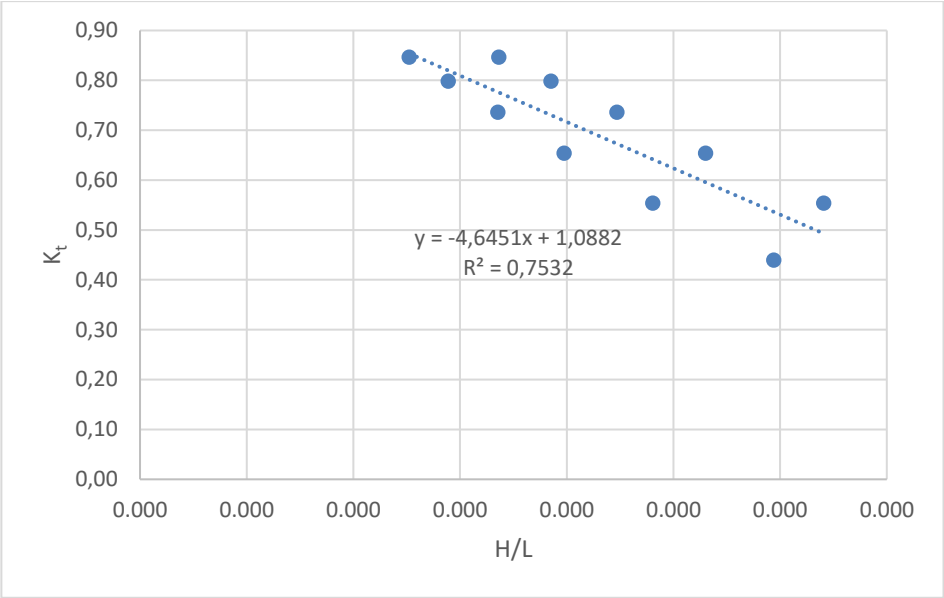

Figure A.5: The change of K_t w.r.t H/L retrieved from Macagnon 1954 for Cylindrical Floating Breakwater

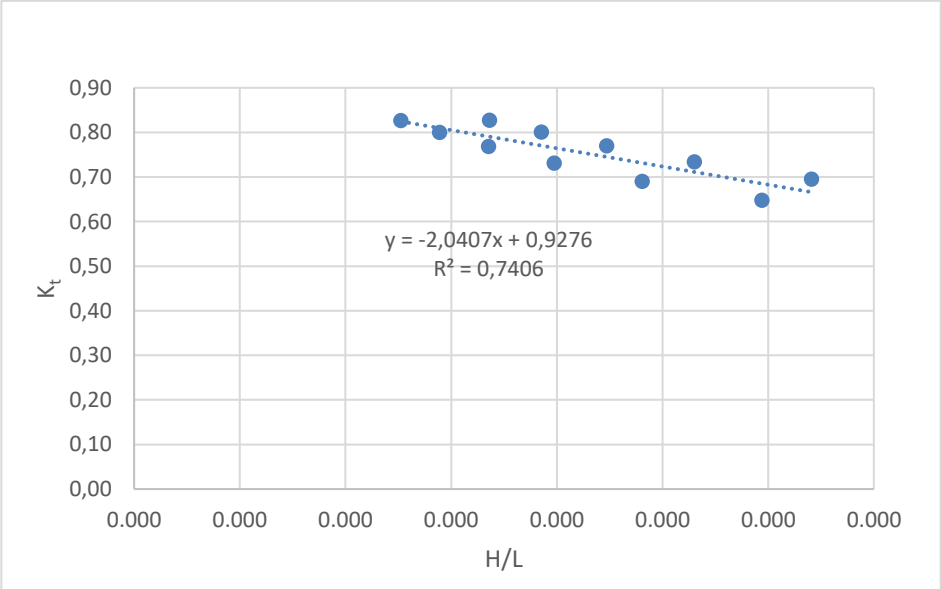

Figure A.6: The of K_t w.r.t H/L retrieved from Abubaker and Türker 2019 for Cylindrical Floating Breakwater

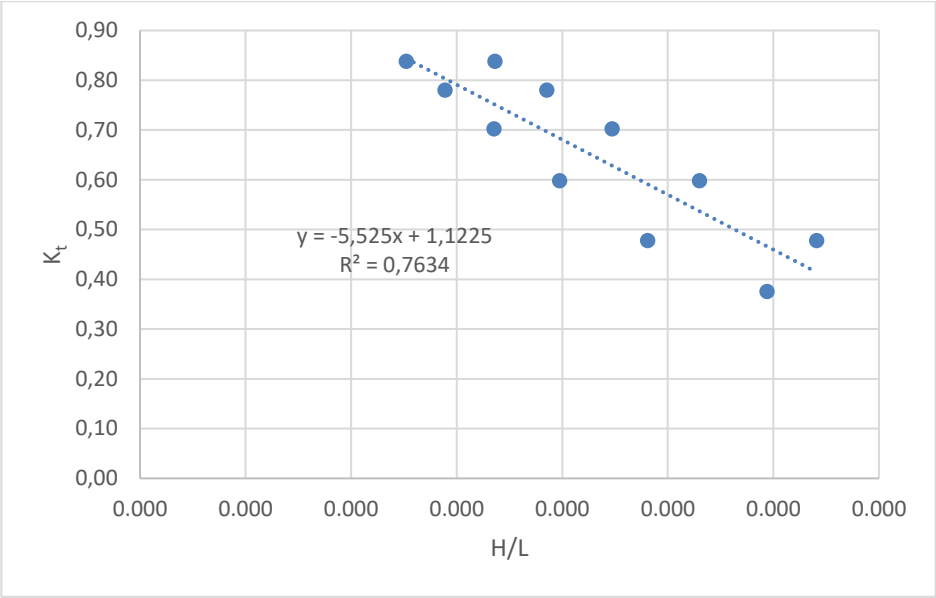

Figure A.7: The change of K_t w.r.t H/L retrieved from Ruol et. al. 2013 for Cylindrical Floating Breakwater

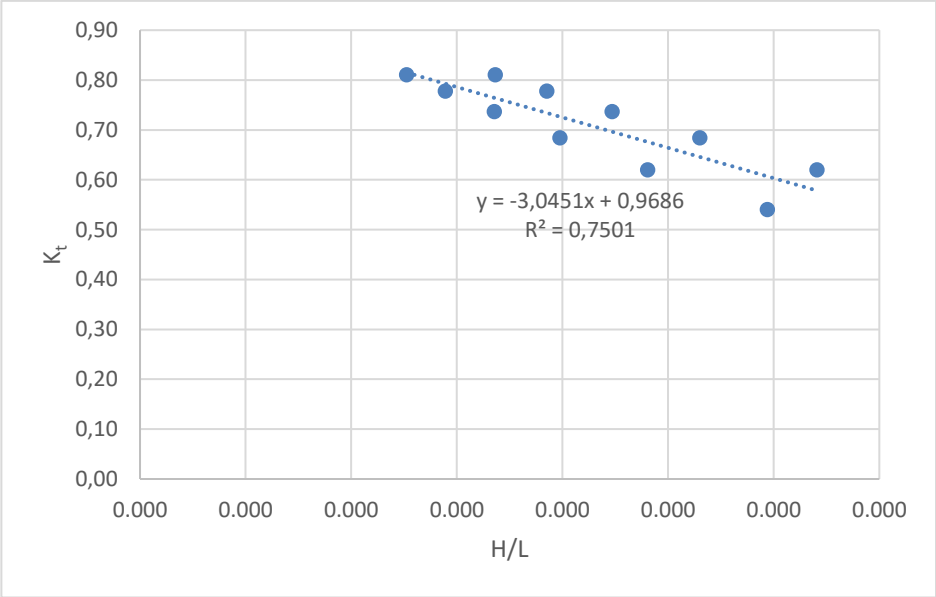

Figure A.8: The change of K_t w.r.t H/L retrieved from Kriebel and Bollmann 1996 for Cylindrical Floating Breakwater

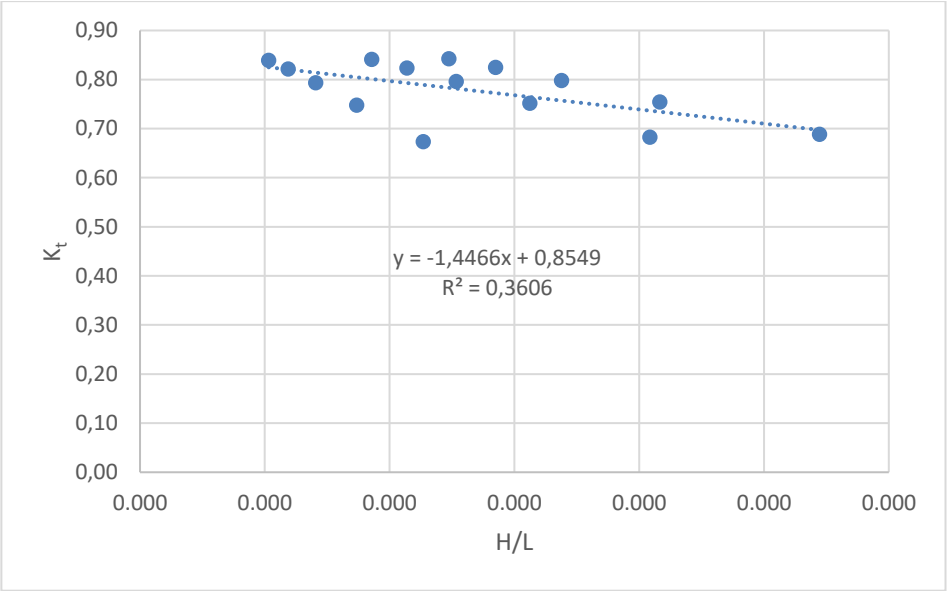

Figure A.9: The change of K_t w.r.t H/L retrieved from Abubaker and Türker 2019 for Board-net Floating Breakwater

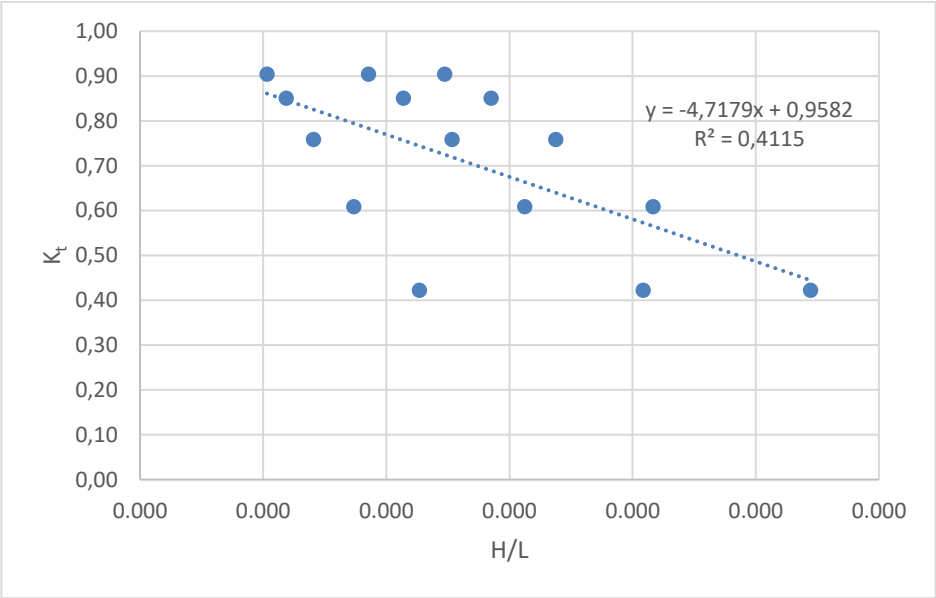

Figure A.10: The change of K_t w.r.t H/L retrieved from Ruol et. al. 2013 for Board-net Floating Breakwater

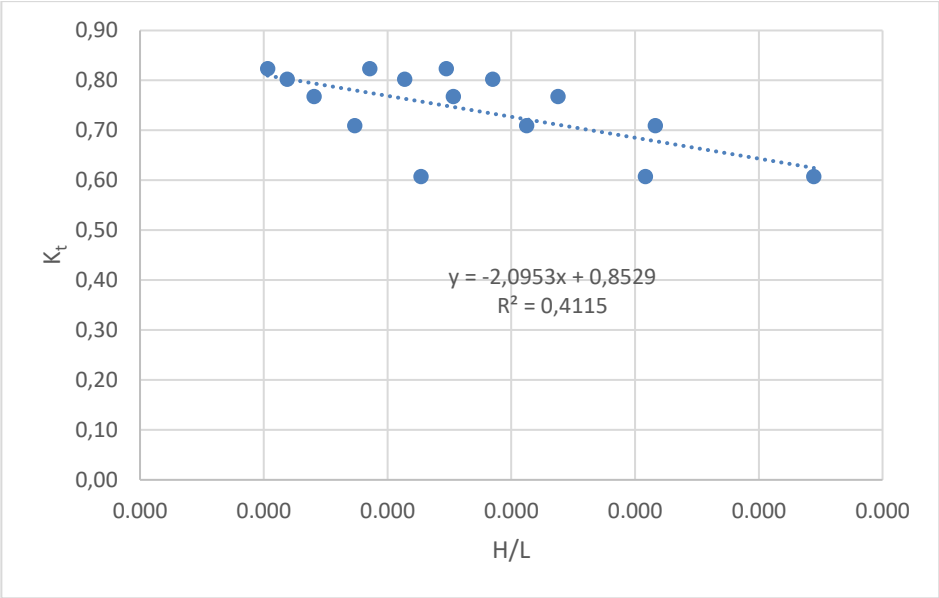

Figure A.11: The change of K_t w.r.t H/L retrieved from Kriebel and Bollmann 1996 for Board-net Floating Breakwater

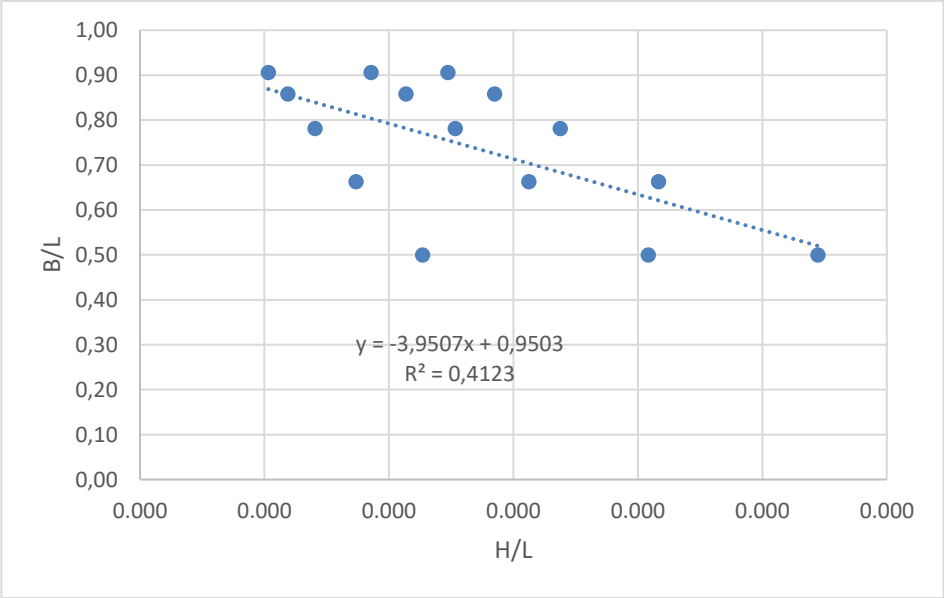

Figure A.12: The change of K_t w.r.t H/L retrieved from Macagnon 1954 for Board-net Floating Breakwater

Appendix B: $P_{absorbed}$ and CWR

For Wave Dragon

Table B.1: Monthly average wave power results by using K_t from Abubaker and Türker 2019

	2010	2011	2012	2013	2014	2015	2016	2017
Jan	30.42	43.17	97.59	79.44	84.89	157.52	86.98	69.68
Feb	29.66	95.26	41.05	224.35	78.97	101.87	120.56	68.11
Mar	28.99	54.57	53.21	-	63.36	93.39	62.26	59.76
Apr	24.52	37.36	28.55	-	26.56	34.06	39.69	31.68
May	15.61	48.07	8.62	62.46	22.33	38.57	21.30	14.37
Jun	13.90	21.46	12.47	20.92	5.97	26.73	16.97	23.06
July	28.29	16.81	-	12.93	14.50	14.66	15.24	20.17
Aug	14.21	14.95	15.96	21.47	20.41	24.82	23.68	16.43
Sep	26.32	54.16	44.72	47.08	20.54	6.79	33.83	40.04
Oct	45.00	64.84	28.50	35.73	59.89	41.55	24.03	47.67
Nov	66.67	66.74	48.99	66.76	34.23	83.65	47.53	55.29
Dec	26.68	124.19	62.34	113.19	116.71	84.74	106.66	77.42

Table B.2: Monthly average wave power results by using K_t from Macagnon 1954

	2010	2011	2012	2013	2014	2015	2016	2017
Jan	20.31	22.87	54.83	35.22	38.46	57.93	39.05	39.71
Feb	15.74	23.62	28.15	65.26	41.76	49.01	51.56	32.82
Mar	21.49	30.39	28.94	-	33.32	46.72	34.77	33.55
Apr	19.58	21.05	24.81	-	20.37	21.31	25.59	22.86
May	14.14	38.47	8.37	36.40	20.32	31.01	18.85	12.93
Jun	12.08	18.33	12.18	18.59	6.37	24.29	15.95	21.40
July	25.56	15.91	-	12.31	14.83	15.15	16.01	19.40
Aug	14.99	15.06	15.75	20.12	20.22	21.15	22.61	16.78
Sep	18.17	40.91	33.23	32.55	13.96	5.65	27.42	31.48
Oct	31.84	43.67	21.68	28.71	40.03	24.72	14.72	36.18
Nov	39.93	38.73	31.27	41.05	20.95	50.19	32.35	35.22
Dec	18.56	58.14	38.82	52.85	51.65	44.45	43.88	42.55

Table B.3: Monthly average wave power results by using K_t from Ruol et. al. 2013

	2010	2011	2012	2013	2014	2015	2016	2017
Jan	18.55	23.40	54.41	39.77	42.88	73.22	43.77	39.12
Feb	16.09	38.96	25.40	96.23	42.77	52.83	59.45	35.35
Mar	18.75	30.30	29.20	-	34.22	49.29	34.61	33.31
Apr	16.59	20.85	20.40	-	17.54	20.06	23.74	20.18
May	11.47	32.57	6.66	35.46	16.46	26.21	15.40	10.51
Jun	9.93	15.16	9.68	15.17	4.98	19.69	12.80	17.24
July	20.75	12.75	-	9.85	11.67	11.90	12.54	15.47
Aug	11.74	11.88	12.48	16.16	16.01	17.50	18.07	13.21
Sep	16.35	35.43	28.97	29.27	12.64	4.72	23.11	26.83
Oct	28.34	39.72	18.73	24.27	36.54	23.84	14.00	31.28
Nov	38.38	37.81	29.15	38.95	19.92	48.20	29.29	32.86
Dec	16.64	63.63	36.62	57.93	58.38	45.71	51.77	42.70

Table B.4: Monthly average wave power results by using K_t from Kriebel and Bollmann 1996

	2010	2011	2012	2013	2014	2015	2016	2017
Jan	38.73	54.90	124.16	100.88	107.82	199.70	110.47	88.66
Feb	37.73	120.38	52.25	283.86	100.44	129.46	153.06	86.56
Mar	36.90	69.43	67.69	-	80.57	118.72	79.21	76.03
Apr	31.18	47.53	36.23	-	33.79	43.36	50.52	40.32
May	19.77	61.12	10.88	79.49	28.29	49.05	27.01	18.21
Jun	17.63	27.25	15.73	26.52	7.44	33.86	21.46	29.19
July	35.85	21.25	-	16.34	18.20	18.38	19.06	25.47
Aug	17.77	18.80	20.11	27.15	25.71	31.52	29.91	20.64
Sep	33.51	68.92	56.91	59.94	26.15	8.62	43.00	50.93
Oct	57.28	82.55	36.26	45.43	76.25	52.88	30.59	60.66
Nov	84.86	84.93	62.37	84.98	43.56	106.47	60.51	70.38
Dec	33.97	157.79	79.35	143.81	148.21	107.77	135.36	98.49

Table B.5: Monthly average capture width ratio results by using K_t from Abubaker and Türker 2019

	2010	2011	2012	2013	2014	2015	2016	2017
Jan	54%	50%	51%	48%	49%	47%	49%	51%
Feb	50%	45%	54%	46%	50%	49%	48%	49%
Mar	56%	51%	51%	-	50%	50%	51%	51%
Apr	57%	51%	60%	-	56%	53%	53%	55%
May	61%	58%	64%	52%	61%	58%	60%	61%
Jun	60%	59%	64%	61%	69%	61%	63%	62%
July	61%	63%	-	63%	67%	67%	68%	64%
Aug	69%	66%	65%	63%	65%	59%	63%	67%
Sep	54%	56%	56%	54%	54%	59%	58%	57%
Oct	55%	54%	56%	58%	54%	52%	52%	56%
Nov	52%	51%	53%	52%	52%	52%	54%	53%
Dec	54%	49%	53%	49%	48%	50%	48%	51%

Table B.6: Monthly average capture width ratio results by using K_t from Macagnon 1954

	2010	2011	2012	2013	2014	2015	2016	2017
Jan	36%	27%	29%	21%	22%	17%	22%	29%
Feb	27%	11%	37%	13%	27%	24%	21%	24%
Mar	41%	28%	28%	-	26%	25%	28%	29%
Apr	46%	29%	52%	-	43%	33%	34%	40%
May	56%	46%	62%	30%	56%	46%	54%	55%
Jun	52%	51%	63%	54%	74%	56%	59%	58%
July	55%	60%	-	60%	68%	70%	72%	61%
Aug	72%	66%	64%	59%	64%	50%	60%	68%
Sep	37%	42%	41%	38%	37%	49%	47%	45%
Oct	39%	36%	43%	46%	36%	31%	32%	43%
Nov	31%	30%	34%	32%	32%	31%	37%	34%
Dec	38%	23%	33%	23%	21%	26%	20%	28%

Table B.7: Monthly average capture width ratio results by using K_t from Ruol et. al. 2013

	2010	2011	2012	2013	2014	2015	2016	2017
Jan	33%	27%	28%	24%	25%	22%	24%	29%
Feb	27%	18%	34%	20%	27%	26%	24%	26%
Mar	36%	28%	28%	-	27%	26%	28%	28%
Apr	39%	29%	43%	-	37%	31%	32%	35%
May	45%	39%	49%	29%	45%	39%	44%	45%
Jun	43%	42%	50%	44%	58%	45%	47%	46%
July	45%	48%	-	48%	54%	55%	56%	49%
Aug	57%	52%	51%	47%	51%	42%	48%	54%
Sep	34%	37%	36%	34%	33%	41%	40%	38%
Oct	34%	33%	37%	39%	33%	30%	30%	37%
Nov	30%	29%	31%	31%	30%	30%	33%	31%
Dec	34%	25%	31%	25%	24%	27%	23%	28%

Table B.8: Monthly average capture width ratio results by using K_t from Kriebel and Bollmann 1996

	2010	2011	2012	2013	2014	2015	2016	2017
Jan	68%	64%	65%	62%	62%	60%	62%	65%
Feb	64%	57%	69%	58%	64%	63%	61%	63%
Mar	71%	65%	64%	-	64%	63%	65%	65%
Apr	73%	65%	76%	-	72%	67%	68%	70%
May	78%	73%	81%	66%	78%	73%	77%	77%
Jun	76%	75%	81%	77%	87%	78%	79%	79%
July	78%	80%	-	80%	84%	84%	85%	80%
Aug	86%	83%	82%	79%	82%	75%	80%	84%
Sep	69%	71%	71%	69%	69%	74%	74%	73%
Oct	70%	69%	72%	73%	68%	66%	67%	72%
Nov	66%	66%	67%	67%	67%	66%	69%	67%
Dec	69%	62%	67%	62%	62%	64%	61%	65%

For Cylindrical Floating Breakwater

Table B.9: Monthly average wave power results by using K_t from Macagnon 1954

	2010	2011	2012	2013	2014	2015	2016	2017
Jan	5.24	8.11	44.84	24.86	28.90	79.70	30.08	24.33
Feb	2.93	23.48	10.63	133.29	28.78	42.90	53.78	19.66
Mar	5.75	14.56	13.42	-	18.56	37.65	19.10	17.70
Apr	4.60	6.31	7.53	-	5.06	6.07	9.02	6.66
May	2.23	17.87	0.56	20.14	5.03	11.90	4.27	1.77
Jun	1.41	3.98	1.68	4.15	0.34	7.21	3.04	5.62
July	7.96	3.04	-	1.67	2.79	2.96	3.38	4.66
Aug	2.98	2.84	3.06	4.97	5.13	5.44	6.30	3.61
Sep	3.94	20.68	14.12	14.17	1.87	-0.21	9.33	12.37
Oct	13.37	25.26	5.82	10.25	21.60	8.83	2.22	16.41
Nov	23.51	22.80	13.82	24.22	5.90	35.93	14.14	17.53
Dec	4.15	60.30	21.56	50.91	51.86	32.66	41.68	28.71

Table B.10: Monthly average wave power results by using K_t from Ruol et. al. 2013

	2010	2011	2012	2013	2014	2015	2016	2017
Jan	4.27	6.69	46.80	23.99	28.44	83.33	29.69	24.31
Feb	1.42	20.65	10.06	141.52	28.90	43.99	55.44	18.68
Mar	5.05	13.67	12.37	-	17.78	38.38	18.57	17.07
Apr	4.01	4.98	7.34	-	4.40	4.99	8.17	5.95
May	1.78	18.41	0.19	19.83	4.75	11.88	3.87	1.29
Jun	0.87	3.50	1.33	3.75	0.10	7.10	2.68	5.42
July	7.90	2.70	-	1.28	2.58	2.78	3.26	4.46
Aug	2.83	2.61	2.80	4.74	5.03	5.04	6.23	3.45
Sep	3.00	21.31	14.08	13.91	0.89	-0.67	9.11	12.33
Oct	13.11	25.94	5.19	10.08	21.90	7.76	1.03	16.64
Nov	23.60	22.72	13.29	24.48	4.76	37.24	13.83	17.30
Dec	3.24	63.05	21.61	52.68	53.48	33.10	41.99	28.97

Table B.11: Monthly average wave power results by using K_t from Kriebel and Bollmann 1996

	2010	2011	2012	2013	2014	2015	2016	2017
Jan	12.80	19.48	59.82	42.91	47.16	105.55	48.66	37.88
Feb	11.79	50.28	19.32	165.09	44.16	61.24	75.27	35.39
Mar	12.32	27.02	25.98	-	32.68	54.84	32.34	30.62
Apr	10.03	16.24	12.67	-	11.05	14.68	18.17	13.79
May	5.68	25.08	2.63	32.81	9.22	18.60	8.57	5.07
Jun	4.80	8.55	4.31	8.37	1.67	11.77	6.44	9.71
July	12.69	6.37	-	4.48	5.39	5.50	5.84	8.21
Aug	5.33	5.58	6.04	8.84	8.45	10.41	10.18	6.38
Sep	10.62	28.98	22.20	23.33	7.59	1.85	15.59	19.43
Oct	22.07	35.84	12.13	16.75	32.09	18.96	9.16	24.38
Nov	36.10	35.87	24.11	36.40	14.70	49.24	23.53	28.41
Dec	10.84	79.85	33.26	70.29	72.49	48.53	63.20	43.36

Table B.12: Monthly average wave power results by using K_t from Abubaker and Türker 2019

	2010	2011	2012	2013	2014	2015	2016	2017
Jan	13.96	21.20	58.21	44.28	48.13	102.50	49.57	38.27
Feb	13.51	53.85	20.13	157.32	44.46	60.63	74.16	36.82
Mar	13.20	28.27	27.37	-	33.85	54.55	33.24	31.62
Apr	10.77	17.83	13.01	-	11.87	15.99	19.27	14.69
May	6.22	24.72	3.04	33.47	9.63	18.80	9.08	5.63
Jun	5.42	9.16	4.73	8.88	1.94	12.01	6.88	10.02
July	12.88	6.80	-	4.95	5.67	5.75	6.03	8.50
Aug	5.53	5.89	6.38	9.18	8.63	10.95	10.36	6.61
Sep	11.73	28.56	22.47	23.85	8.71	2.35	15.99	19.66
Oct	22.58	35.43	12.93	17.10	32.07	20.32	10.52	24.37
Nov	36.35	36.32	24.94	36.48	16.07	48.26	24.11	28.94
Dec	11.92	77.54	33.54	69.00	71.39	48.51	63.47	43.50

Table B.13: Monthly average capture width ratio results by using K_t from Macagnon 1954

	2010	2011	2012	2013	2014	2015	2016	2017
Jan	9%	9%	23%	15%	17%	24%	17%	18%
Feb	5%	11%	14%	27%	18%	21%	21%	14%
Mar	11%	14%	13%	-	15%	20%	16%	15%
Apr	11%	9%	16%	-	11%	9%	12%	12%
May	9%	21%	4%	17%	14%	18%	12%	8%
Jun	6%	11%	9%	12%	4%	17%	11%	15%
July	17%	11%	-	8%	13%	14%	15%	15%
Aug	14%	13%	12%	14%	16%	13%	17%	15%
Sep	8%	21%	18%	16%	5%	-2%	16%	18%
Oct	16%	21%	12%	17%	19%	11%	5%	19%
Nov	18%	18%	15%	19%	9%	22%	16%	17%
Dec	8%	24%	18%	22%	22%	19%	19%	19%

Table B.14: Monthly average capture width ratio results by using K_t from Ruol et. al. 2013

	2010	2011	2012	2013	2014	2015	2016	2017
Jan	8%	8%	24%	15%	16%	25%	17%	18%
Feb	2%	10%	13%	29%	18%	21%	22%	14%
Mar	10%	13%	12%	-	14%	20%	15%	15%
Apr	9%	7%	15%	-	9%	8%	11%	10%
May	7%	22%	1%	16%	13%	18%	11%	5%
Jun	4%	10%	7%	11%	1%	16%	10%	15%
July	17%	10%	-	6%	12%	13%	15%	14%
Aug	14%	11%	11%	14%	16%	12%	17%	14%
Sep	6%	22%	18%	16%	2%	-6%	16%	18%
Oct	16%	22%	10%	16%	20%	10%	2%	20%
Nov	18%	18%	14%	19%	7%	23%	16%	17%
Dec	7%	25%	18%	23%	22%	20%	19%	19%

Table B.15: Monthly average capture width ratio results by using K_t from Kriebel and Bollmann 1996

	2010	2011	2012	2013	2014	2015	2016	2017
Jan	23%	23%	31%	26%	27%	31%	27%	28%
Feb	20%	24%	25%	34%	28%	30%	30%	26%
Mar	24%	25%	25%	-	26%	29%	26%	26%
Apr	24%	22%	27%	-	24%	23%	24%	24%
May	22%	30%	20%	27%	25%	28%	24%	22%
Jun	21%	24%	22%	24%	19%	27%	24%	26%
July	27%	24%	-	22%	25%	25%	26%	26%
Aug	26%	25%	25%	26%	27%	25%	27%	26%
Sep	22%	30%	28%	27%	20%	16%	27%	28%
Oct	27%	30%	24%	27%	29%	24%	20%	29%
Nov	28%	28%	26%	29%	22%	31%	27%	27%
Dec	22%	32%	28%	30%	30%	29%	28%	28%

Table B.16: Monthly average capture width ratio results by using K_t from Abubaker and Türker 2019

	2010	2011	2012	2013	2014	2015	2016	2017
Jan	25%	25%	30%	27%	28%	31%	28%	28%
Feb	23%	25%	27%	32%	28%	29%	30%	27%
Mar	25%	26%	26%	-	27%	29%	27%	27%
Apr	25%	24%	27%	-	25%	25%	26%	26%
May	24%	30%	23%	28%	26%	28%	26%	24%
Jun	23%	25%	24%	26%	23%	28%	25%	27%
July	28%	25%	-	24%	26%	26%	27%	27%
Aug	27%	26%	26%	27%	28%	26%	28%	27%
Sep	24%	30%	28%	28%	23%	20%	27%	28%
Oct	27%	29%	26%	28%	29%	25%	23%	29%
Nov	28%	28%	27%	29%	25%	30%	27%	28%
Dec	24%	31%	28%	30%	30%	29%	28%	29%

For Board-net Folating Breakwater:

Table B.17: Monthly average wave power results by using K_t from Abubaker and Türker 2019

	2010	2011	2012	2013	2014	2015	2016	2017
Jan	19.2	29.2	72.3	58.2	62.6	127.1	64.4	49.3
Feb	19.3	73.1	26.7	191.1	57.1	76.6	93.3	48.8
Mar	17.9	37.6	36.7	-	44.7	69.3	43.6	41.6
Apr	14.7	24.7	17.0	-	16.1	22.0	25.9	19.9
May	8.6	31.1	4.4	43.5	12.8	24.3	12.2	7.9
Jun	7.7	12.4	6.5	12.0	2.8	15.6	9.3	13.2
July	16.7	9.2	-	6.9	7.6	7.7	7.9	11.2
Aug	7.3	7.9	8.6	12.1	11.3	14.6	13.5	8.7
Sep	16.3	35.9	29.0	31.1	12.5	3.6	20.9	25.4
Oct	29.4	44.7	17.5	22.3	40.9	27.6	15.1	31.1
Nov	46.7	46.9	32.8	46.7	22.2	60.4	31.5	37.6
Dec	16.5	96.1	43.2	86.5	89.8	61.9	81.4	55.7

Table B.18: Monthly average wave power results by using K_t from Macagnon 1954

	2010	2011	2012	2013	2014	2015	2016	2017
Jan	17.14	26.07	78.10	56.80	62.27	137.74	64.23	49.90
Feb	15.95	67.09	25.63	214.37	58.13	80.30	98.58	46.94
Mar	16.44	35.88	34.54	-	43.29	71.99	42.77	40.54
Apr	13.40	21.78	16.75	-	14.75	19.65	24.19	18.38
May	7.61	32.85	3.56	43.32	12.24	24.50	11.41	6.82
Jun	6.47	11.42	5.78	11.15	2.26	15.54	8.59	12.85
July	16.74	8.50	-	6.02	7.16	7.30	7.73	10.87
Aug	7.06	7.42	8.03	11.72	11.16	13.84	13.43	8.45
Sep	14.26	37.96	29.26	30.82	10.28	2.55	20.61	25.61
Oct	29.16	46.98	16.16	22.12	42.17	25.31	12.39	32.04
Nov	47.52	47.28	31.93	47.87	19.70	64.41	31.10	37.50
Dec	14.54	104.20	43.80	91.97	94.93	63.78	83.15	57.03

Table B.19: Monthly average wave power results by using K_t from Ruol et. al. 2013

	2010	2011	2012	2013	2014	2015	2016	2017
Jan	18.50	28.16	86.00	61.96	68.06	151.71	70.23	54.64
Feb	17.03	72.68	27.91	236.68	63.68	88.19	108.36	51.13
Mar	17.81	39.04	37.54	-	47.19	79.01	46.69	44.22
Apr	14.50	23.48	18.29	-	15.97	21.22	26.26	19.93
May	8.20	36.10	3.79	47.35	13.33	26.82	12.38	7.33
Jun	6.93	12.37	6.23	12.10	2.41	16.99	9.30	14.02
July	18.31	9.21	-	6.48	7.78	7.94	8.44	11.85
Aug	7.69	8.06	8.73	12.77	12.19	15.04	14.69	9.21
Sep	15.35	41.72	32.02	33.67	10.97	2.66	22.51	28.02
Oct	31.86	51.61	17.53	24.18	46.25	27.41	13.23	35.14
Nov	52.06	51.75	34.82	52.48	21.25	70.85	33.97	40.99
Dec	15.67	114.77	47.97	101.14	104.35	69.95	91.12	62.51

Table B.20: Monthly average wave power results by using K_t from Kriebel and Bollmann 1996

	2010	2011	2012	2013	2014	2015	2016	2017
Jan	21.14	32.06	81.68	64.78	69.87	143.62	71.88	55.18
Feb	21.04	80.63	29.64	217.22	63.97	86.18	105.04	54.15
Mar	19.76	41.72	40.59	-	49.64	77.82	48.51	46.27
Apr	16.16	27.10	18.96	-	17.80	24.19	28.69	21.93
May	9.45	35.03	4.76	48.58	14.19	27.12	13.52	8.62
Jun	8.38	13.73	7.19	13.23	3.04	17.44	10.30	14.66
July	18.64	10.17	-	7.54	8.41	8.49	8.82	12.47
Aug	8.13	8.74	9.48	13.47	12.55	16.21	15.02	9.71
Sep	17.88	40.47	32.45	34.67	13.57	3.84	23.29	28.39
Oct	32.84	50.32	19.31	24.83	45.90	30.43	16.39	34.88
Nov	52.31	52.45	36.53	52.32	24.37	68.08	35.10	41.98
Dec	18.14	108.64	48.29	97.49	101.10	69.44	91.15	62.43

Table B.21: Monthly average capture width ratio results by using K_t from Abubaker and Türker 2019

	2010	2011	2012	2013	2014	2015	2016	2017
Jan	34%	34%	38%	36%	36%	38%	36%	36%
Feb	33%	34%	35%	39%	36%	37%	37%	35%
Mar	34%	35%	35%	-	35%	37%	36%	36%
Apr	34%	34%	36%	-	34%	34%	35%	35%
May	34%	37%	33%	36%	35%	36%	35%	33%
Jun	33%	34%	34%	35%	33%	36%	34%	36%
July	36%	35%	-	34%	35%	35%	36%	35%
Aug	35%	35%	35%	35%	36%	35%	36%	35%
Sep	34%	37%	36%	36%	33%	31%	36%	36%
Oct	36%	37%	35%	36%	37%	34%	33%	37%
Nov	36%	36%	35%	37%	34%	38%	36%	36%
Dec	34%	38%	36%	37%	37%	37%	36%	37%

Table B.22: Monthly average capture width ratio results by using K_t from Macagnon 1954

	2010	2011	2012	2013	2014	2015	2016	2017
Jan	30%	30%	41%	35%	36%	41%	36%	37%
Feb	27%	32%	34%	44%	37%	39%	39%	34%
Mar	32%	33%	33%	-	34%	38%	35%	35%
Apr	31%	30%	35%	-	31%	30%	32%	32%
May	30%	39%	26%	36%	34%	37%	32%	29%
Jun	28%	32%	30%	32%	26%	36%	32%	35%
July	36%	32%	-	29%	33%	33%	35%	34%
Aug	34%	33%	33%	34%	36%	33%	36%	34%
Sep	29%	39%	36%	36%	27%	22%	35%	37%
Oct	35%	39%	32%	36%	38%	32%	27%	38%
Nov	37%	36%	34%	38%	30%	40%	35%	36%
Dec	30%	41%	37%	40%	39%	38%	37%	37%

Table B.23: Monthly average capture width ratio results by using K_t from Ruol et. al. 2013

	2010	2011	2012	2013	2014	2015	2016	2017
Jan	33%	33%	45%	38%	39%	45%	39%	40%
Feb	29%	34%	37%	48%	41%	43%	43%	37%
Mar	34%	36%	36%	-	37%	42%	38%	38%
Apr	34%	32%	38%	-	34%	33%	35%	35%
May	32%	43%	28%	39%	37%	40%	35%	31%
Jun	30%	34%	32%	35%	28%	39%	34%	38%
July	40%	35%	-	32%	36%	36%	38%	37%
Aug	37%	36%	35%	37%	39%	36%	39%	37%
Sep	32%	43%	40%	39%	29%	23%	39%	40%
Oct	39%	43%	35%	39%	41%	34%	29%	41%
Nov	41%	40%	38%	41%	32%	44%	39%	39%
Dec	32%	45%	40%	44%	43%	41%	41%	41%

Table B.24: Monthly average capture width ratio results by using K_t from Kriebel and Bollmann 1996

	2010	2011	2012	2013	2014	2015	2016	2017
Jan	37%	37%	43%	40%	40%	43%	40%	41%
Feb	36%	38%	39%	44%	41%	42%	42%	39%
Mar	38%	39%	39%	-	39%	41%	40%	40%
Apr	38%	37%	40%	-	38%	37%	38%	38%
May	37%	42%	35%	40%	39%	41%	38%	37%
Jun	36%	38%	37%	38%	35%	40%	38%	40%
July	40%	38%	-	37%	39%	39%	40%	39%
Aug	39%	39%	39%	39%	40%	39%	40%	39%
Sep	37%	42%	40%	40%	36%	33%	40%	40%
Oct	40%	42%	38%	40%	41%	38%	36%	41%
Nov	41%	40%	39%	41%	37%	42%	40%	40%
Dec	37%	43%	41%	42%	42%	41%	41%	41%